MOLECULAR DIFFERENCES BETWEEN EPITHELIAL & MESENCHYMAL-LIKE CANCER CELLS AS CANDIDATES FOR THERAPEUTIC TARGETS AND BIOMARKERS FOR PANCREATIC ADENOCARCINOMA

By

Arkadeep Sinha

A DISSERTATION

Submitted to
Michigan State University
in partial fulfillment of the requirements
for the degree of

Genetics- Doctor of Philosophy

2014

ABSTRACT

MOLECULAR DIFFERENCES BETWEEN EPITHELIAL & MESENCHYMAL-LIKE CANCER CELLS AS CANDIDATES FOR THERAPEUTIC TARGETS AND BIOMARKERS FOR PANCREATIC ADENOCARCINOMA

By

Arkadeep Sinha

The standard treatments for pancreatic cancer are frustratingly ineffective for long-term benefit with a 5-year survival rate of approximately only 5%. Surgical removal of the tumor extends survival and chemotherapeutic treatment can reduce the bulk of tumors, but neither method completely eliminates cancer cells or their ability to spread and grow. As a result, disease recurrence is the norm. The failure of surgical removal to obtain complete remission indicates that, by the time a cancerous mass in the pancreas is recognized, some of the cancer cells have already disseminated to other parts of the body and established metastatic sites. Likewise, the failure of drugs to kill all cancer cells suggests that certain cells within the tumor have increased resistance to existing treatments. The cause for the failure of these treatments can thus be traced to a subpopulation of cancer cells within each tumor.

There is evidence showing that the process of epithelial to mesenchymal transition (EMT) gives rise to a more aggressive and chemoresistant subpopulation akin to the above-mentioned subpopulation of cancer cells. So, the over-arching hypothesis of this research is that targeting the EMT-derived mesenchymal-like subpopulation of pancreatic cancer cells will lead to better prognosis. The specific hypotheses tested in this study are 1) Mesenchymal-like cancer cells have distinct genetic alterations and

gene expression features relative to their epithelial-like counterparts; and 2) Presence of increased levels of mesenchymal-like cancer cells in a tumor confers a poor prognosis.

To test the first hypothesis, we used Affymetrix microarrays and CGH microarrays to compare gene expression and gene amplification measurements, respectively, between mesenchymal-like and epithelial-like cancer cells in model systems. We identified major gene expression changes that occur during the process of EMT and identified changes in glycogenes affecting sulfation as well as in genes known to bind sulfated molecules like MRC2. We also identified 20 genes with differential copy numbers between the epithelial and mesenchymal-like cells. A study of 11 primary tissues also supported our findings providing additional candidates to target the mesenchymal-like cancer cells and for use as prognostic biomarkers. To test the second hypothesis, we pursued additional investigations of MRC2. First, we performed functional analysis on MRC2 to determine that it is needed for the migration and invasion of cancer cells, and we studied expression in primary tissue to reveal that it is significantly upregulated in the pancreatic cancer tissues compared to the adjacent non-cancerous tissue. To enable more specific detection of mesenchymal-like cancer cells, we developed a novel system of identifying co-expression of MRC2 and the epithelial marker Epcam. We currently are using this system to test whether an increased presence of co-expressing cells associates with poor prognosis. These complementary approaches provide a broader molecular understanding of the mesenchymal-like aggressive subpopulation of cancer cells and lay a solid foundation to test the over-arching hypothesis.

ACKNOWLEDGEMENTS

This dissertation is dedicated to my family, friends and colleagues without the support of whom, I would not have had the opportunity to write this. I would like to thank my family especially my mother Mrs. Ruma Sinha, my dad, Late Ratan Kumar Sinha and my fiancé Jessica Yadav for their unconditional support. I would like to convey my regards to my dissertation advisor, Dr. Brian B. Haab for his guidance, training and support for my graduate study. Next, I want to take the opportunity to thank my dissertation committee, Dr. Hua Xiao and Dr. Brian C Schutte from Michigan State University, Dr. Steven J. Triezenberg from the Van Andel Institute and Dr. Venkateshwar G. Keshamouni from the University of Michigan for their constructive inputs and supervision of my dissertation work and guidance in making me improve as a scientist. My sincere regards go to the Genetics Program, for providing me an excellent opportunity to follow my passion and pursue my PhD. I would like to send my appreciation to all current and former lab members in the Lab of Cancer Immunodiagnostics, as well as other colleagues at Van Andel Research Institute and Michigan State University. I want to thank the Van Andel Research Institute (VARI) and the Michigan State University-College of Natural Sciences for their sponsorship and support.

TABLE OF CONTENTS

LIST OF TABLES vii

LIST OF FIGURES viii

KEY TO SYMBOLS AND ABBREVIATIONS x

CHAPTER ONE: INTRODUCTION 1
- Introduction 2
  - Cells of the Pancreas 2
  - Pancreatic Disorders 4
  - Pancreatic Adenocarcinoma 5
  - Epithelial to Mesenchymal Transition (EMT) 9
  - TGF-β Signaling and EMT 12
  - Hypothesis 14

CHAPTER TWO: DIFFERENCES IN THE MUTATION SPECTRUM OF EPITHELIAL AND MESENCHYMAL-LIKE CANCER CELLS 17
- Introduction 18
- Materials and Methods 22
  - Cell culture 22
  - Flow cytometry 22
  - Comparative Genomic Hybridization (CGH) 23
  - Identification of genes with differential alterations 23
  - Quantitative PCR validation of genomic amplifications and deletions 24
  - Correlation with gene expression 25
  - Hierarchical Clustering 25
- Results 27
  - Genomic differences between epithelial-like and mesenchymal-like cell lines 27
  - Genomic alterations common to both groups 51
  - Validation of selected copy number changes 52
  - Relationship of copy number to gene expression 54
  - Gains and losses of the selected genes in primary tumors 58
- Discussion 63

CHAPTER THREE: GENE EXPRESSION ALTERATIONS DURING EMT AS CANDIDATE THERAPEUTIC TARGETS & PROGNOSTIC MARKER 68
- Introduction 69
- Materials and Methods 72
  - Cell culture and RNA extraction for microarray analysis 72
  - Microarray data collection and analysis 72
  - Sulfated glycosaminoglycan assay 73
  - Cell culture and induction of EMT 74

Immunofluorescence assay 75
Western blot 76
MRC2 knockdown 76
Scratch assay 77
Proliferation assay 77
Chemotaxis assay 77
Invasion assay 78
Immunohistochemistry 78
Fluroescence Intensity Thresholding and Colocalization (FITC) 80
Results 82
Alterations in glycogenes upon TGF-β induced EMT 82
Functional assessment of top alterations 86
Mannose Receptor C-Type 2 (MRC2) 88
MRC2 in primary tissues 93
Functional role of MRC2 96
Prognostic value of MRC2 101
MRC2/Epcam dual positive cells as prognostic biomarker 103
Discussion 114

CHAPTER FOUR: SYNTHESIS AND FUTURE WORK 117
Summary 118
Copy number differences between epithelial and mesenchymal cancer cells 118
Gene expression changes during EMT 119
MRC2 association with prognosis 120
Fluorescence intensity thresholding and colocalization 121
Future studies 121

BIBLIOGRAPHY 124

LIST OF TABLES

Table 1. Classification of the cell lines..... 31

Table 2. Genes with the highest average alterations. 36

Table 3. Genes with alterations that are selectively enriched in one of the groups. 39

Table 4. Alterations common to both mesenchymal-like and epithelial cells. 51

Table 5. DNA-mRNA correlations. 55

Table 6. Analysis of glycogene enrichment in Panc-1 upon TGF-β treatment..... 83

LIST OF FIGURES

Figure 1. Morphology of cell lines in 2D & 3-D cultures. 30

Figure 2. Hierarchical Clustering. 33

Figure 3. Top hits based on t-test comparisons. 35

Figure 4. Enriched deletions and amplifications in mesenchymal-like cancer cells. 41

Figure 5. Rates of alterations of selected genes. 45

Figure 6. Distribution of altered probes throughout the genome for epithelial cell lines. 46

Figure 7. Distribution of altered probes throughout the genome for mesenchymal-like cell lines. 47

Figure 8. Difference in the incidence of mutations between the epithelial and mesenchymal-like cell lines. 48

Figure 9. Detailed view of chromosome 9. 50

Figure 10. Q-PCR validation of DNA alterations. 53

Figure 11. DNA-mRNA correlation. 57

Figure 12. Genomic alterations in primary tumors. 60

Figure 13. Distribution of Mutated probes throughout the genome for the primary tissues. 62

Figure 14. Alcian Blue assay for comparison of overall sulfation levels for treated and untreated Panc-1. 85

Figure 15. TGF-β1-induced changes in MRC2 protein levels. 91

Figure 16. Correlation between SMAD4 and MRC2 staining intensity. 92

Figure 17. Correlation between different MRC2 antibodies. 93

Figure 18. MRC2 staining in vivo. 95

Figure 19. MRC2 Knockdown. 97

Figure 20. MRC2 contribution to migration, chemotaxis, and invasion. 99

Figure 21. Association of MRC2 staining with prognosis..... 102

Figure 22. Dual fluorescence images along with H&E. 106

Figure 23. Confocal Images showing presence of probable dual positive cancer cells. 108

Figure 24. Confocal Images able to distinguish red blood cells from true positives. ... 109

Figure 25. FITC Results. 113

KEY TO SYMBOLS AND ABBREVIATIONS

Abbreviation/Symbol	Definition
ADM	Acinar to ductal metaplasia
A549	Adenocarcinomic human alveolar basal epithelial cell line
AF103097	Putative gene on chromosome 14
Akt	Protein kinase B
ALDH	Aldehyde dehydrogenase
ARPCIA	Subunit of the Arp2/3 complex
BCA	Bicinchoninic acid assay
BCR E3 ligase	BTB-Cul3-Rbx1 E3 Ubiquitin Ligase
BMPs	Bone morphogenetic proteins
BRCA2	Breast cancer 2
BSA	Bovine serum albumin
BxPC3	Human adenocarcinoma cell line
c-MET	MET/HGFR
CA	California
CA199	Carbohydrate antigen 19-9
CCLE	Cancer Cell Line Encyclopedia
CD24	Heat stable antigen
CD44	cell surface glycoprotein encoded by CD44 gene
CDKN2A	Cyclin-dependent kinase inhibitor 2A
CDKN2B	Cyclin-dependent kinase inhibitor 2B

CGH	Comparitive Genomic Hybridization
CHST11	Carbohydrate sulfotransferase 11
CHST3	Carbohydrate sulfotransferase 3
CT	Computerized tomography
Cy-5	Cyanine-5
DAB	3, 3'-Diaminobenzidine
DAPI	4', 6-Diamidino-2-Phenylindole
DEC-205	Type I cell surface protein expressed primarily by dendritic cells, mannose receptor family member
DMSO	Dimethylsulfoxide
DNA	Deoxyribonucleic acid
DQ515897	putative gene on chromosome 8 located near MYC
dUTP	2´-Deoxyuridine, 5´-Triphosphate
E-Cadherin	Epithelial cadherin
E13.5	Embryonic day 13 .5
ECM	Extracellular matrix
EDTA	Ethylenediaminetetraacetic acid
EGF	Epidermal growth factor
EGFR	Epidermal growth factor receptor
EMT	Epithelial to Mesenchymal Transition
ESA	Epithelial specific antigen
FBS	Fetal bovine serum
FDA	Food and Drug Administration

FFPE	Formaldehyde fixed-paraffin embedded
FGF	Fibroblast growth factor
FISH	Fluorescence in-situ hybridization
FITC	Fluorescence Intensity Thresholding and Colocalization
FSP1	Fibroblast specific protein 1
GAG	Glycosaminoglycan
H&E	Hematoxylin and eosin
HAS2	Hyaluronan synthase 2
HDAC2	Histone deacetylase 2
HGF	Hepatocyte growth factor
HRP	Horseradish peroxidase
Hs799T	Pancreatic cancer cell line isolated from lymph node metastasis
IA	Iowa
IF	Immunofluorescence
IGF II	Insulin-like growth factor 2
IgG	Immunoglobulin G
IHC	Immunohistochemistry
IL	Illinois
IN	Indiana
ITGA3	Integrin, alpha 3
ITGA5	Integrin, alpha 5
ITGB3	Integrin, beta 3

KIAA1797	Gene on chromosome 9
KLHL9	Kelch-like family member 9
KRAS	V-Ki-ras2 Kirsten rat sarcoma viral oncogene homolog
LAMC2	Laminin, gamma 2
M34428	Putative gene on chromosome 8 located near MYC
MD	Maryland
MET	Mesenchymal to epithelial transition
Miapaca-2	Cell line established from the tumor tissue of the pancreas obtained from a 65-year-old Caucasian male
MMP2	Matrix metalloproteinase 2
MMP9	Matrix metalloproteinase 9
MR	Mannose receptor
MRC2	Mannose receptor C type 2
mRNA	Messenger RNA
MYC	Oncogene
N-Cadherin	Neural cadherin
NAG	Neuroblastoma Amplified Gene
Ngn3	Neurogenin 3
NY	New York
OST3P	Subunit of the oligosaccharyltransferase complex
p53	Oncogene coded by TP53 gene
Panc-1	Human pancreatic carcinoma, epithelial-like cell line
PanIN	Pancreatic intraepithelial neoplasia

PBS	Phosphate-buffered saline
PBST	Phosphate-buffered saline with tween
PCR	Polymerase chain reaction
PDAC	Pancreatic adenocarcinoma
PDGF	Platelet-derived growthf actor
Pdx-1	Pancreatic and duodenal homeobox 1
PI3K	Phosphoinositide 3-kinase
PLA(2)R	Phospholipase A2 receptor
PP cells	Pancreatic polypeptide producing cells
Ptf1a	Pancreas specific transcription factor, 1a
PVDF	polyvinylidene
Ras-Raf-MAPK	MAPK/ERK pathway
Rho-ROCK	Rho-associated protein kinase
RIPA	Radio-Immunoprecipitation Assay
RNA	Ribonucleic acid
SGCZ	Sarcoglycan zeta
shRNA	Short hairpin RNA
SMAD2/3/4	SMAD family member proteins 2, 3 & 4.
SMURF1	SMAD specific E3 ubiquitin protein ligase 1
SPOCK1	Gene encoding the protein core of plasma proteoglycan containing chondroitin- and heparan-sulfate chains
STK19	Serine/threonine-protein kinase 19
SULF2	Sulfatase 2

SW1990	Cell line from spleen metastasis of a grade II pancreatic adenocarcinoma derived from the exocrine pancreas
TBS	Tris-buffered saline
TBST	Tris-buffered saline with tween
TGF	Transformation growth factor
TGF-βR1	Transformation growth factor beta receptor 1
TGF-βR2	Transformation growth factor beta receptor 2
TMA	Tissue microarray
TP53	Tumor protein p53
TUSC3	Tumor suppresor candidate 3
um	Micron
VA	Virgnia
VEGF	Vascular endothelial growth factor
α	Alpha
α-SMA	Alpha-smooth muscle actin
β	Beta

CHAPTER ONE: INTRODUCTION

Introduction

The pancreas is an integral part of the digestive system required for glucose metabolism. It is a slender, pink organ with a nodular consistency which lies within the abdomen-pelvis cavity between the stomach and small intestine. The adult pancreas ranges between 20-25 centimeters in length and weighs approximately 80 grams. The head of the pancreas lies close to the duodenum and the slender body extends toward the spleen where the tail is rounded. It is connected to the duodenum by the ampulla of Vater [1-3].

The pancreas is often described as two organs in one because of the distinct organization and function of the endocrine and exocrine functions [4]. It serves two major functions with the exocrine pancreas being responsible for the production of digestive enzymes which are secreted to eventually end up in the stomach, while the endocrine pancreas is involved in the synthesis of several hormones that are involved in food uptake and metabolism, and secreted into the bloodstream [2, 5].

Cells of the Pancreas

With distinct functions to perform, there are different cell types which are present within the pancreas. Acinar cells forming the exocrine component are the major cell type in the pancreas arranged in the form of lobules. The acinar cells have basal nuclei with regular arrays of rough endoplasmic reticulum and numerous secretory granules containing the digestive enzymes. The acinar cells secrete a minimum of 22 different digestive enzymes like trypsin, amylase and lipase that drains into a highly branched ductal

network which ultimately merges with the common bile duct. The accessory duct and pancreatic duct perforate the wall of the duodenum to discharge pancreatic juice. These enzymes are secreted in an inactive form and are activated after they reach the duodenum where they are required for the breakdown of the carbohydrates, lipids and proteins. Secretion of pancreatic juices is regulated by hormones like secretin, gastrin and others [1-3].

The endocrine pancreas is present in the form of clusters of cells known as pancreatic islets or the islets of Langerhans. The islets are scattered among the exocrine part of the organ and account for only 1% of the total pancreatic cell population [4]. The islets are comprised of a variety of cells including the alpha cells which produce glucagon and beta cells which secrete insulin; both of them play irreplaceable roles in regulating blood glucose levels. In addition to these cells, delta cells, PP cells and epsilon cells are also present in the islets which produce somatostatin, pancreatic polypeptide and ghrelin respectively performing various regulatory functions [1, 3].

The ducts of the pancreas are lined with columnar epithelial cells with small number of goblet cells in the larger ducts. The junction between the acini and the ducts are lined with centroacinar cells which secrete non-enzymatic components of the pancreatic juices like bicarbonates which help neutralize the acids coming into the small intestine from the stomach[2].

Pancreatic Disorders

Given the importance of this organ, several diseases are associated with the improper functioning of the pancreas; the most prevalent of them being Type 1 diabetes wherein the body loses its ability to control blood sugar levels because of the lack or deficiency of insulin secretion by the pancreas. It's mostly caused by the destruction of pancreatic beta cells because of autoimmune disorder. It affects approximately 3 million people in the United States and accounts for approximately $15 billion per year in healthcare costs [1, 3, 6].

Pancreatitis is another pancreas related condition where the pancreatic enzymes that are intended to be activated in the small intestine get activated in the pancreas itself, causing injury to the pancreatic tissue leading to fibrosis and acinar cell atrophy which leads to endocrine and exocrine insufficiency [1, 3, 7].

Recently, pancreatic cancer has received greater attention because of the high mortality rates associated with it. A closer look at the statistics hints towards the severity of the problem. Prostate cancer is one of the most common cancers affecting approximately 233,000 patients each year. On the contrary, pancreatic cancer only affects approximately 46,000 patients annually making it the 12^{th} most common cancer type. However, the number of people succumbing to pancreatic cancer (approx. 40,000) is vastly greater than the number of people expiring because of prostate cancer (approx. 30,000) alluding towards the high mortality rate associated with pancreatic cancer [8].

Pancreatic Adenocarcinoma

Pancreatic adenocarcinoma is by far the most common pancreatic cancer accounting for approximately 85-90% of the cases globally [9, 10]. Smoking and obesity have been shown to increase the risk of pancreatic cancer. History of pancreatitis and diabetes make a person more susceptible to pancreatic cancer [10, 11]. One of the major reasons why pancreatic cancer is so deadly is because the symptoms of the disease are not really specific. The similarity of its symptoms with other conditions like jaundice and the lack of effective screening tools against asymptomatic pre or early malignant tumors have prevented early intervention [10]. Given the location of the pancreas as well as presence of body fat and bowel gas, ultrasound scans can often miss pancreatic tumors [12]. Computerized tomography (CT) is the initial comprehensive imaging technique applied to patients suspected to have pancreatic cancer. However, non-contrast CT has very poor sensitivity and specificity for pancreatic tumors because of the hypovascular nature of pancreatic tumors. Because of these limitations, pancreatic cancers often go undetected till later stages resulting in the median size of pancreatic adenocarcinoma to be 31 millimeters at the time of diagnosis. Only 7% of the tumors over 30 millimeters are resectable compared to 83% of tumors under the size of 20 millimeters [12]. Other than an increase in the size of primary tumor, metastatic lesions also develop by the time a pancreatic tumor is detected with the liver being the primary site for metastatic lesions. The 5-year survival rate is a measly 6.7 % [8].

Anatomically, pancreatic adenocarcinoma produces a firm, highly fibrotic mass with poorly defined boundaries. Normal pancreas has a minimal fibrotic compartment but

pancreatic cancer is associated with intensive desmoplasia leading to a proliferation of fibroblasts and deposition of ECM components where the actual neoplastic cells are only a minority. The cancer cells are ductal in nature and therefore initially thought to arise from the ductal cells [13]. Recent evidence from mouse models using lineage tracing studies, acinar cells has been identified as the cells of origin for pancreatic cancer. The process of acinar to ductal metaplasia (ADM) gives rise to the neoplastic ductal cells in adenocarcinoma [9, 14-16]. ADM also happens in pancreatitis which might make pancreatitis a risk factor for pancreatic cancer [14]. The progression of pancreatic cancer begins with the transformation of histologically normal epithelium to low grade pancreatic intraepithelial neoplasia (PanIN) followed by its passage to the other PanIN grades to ultimately develop PDAC. PanINs are classified into 4 categories -1A, 1B, 2 and 3 with each level accruing more mutations (Fig 2). KRAS mutations happen very early, with more than 90% of pancreatic adenocarcinoma containing them. The KRAS activation is followed by inactivation of CDKN2A (p16) followed by mutations to SMAD4, TP53 and BRCA2. These mutations become increasingly more common with the progression of the disease. Given that most of the mutations are in tumor suppressors, therapeutic intervention based on these genes has been difficult till date [10, 17, 18].

In general, most cancer cells acquire the same set of 6 functional capabilities during their development; the process of acquisition of these traits varying from one tumor to another. These capabilities include self sufficiency in growth signals, insensitivity to anti-growth signals, tissue invasion and metastasis, limitless replicative potential, sustained

angiogenesis, avoiding apoptosis, reprogramming of energy metabolism and evading immune destruction [19, 20]. The KRAS mutation commonly seen in pancreatic cancer makes the protein and the pathway Ras-Raf-MAPK constitutively active irrespective of the upstream signaling like EGFR, providing growth signal sufficiency. The mutations in CDKN2A, SMAD4 provide insensitivity to growth inhibitory signals while mutations in TP53 as well as overexpression of Akt in the PI3K-AKT pathway help the cells evade apoptosis. To escape undergoing senescence, most pancreatic cancers (approximately 95%) undergo activation of telomerase to maintain their telomere lengths and continue the process of cell division [21]. Sustained angiogenesis is acquired through the upregulation of vascular endothelial growth factor which has also been correlated with poor prognosis in pancreatic cancer [22]. The capability of tissue invasion and metastasis is an area of active research with several genes and events like the epithelial to mesenchymal transition having been shown to influence it. Cancer cells have been shown to alter their energy metabolism by limiting their energy metabolism largely to glycolysis even under aerobic conditions with relatively little pyruvate being dispatched to the oxygen-consuming mitochondria. Even though this process is highly energy-inefficient, it is favored by cancer cells possibly for diverting glycolytic intermediates into various biosynthetic pathways for rapid cellular division. It has been observed that tumors arise more frequently and grow more rapidly in immunodeficient mice compared to their immunocompetent controls. This has inspired studies about the role of the immune system in resisting or the progression of tumors [20].

Another area of active research in pancreatic cancer is biomarker identification. By the time of clinical diagnosis, metastatic lesions are already present leaving only a minority of patients with the option of undergoing surgery. This indicates the requirement for better diagnostic tools to identify the pancreatic cancer at an earlier stage. The only FDA approved biomarker for pancreatic cancer is CA19-9, a carbohydrate molecule that is upregulated during the formation, and is associated with the progression of the disease. The addition of carbohydrate moieties to proteins, lipids and other organic molecules happens through a process known as glycosylation. It is a dynamic process that involves an interplay between various glycosyltransferases in the endoplasmic reticulum and golgi apparatus and has important functional connotations. Proper glycosylation is required for proper protein folding and increases the stability of proteins. Abnormal glycosylation has been implicated in several pathologic conditions with glycosylation playing an important role in mediating essential processes in development, host-pathogen interactions, immune cell recognition as well as cancer development and progression. Alterations in cancer cell glycosylation have been shown to frequently modulate the invasive potential of tumor cells and their interactions with other stromal components (22). The carbohydrate structures on cell surface and secreted proteins are good indicators of cell type and status as they specifically change in association with development. However, the performance of CA19-9 as a biomarker has been debated in recent times and due to the lack of effective biomarkers, vascular and perineural invasion are present in the majority of surgically resected cancers, and metastases to regional lymph nodes, the liver, and distant sites are prevalent.

The poor performance of drugs in pancreatic cancer is often attributed to the desmoplasia associated with pancreatic cancer. Conflicting reports are available regarding the role of the stromal component; with some evidence suggesting the stromal compartment prevents the penetration of drugs to the neoplastic cells while other studies suggesting the stromal component acting as a physical barrier preventing metastasis, showing that targeting the stromal cells showing an increase in tumorigenicity [10, 23]. Irrespective of the direction of effect, it suggests a very important role of the tumor associated stroma in pancreatic cancer. One of the major processes implicated in the fibrotic process is epithelial to mesenchymal transition.

Epithelial to Mesenchymal Transition (EMT)

The early embryo and most adult organs of the human body including the pancreas are composed of cells of epithelial origin. Epithelial cells generally contact with other epithelial cells as well as with the basement membrane. They display apical-basal polarity and have contact with each other through tight junctions, adherens junctions, gap junctions as well as desmosomes. Apart from epithelial cells, another class of cells present in the body is mesenchymal cells. Given that the early embryo consists of only epithelial cells and the adult body contains both epithelial and mesenchymal tissue, Elizabeth Hay identified the process of epithelial to mesenchymal transition, a reversible process which allows the evolution of mesenchymal cells from cells of epithelial origin [24]. The reverse process where mesenchymal cells turn back to epithelial cells is known as mesenchymal-epithelial transition. The process of EMT is a critical biological process primarily required during the process of embryogenesis and also induced in

adults during processes of wound healing and tissue regeneration. EMT therefore is responsible for generating cells with a distinct phenotype and function as well as facilitating the movement of cells for purposes ranging from wound healing to cancer metastasis.

Key events in EMT involve the dissolution of epithelial cell-cell junctions, loss of apical-basal polarity as well as increased cell motility and protrusions. Additionally cells that have undergone EMT acquire resistance to senescence and apoptosis as well as an elevated ability to degrade the extracellular matrix. Upon the initiation of EMT, cells downregulate genes affecting cell junctions leading to downregulation of adherens junctions, tight junctions and others involved in contact and communication between epithelial cells. Epithelial cadherin (E-Cadherin) is cleaved and degraded and other mesenchymal cell specific adhesion molecules like neural-cadherin (N-cadherin) are expressed in its place leading to a cadherin switch which increases the affinity of these cells for mesenchymal cells. N-Cadherin mediated junctions are weaker than E-cadherin junctions and facilitate migration and invasion of these cells. Along with the changes in adhesion molecules, several matrix metalloproteinases like MMP2, MMP9 are also upregulated during EMT which play a major role in the remodeling of ECM, which is an integral part of cancer metastasis [25].

EMT can be classified into three subtypes based on their biological setting. Though the differences in the specific signals between the three subtypes are not lucid, functional distinctions are well classified.

Type 1 EMT is classified as the EMT associated with implantation, embryo formation and organ development. This generates diverse cell types and neither causes fibrosis or induce an invasive phenotype. Most of the mesenchyme generated by this process undergoes MET to generate secondary epithelia. The EMT associated with gastrulation is dependent on the Wnt signaling pathway with TGF-β superfamily proteins mediate the actions of Wnt.

Type-2 EMT induces the processes associated with wound healing, tissue regeneration and organ fibrosis. This process is associated with repair and generates fibroblasts and other related cells to reconstruct tissues following trauma and inflammatory injury. This process is generally associated with inflammation and ceases once inflammation is attenuated. Macrophages and activated fibroblasts accumulate at sites of injury releasing cytokines like transformation growth factor (TGF), Platelet derived growth factor (PDGF), epidermal growth factor (EGF) amongst others which can induce the EMT process. If inflammation remains unchecked, EMT derived fibrosis can lead to organ destruction.

Type-3 EMT occurs in neoplastic cells, allowing it to invade surrounding tissue and metastasize to various organs of the body. Cancer cells undergo the process to varying extents with some cells retaining many epithelial traits while gaining more mesenchymal traits while certain cells shed all vestiges of their epithelial origin. These mesenchymal

cells are typically seen at the invasive front of the primary tumors and considered responsible for subsequent steps of invasion-metastasis cascade.

Type-3 EMT can be triggered by a wide variety of cytokines like EGF, hepatocyte growth factor (HGF), fibroblast growth factor (FGF) and TGF, most likely released by the tumor associated stroma. Once activated by the transcription factors, the cells use a variety of intracellular signaling networks and signal-transducing proteins like SMADs, ERK, MAPK etc. to implement the transition [26].

TGF-β Signaling and EMT

TGF-β signaling plays a significant role during development with experimental evidence of involvement in palate fusion and the formation of endocardial cushions. EMT is used to induce mesenchymal cells to generate newer tissue with diverse function during embryogenesis. During development, the first set of mesenchymal cells, the primary mesenchyme is generated through the process of EMT which subsequently gives rise to epithelial tissue through the process of MET to form various organs [25, 27].

In the canonical TGF-β signaling pathway, TGF-β ligands bind to the Type II TGF-β receptor which is a serine/threonine receptor kinase. The different kinds of ligands include three different kinds of TGF-β, 2 kinds of activins, and many bone morphogenetic proteins (BMPs) 13. Upon binding of the ligand, the dimer of TGF-βR2 binds to a dimer of TGF-βR1 and phosphorylates it. The tetramer of TGF-βR complex then binds to the SMAD2/3 phosphorylating it at 2 C-terminal serines. Two

phosphorylated Smad proteins then bind to a co-SMAD like SMAD4 to form a trimeric complex. The SMAD complex then moves to the nucleus and regulates transcription of target genes through physical interaction with the DNA and cooperation with DNA-binding transcription factors [25, 28].

In adults, it occurs during wound healing, organ regeneration and organ fibrosis. However, this process is also hijacked by cancer cells for their own benefit [27]. Most organs of the body including the pancreas are made up of epithelial cells which have strong contacts with each other and with the basement membrane. If they lose contact with other cells or the basement membrane, they under cell-death through a process called anoikis. On the other hand, mesenchymal cells are spindle shaped elongated cells akin to fibroblasts. They do not have any contact with basement membrane and are immune to anoikis. They generally form the support structure to most organs. Once, cells undergo the process of EMT, they become much more motile, invasive and adopt anoikis resistance. Cancer cells utilize it to metastasize to other organs in the body [25]. Carcinoma cells that have undergone EMT are typically seen at the invasive front of the cancer. They pass through this process in varying degrees with several cells retaining some epithelial traits while acquiring new mesenchymal traits while some cells lose all vestiges of epithelial cells becoming completely mesenchymal expressing markers like alpha-SMA, FSP1, vimentin and desmin [26].

Hypothesis

With existing therapies, like most cancer treatments, initial treatment is associated with a reduction of bulk tumor tissue followed by a resistant and more aggressive tumor recurrence. Also studies have shown that a subset of dysplastic cells can disseminate and form micro-metastasis even before the formation of primary tumor which might explain the relapses even in patients with organ-restricted cancers [29]. This points toward the presence of a subpopulation of cancer cells which are highly aggressive and resistant to chemotherapeutics and suggest that targeting this subpopulation of cancer cells might improve patient prognosis. EMT has been shown to play a vital role in the metastasis of cancers forming mesenchymal-like cancer cells with elevated propensity to migrate and increased chemoresistance. Hence, the over-arching hypothesis of the study is that targeting the EMT-derived mesenchymal-like cancer cells would lead to better prognosis of pancreatic cancer patients.

To test the overarching hypothesis, the initial step is to identify molecules that can be used to target the mesenchymal-like subpopulation of cells. Molecules like E-cadherin, vimentin, Zeb1 are known molecules that can differentiate between epithelial and mesenchymal cells. However, targeting the mesenchymal-like cancer cells with these molecules have been difficult to achieve without significant side effects as most of these known molecules are either transcription factors or adhesion molecules. Hence, there is a need for the identification of new molecules that can not only differentiate between the cell types but also be able to target them.

Several molecules are known to induce EMT while others are known to prevent or reverse it. Alterations in these genes might affect the process of EMT. The induction of EMT in only a small subset of cancer cells alludes to the fact that only a subset of cells with specific mutations might undergo EMT. Hence, we formed the hypothesis that EMT-derived mesenchymal-like cancer cells have distinct genetic alterations and gene expression features relative to their epithelial counterparts. The genetic differences and molecular differences between the groups can serve as suitable candidates for drug targets and possibly also serve as biomarkers.

One of the prerequisites for the success of any targeted therapy is to identify whether the molecules which is being targeted has any relation with the disease prognosis or progression. With our over-arching hypothesis, it was necessary to determine whether the mesenchymal-like cancer cell subset is associated with poor prognosis. Hence, we came up with the second hypothesis that the presence of increased levels of mesenchymal-like cancer cells in a tumor confers a poor prognosis. The identified differences between epithelial and mesenchymal-like cancer cells can be used as markers for the mesenchymal-like subset of cancer cells to test this hypothesis. Hence, with the over-arching hypothesis in place, these specific hypotheses were tested in this study

1. EMT-derived mesenchymal-like cancer cells have distinct genetic alterations and gene expression features relative to their epithelial counterparts.

2. The presence of increased levels of mesenchymal-like cancer cells in a tumor confers a poor prognosis.

CHAPTER TWO: DIFFERENCES IN THE MUTATION SPECTRUM OF EPITHELIAL AND MESENCHYMAL-LIKE CANCER CELLS

The results of this chapter have been published separately as

Sinha A, Cherba D, Bartlam H, Lenkiewicz E, Evers L, Barrett MT & Haab BB. (2014) Mesenchymal-like pancreatic cancer cells harbor specific genomic alterations more frequently than their epithelial-like counterparts. (DOI: 10.1016/j.molonc.2014.04.007)

Introduction

Pancreatic cancer continues to bring a dismal prognosis to afflicted patients, with a five year survival rate of only about 5%. This cancer is highly resistant to current therapeutics, with the most effective drug, gemcitabine, only increasing survival time by an average of two months. Therapies that specifically target aberrant pathways in cancer cells hold promise for more effective action with fewer side effects. Many targeted therapeutics have been tested for pancreatic cancer, such as farnasyltransferase inhibitors to target the KRAS pathway [30] and VEGF inhibitors such as avastin to reduce angiogenesis [31]. Erlotinib, which blocks the epidermal growth factor receptor, is used in combination with gemcitabine and is the only FDA-approved targeted therapy for pancreatic adenocarcinoma, although the increase in survival is minimal [32]. Dramatic advances in pancreatic cancer therapeutics are critically needed.

A major difficulty in the development of drugs against pancreatic cancer and other cancers is the achievement of complete and durable responses. Most tumors respond initially to certain treatments with major shrinkage of the primary tumor, yet the remaining cells eventually develop into a more aggressive and resistant cancer. This situation suggests the existence of a subset of particularly resistant cells among the heterogeneous cancer cell populations. That possibility is supported by the observation of tumor-initiating cells, existing within the bulk of the tumor, that have an enhanced ability to proliferate and produce differentiated progeny [33]. This subpopulation of cancer cells can be distinguished from other cancer cells by specific molecular markers, such as c-MET, ALDH, CD44, ESA, and CD24 [34-36]. However, cancer cell

subpopulations can also be defined by more general traits of cellular differentiation. For example, cancer cells induced to undergo epithelial-to-mesenchymal transition (EMT) show traits of stem cells and have elevated rates of migration akin to normal mesenchymal cells [26, 37]. The metastatic dissemination of pancreatic cancer requires cells to break away from the epithelial ductal structures and make their way through the extracellular matrix to reach the lymphatic, circulatory or serous system. The characteristics conferred by epithelial to mesenchymal transition might help cells to go through this dissemination process more efficiently. While most primary pancreatic cancer cells have epithelial traits and are part of ductal structures, solitary cancer cells with mesenchymal traits have been observed in tissue sections [34, 38]. These observations lead to the possibility that pancreatic cancer cells with mesenchymal traits are particularly aggressive and represent an important subpopulation for drug targeting [34, 39]. There is an apparent need for gaining insight into this phenotypic switch in cancer cells, and to understand this, the primary step is to characterize the molecular alterations associated with this transition.

The conditions required for the induction of EMT typically are present in the inflammatory environment of most pancreatic tumors, such as release of cytokines like TGF-β, reorganization and expression of particular cytoskeletal proteins, hypoxia, production of extracellular matrix-degrading enzymes, and changes in the expression of specific microRNAs [26]. At the same time, several molecules can counter the process of EMT. BMP7 can reverse TGF-β induced EMT by expression of E-cadherin, and the expression of miR-200 family can prevent TGF-β-induced EMT [40, 41]. Not all cancer

cells undergo EMT, as most of the cancer cells in established pancreatic tumors have an epithelial morphology. Given the myriad routes of initiating EMT and the abundance of EMT-inducing factors in most pancreatic tumors, the question arises why only a subset of cancer cells undergo this process. One possibility is that only certain cells are predisposed to respond to the external factors, EMT could occur selectively in cells that harbor specific, enabling genomic alterations.

The most common mutations in pancreatic cancers are in KRAS, TP53, SMAD4, and CDKN2A [42-46], and other regions of genetic amplification and deletion frequently appear at multiple loci [47-53]. Such mutations likely contribute to the initiation of cancer and may not necessarily be involved in the progression of a subset of cells to an invasive and resistant phenotype. A study finding specific amplifications and deletions enriched in patients with venous invasion and shortened survival [54] points to genetic hits that affect cancer cell progression, similar to findings that amplifications at the 7q21-q22 locus involving the SMURF1 and ARPCIA genes promote cellular invasiveness [55, 56]. However, most of these studies identified genes that were altered in a very small subset of the cell lines/tissues being studied.

Here we examined the hypothesis that EMT derived mesenchymal cancer cells have distinct genetic alterations compared to their epithelial counterparts. Cultured pancreatic cancer cells provided a good model system to test this hypothesis, since they tend to take on either a mesenchymal-like or an epithelial phenotype. In this study we examined differences in gene copy number gains and losses using Comparative Genomic

Hybridization (CGH). Unlike previous studies, we aimed to identify only those genes that were altered in a significant number of the cell lines being examined. After the identification of candidates using cell lines, we validated for the presence of these alterations in primary tissues.

Materials and Methods

Cell culture

The pancreatic cell lines were obtained from the American Type Culture Collection (Manassas, VA) and passaged for fewer than 6 months after resuscitation. The cells were maintained in RPMI medium (Invitrogen, Carlsbad, CA) supplemented with 10% fetal bovine serum (FBS) and penicillin/streptomycin (Invitrogen). The three-dimensional cell cultures were performed in a 75:25 mixture of Matrigel (BD Biosciences, Bedford, MA) and DMEM media (Invitrogen) with a protocol similar to the 'thin gel method' advised by BD. The cells were recovered from the Matrigel using the Cell Recovery Solution (BD Biosciences) following the protocol supplied.

Flow cytometry

Pancreatic ductal adenocarcinoma samples were obtained under a WIRB protocol (20040832) for an NIH funded biospecimen repository (NCI P01 Grant CA109552). Biopsies were minced in the presence of NST buffer and DAPI according to published protocols. Briefly, nuclei were disaggregated then filtered through a 40 μm mesh prior to flow sorting with an Influx cytometer (Becton-Dickinson, San Jose, CA) with ultraviolet excitation. DAPI emission was collected at >450 nm. DNA content and cell cycle were analyzed using the software program MultiCycle (Phoenix Flow Systems, San Diego, CA).

Comparative Genomic Hybridization (CGH)

DNAs were extracted using Qiagen micro kits (Qiagen, Valencia, CA). For each hybridization, 1 µg of genomic DNA from each sample and 1 µg of pooled commercial 46XX reference DNA (Promega Corp., Madison, WI) were digested with DNaseI and labeled with Cy-5 dUTP and Cy-3 dUTP, respectively, using a BioPrime labeling kit (Invitrogen). All labeling reactions were assessed using a Nanodrop assay (Nanodrop, Wilmington, DE). We used Agilent 244K chips to obtain copy number data from the cell lines and patient samples as previously described [57].

Identification of genes with differential alterations

We averaged the $\log_{10}$ ratios of each probe within each group (X_{avg}) and then smoothed the values using a sliding window of 5 probes using the formula (X_{smooth} at probe N = 0.1*X_{avg} probe (N-2) + 0.2* X_{avg} probe (N-1) + 0.4* X_{avg} probe N + 0.2* X_{avg} probe (N+1) + 0.1* X_{avg} probe (N+2)), where probes N-2 to N+2 are adjacent on a chromosome. We filtered out probes showing low average levels of amplification or deletion by retaining probes with an absolute value of X_{smooth} > 0.3, indicating a two-fold change relative to the reference DNA. For subsequent analyses, we selected the probe from each gene with the highest fold change, using the non-smoothed values. We next calculated, for each probe, the percentage of cell lines in each group for which the probe had an absolute value > 0.3. We selected the probes that exceeded the 0.3 threshold in at least 50% of the cell lines in both group and that had at least a two-fold difference between the groups in the percentage of cell lines altered. For example, a probe that was altered (defined as greater than two-fold change) in 60% of the cell lines in one group and in

25% of the other group passed this criterion. We separately searched for probes altered in at least 50% of both groups.

Quantitative PCR validation of genomic amplifications and deletions

We extracted genomic DNA using the PrepEase genomic DNA isolation kit (Affymetrix, Santa Clara, CA) following the kit protocol, except using pipetting to homogenize cells instead of a homogenizer. We determined genomic DNA concentrations using UV absorption (Nanodrop, Thermo Scientific) with semi-quantitative confirmation by gel electrophoresis. Neuroblastoma Amplified Gene (NAG) protein from chromosome 2 was used as a loading control, as according to the CGH data it was in a region where none of the cell lines showed any major alteration. The primers were from Integrated DNA Technologies (Coralville, IA).

We used the Taq PCR Master Mix Kit (QIAGEN, Germantown, MD) to confirm the primer fidelity and performed gradient PCR to identify the optimum annealing temperature of 64□ C. Power SYBR Green PCR master mix (Life Technologies, Carlsbad, CA) was used for qPCR which was measured using the StepOne Plus RT-PCR system (Applied Biosystems, Carlsbad, CA). A standard curve was made for NAG using template DNA from the Su86.86 cell line to calibrate the data. The qPCR was performed twice to confirm reproducibility.

Correlation with gene expression

We used gene expression measurements from the Cancer Cell Line Encyclopedia (CCLE) project [58]. Gene expression data was available for 25 out of the 26 cell lines that were used in the study. In case of multiple probes (3 or more) for a particular gene, the correlation between the different probes was obtained. If correlation was above 0.75, the values were averaged. If a single probe did the correlate well with the other ones, the outlier was removed while averaging. In case of only two probes and a poor correlation, their correlation with copy numbers was calculated separately as in the case of M34428. We also performed reverse transcription PCR for five genes for which probes were not present in the chip. mRNA was extracted using RNeasy Mini Kit (Qiagen) and treated with DNase I to remove genomic DNA contamination (Thermo Scientific, Pittsburgh PA). Conversion to cDNA was done using the iScript select cDNA synthesis kit (BIO-RAD, Hercules, CA). A standard curve based on GAPDH expression was used to calibrate the expression levels of the genes. We calculated the significance of the correlation between gene expression and relative gene copy number using Microsoft Excel, with the formula $t = r \sqrt{((n-2)/(1-r^2))}$, where t is the value from the student's t distribution. Using the formula, it was found that r values greater than 0.34 were significant at $p<0.05$.

Hierarchical Clustering

To account for bias, hierarchical clustering was performed on the gene expression data from the Cancer Cell Line Encyclopedia (CCLE) Project. The gene expression data was

logged to the base 2 and then mean centered before clustering using average linkage and Euclidean distance.

Results

Genomic differences between epithelial-like and mesenchymal-like cell lines

In order to test the hypothesis that specific genomic changes are more prevalent in pancreatic cancer cells with a mesenchymal-like phenotype, we classified 26 different pancreatic cancer cell lines into either an epithelial group (n = 17) or a mesenchymal-like (n = 9) group (Table 1). We observed molecular and morphological diversity between the cell lines and classified most of the cell lines into one of these broad categories, as in a previous study [59]. We based the classification on morphology and expression levels of E-cadherin, vimentin, and ZEB1, which we obtained from gene expression experiments or published information (Table 1). In cases where we did not have gene expression measurements for the molecular markers, we based the classification on the state of apical-basolateral organization, judging that mesenchymal-like cells typically lose such organization [60]. We found that the cell lines showed correspondence between 2D and 3D cultures in morphology and E-cadherin expression (Figure 1), a result that agrees with previous findings using xenografts [61]. This result supports the use of phenotypes in 2-D cell cultures as a means of classification. We also asked whether whole-genome expression profiling would reveal major differences between the cell lines that might represent a more accurate or natural way to group the cells. Un-supervised clustering resulted in no coherent grouping among the cells (Figure 2A), indicating that the cell lines do not have fundamental differences that result in genome-wide transcriptional differences. But when we clustered the cells using only 20 genes involved in EMT [62], the cell lines segregated generally according to our

classification (Figure 2B), confirming a transcriptional difference relating to their mesenchymal-like and epithelial phenotypes.

We obtained measurements of relative genomic amplifications and deletions for each cell line using a 244K-probe microarray with an average spatial resolution of approximately 8.9kb. We then tested whether the mesenchymal-like cells harbored particular genomic alterations more frequently than the epithelial-like cells. We initially used the student's t-test to identify regions with significantly different levels between the groups but found the method insufficient to distinguish meaningful from irrelevant information, mainly because the test does not include a threshold for minimum level of amplification or deletion. For example, the TTN gene on chromosome 2 was significantly different between the groups ($p < 0.0001$), but none of the individual cell lines showed major amplification or deletion for that probe (defined as a two-fold change relative to the reference DNA) (Figure 3).

Therefore, we based our search on the percentage of cell lines in each group with significant amplifications or deletions, searching for regions that were altered frequently in one group but not the other. First we selected the probes with high average levels of amplifications or deletions, and we then searched for probes with differences between the epithelial and mesenchymal-like groups in frequency of amplification or deletion. For the first step we chose probes with at least an average two-fold amplification or deletion in either group, resulting in 783 probes spanning 72 genes. For each gene, we found the probe with the highest average alteration (Table 2) and calculated the difference

between the groups in the percentage of cell lines showing either amplification or deletion of that probe. We searched for probes with at least a two-fold difference between the groups in frequency of alteration and at least 50% alteration in either of the groups. We also required the immediately adjacent probes on either side to be affected in the same direction as the probe being tested. We used these stringent criteria in order to identify the loci that have the highest likelihood of functional contributions to the mesenchymal-like phenotype.

The search returned 20 genes (Figure 4A, Table 3). All of the 20 alterations were more prevalent in the mesenchymal-like group. This highly non-random, preferential enrichment suggested either that the mesenchymal-like pancreatic cancer cells have evolved beyond the epithelial pancreatic cancer cells or that they have acquired more total genomic alterations. The total number of altered probes was not significantly different between the two groups (Figure 4B), supporting the former proposition. Furthermore, 18 of the 20 alterations were deletions. The total number of amplifications and deletions were similar to each other (Figure 4B), suggesting a higher selection for deletions in the mesenchymal-like cells (Figure 4C).

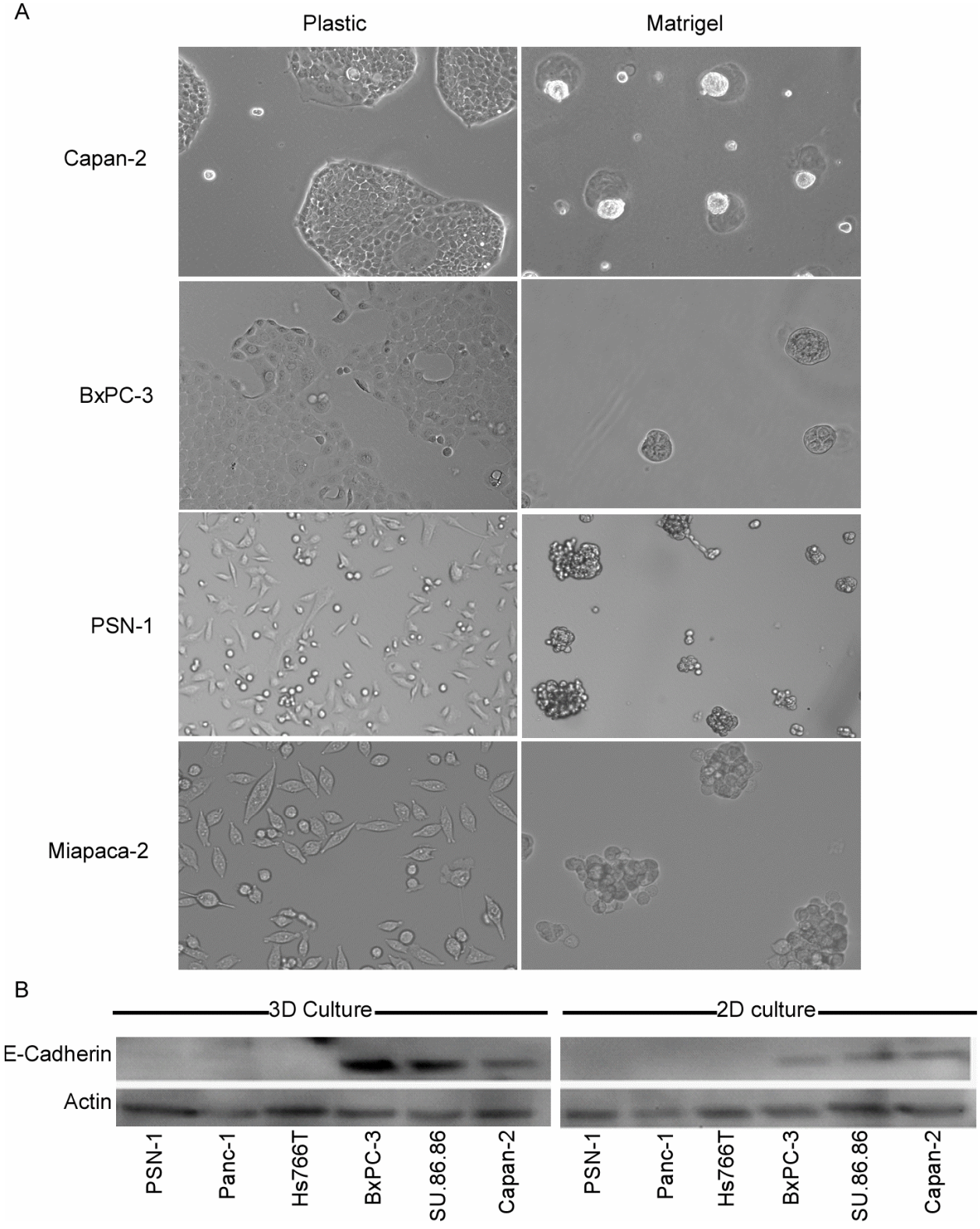

Figure 1. Morphology of cell lines in 2D & 3-D cultures. (A) Morphology of cell lines in 2D (Plastic) and 3D (Matrigel) cultures. (B) E-Cadherin levels for cells grown in 2D and 3D cultures with Actin as control.

Table 1. Classification of the cell lines. The column called "Classification Basis" gives the basis used to classify the cells. The epithelial cells generally had higher E-cadherin, lower vimentin, lower zeb-1, and epithelial-like morphology. In some cases the classification was based on other traits as indicated

Cell line	Classification Basis	References	Origin of tissue	Classification
BxPC-3	E-cadherin (E-cad), Vimentin (Vim), Zeb1, Morphology	[59]	Primary	Epithelial
Capan1	E-cad, Vim, Zeb1	[63, 64]	Metastasis (liver)	Epithelial
Capan-2	E-cad, Vim, Zeb1	[59, 63]	Primary	Epithelial
DAN-G	Morphology	[65, 66]	Primary	Epithelial
HPAC	E-cad, Vim, Zeb1	[63, 64]	Primary	Epithelial
HPAF-II	E-cad, Vim, zeb1	[63, 64]	Metastasis (ascites)	Epithelial
HUP-T4	Morphology	[67]	Metastasis (ascites)	Epithelial
KC1-MOH1	Morphology, Susceptibility to drugs	[68-70]	Primary	Epithelial
Panc02.03	Vim, E-cad, Zeb1	[59, 64]	Primary	Epithelial
Panc03.27	Vim, E-cad, Zeb1	[59, 64]	Primary	Epithelial
Panc04.03	E-cad, vim, Zeb1	[64, 71]	Primary	Epithelial
Panc05.04	Vim, E-cad, Zeb1	[59, 64]	Primary	Epithelial
Patu8902	E-cad, Morphology	[72-74]	Primary	Epithelial
Patu8988T	Polar cells with apical-basolateral organization	[75]	Metastasis (Liver)	Epithelial
Su86.86	Vim, E-cad, Zeb1	[59, 64]	Metastasis (Liver)	Epithelial
SW1990	Morphology	[76]	Primary/ Metastasis (spleen)	Epithelial
YAPC	Morphology, moderate-poorly differentiated tumors formed *in vivo*	[77]	Metastasis (ascites)	Epithelial
Aspc1	E-cad, Zeb1, Vim	[59]	Metastasis (ascites)	Mesenchymal-like
Hs700T	Poorly differentiated tumors formed *in vivo*, Morphology	[64, 78]	Metastasis (pelvis)	Mesenchymal-like
Hs766T	E-cad, Zeb1, Vim	[59]	Metastasis (Lymph node)	Mesenchymal-like

Table 1 (cont'd)

Hup-T3	Poorly differentiated tumor formed in vivo	[67]	Metastasis (ascites)	Mesenchymal-like
Miapaca-2	E-cad, Zeb1, Vim	[59]	Primary	Mesenchymal-like
Panc-1	E-cad, Zeb1, Vim	[59]	Primary	Mesenchymal-like
Panc8.13	E-cad, Zeb1, Vim	[59]	Primary	Mesenchymal-like
Patu8988s	No apical-basolateral organization	[75]	Metastasis (Liver)	Mesenchymal-like
PSN-1	E-cad, Zeb1, Vim	[71]	Primary	Mesenchymal-like

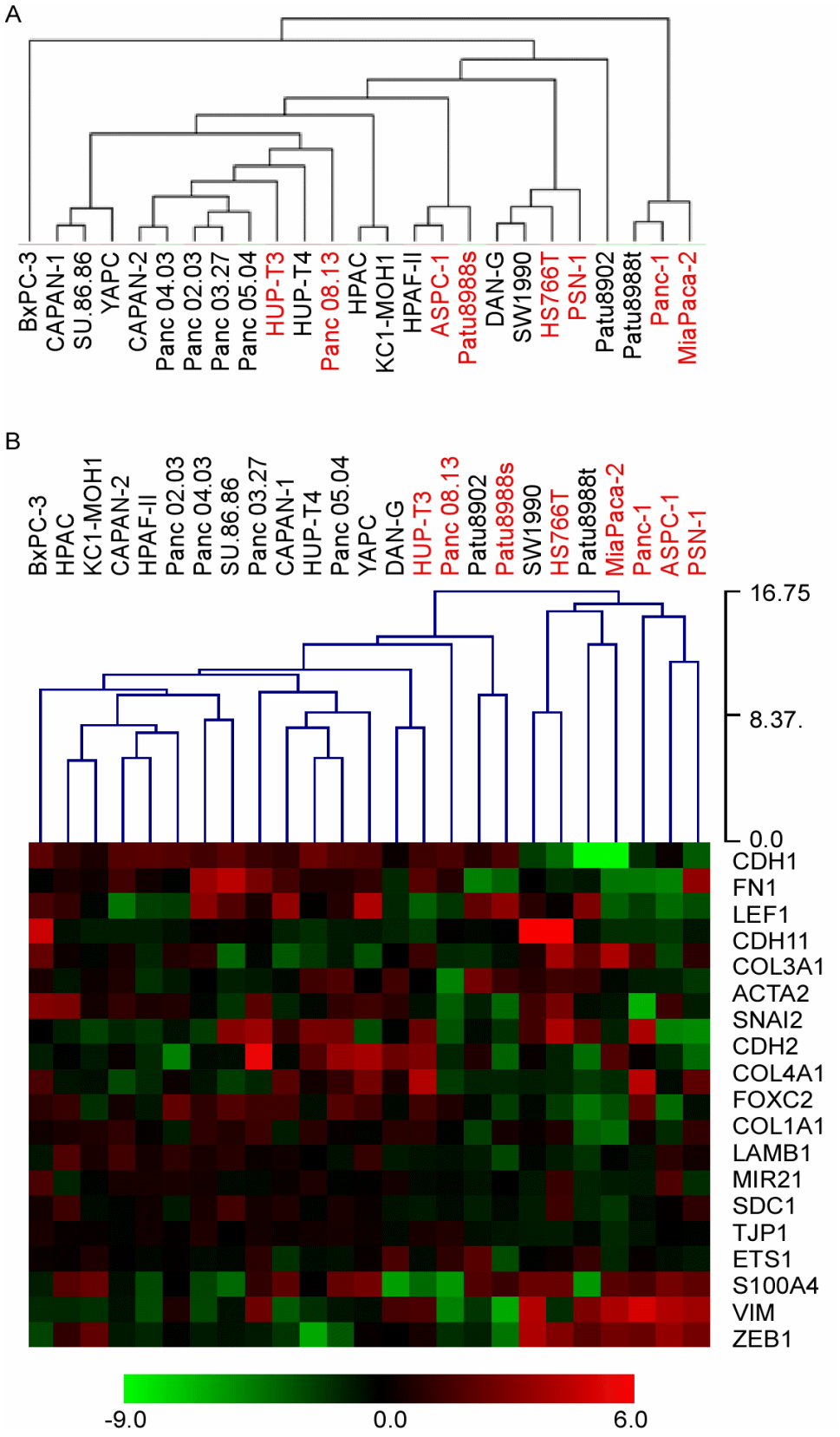

Figure 2. Hierarchical Clustering.

Figure 2. (cont'd) Euclidean distance and average linkage were used for clustering. The cell lines that we had classified as mesenchymal-like are marked in red. (A) Clustering based on the entire genome expression. (B) Clustering based on expression of 20 genes with functions related to the epithelial-mesenchymal transition. Using the whole genome, the cell lines do not segregate according to our classification, but using the 20 genes, the cells classified as mesenchymal-like mainly fall in the right branch.

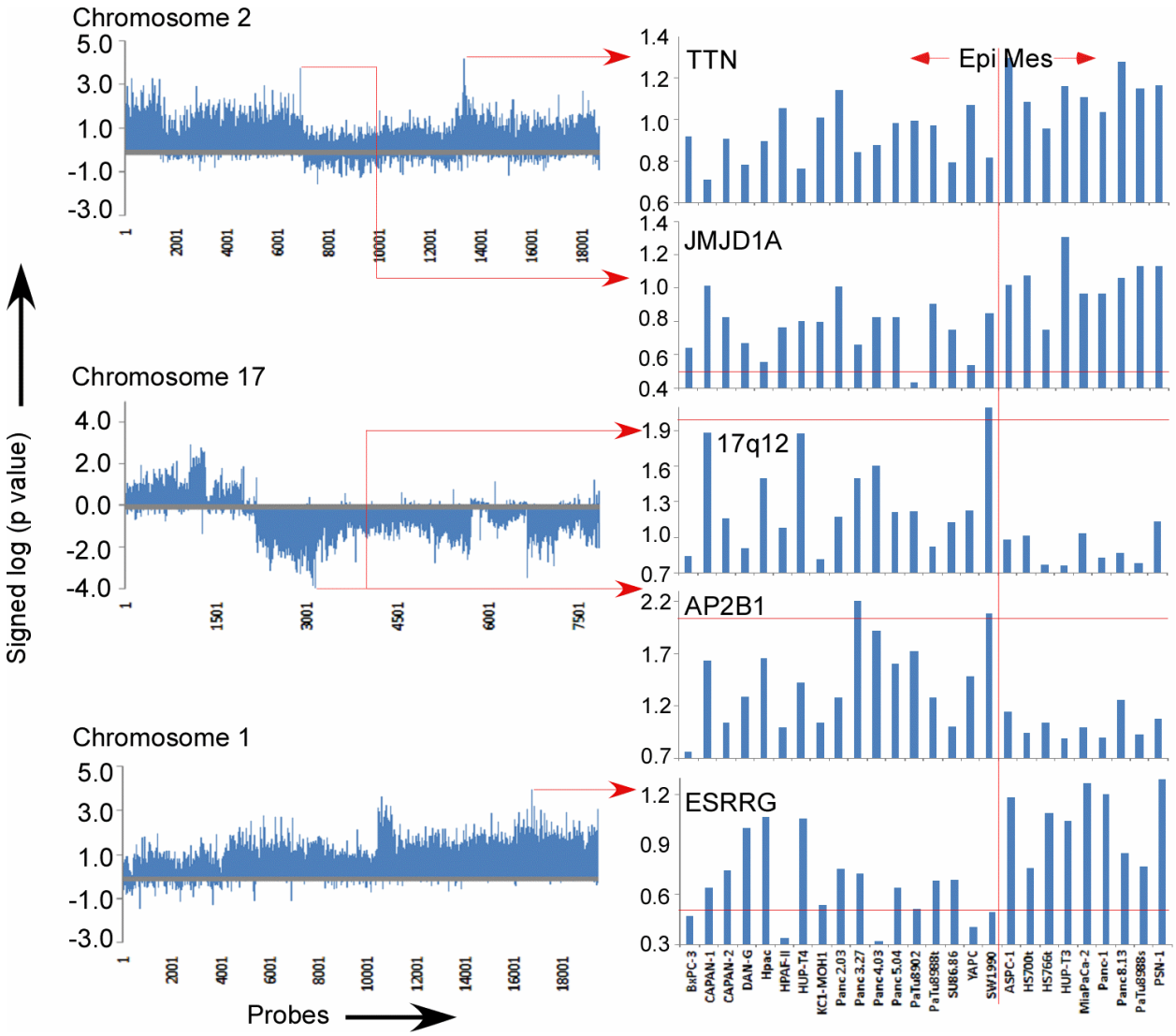

Figure 3. Top hits based on t-test comparisons. The graphs show the logged p values of the comparison of CGH ratios between the mesenchymal-like and epithelial cells, for each probe on a chromosome. The logged p values were signed based on the difference between the Mesenchymal (Xavg) - Epithelial (Xavg). Positive values indicate the mesenchymal-like cells had a higher average raw value at a given probe, and vice versa. The right graphs show the unlogged raw CGH values for 5 probes in all cell lines. An alteration was classified as a value below 0.5 or above 2.

Table 2. Genes with the highest average alterations. The 73 genes that have an average alteration of 2-fold (raw value of +/- 0.3) or more in either group. The table presents the percentage of cell lines in each group that have a greater than 2-fold change for each gene. The percentages in columns 3 and 4 have been rounded off as per the confidence level based on the number of samples. The ratio between the groups has been calculated based on the unrounded percentages.

Chromosome	Gene	% epithelial cells showing the change	% mesenchymal-like cells showing the change	direction of change	probe	Ratio of mes/epi
8p22	SGCZ	10	60	Deletion	A_16_P18225623	9.4
8p23	AF123758	10	40	Deletion	A_16_P38280697	7.5
8q24	CR593328	10	40	Amplification	A_16_P02022039	7.5
8q24	BC033263	10	30	Amplification	A_16_P18482483	5.6
14q32	AF103097	10	60	Deletion	A_16_P02991441	4.7
8q24	DQ515897	10	60	Amplification	A_16_P18480870	4.7
8q24	M34428	10	60	Amplification	A_16_P02020073	4.7
8p22	AK022085	10	40	Deletion	A_16_P18226867	3.7
17p12	ZNF18	10	20	Deletion	A_16_P20589123	3.7
8q24	MYC	10	40	Amplification	A_14_P128991	3.7
9p21	KIAA1797	20	70	Deletion	A_16_P02074946	3.7
9p21	PTPLAD2	20	70	Deletion	A_16_P38673538	3.7
9p22	MLLT3	20	60	Deletion	A_16_P18575142	3.1
9p21	IFNB1	20	70	Deletion	A_14_P124911	2.8
9p22	IFNW1	20	70	Deletion	A_14_P131521	2.8
8q24	AY423624	10	30	Amplification	A_16_P18485764	2.8
8q24	BC042052	20	40	Amplification	A_16_P38576934	2.5
8q24	M13930	20	40	Amplification	A_14_P123915	2.5
8q24	M34429	20	40	Amplification	A_16_P18482128	2.5
9p22	VOO541	20	60	Deletion	A_14_P116804	2.3
9p21	CR627240	20	60	Deletion	A_16_P18581686	2.3
18q21	DCC	20	60	Deletion	A_16_P20866259	2.3
9p23	PTPRD	20	60	Deletion	A_16_P18547744	2.3
18q21	MBD2	20	60	Deletion	A_16_P20867858	2.3
8p22	TUSC3	30	70	Deletion	A_16_P18226308	2.2
9p22	KLHL9	30	70	Deletion	A_16_P02075542	2.2

Table 2 (cont'd)

9p21	AK124391	30	70	Deletion	A_16_P18577258	2.2
9p21	DMRTA1	30	70	Deletion	A_16_P02077035	2.2
18q21	ME2	30	70	Deletion	A_16_P41038127	2.2
18q21	SMAD4	30	70	Deletion	A_16_P20859969	2.2
9p21	ELAVL2	20	40	Deletion	A_16_P38679859	1.8
20q13	RTEL1	30	60	Amplification	A_16_P21187557	1.8
6q27	AK054947	30	60	Deletion	A_16_P37885906	1.8
9p21	IFNE1	40	70	Deletion	A_14_P101271	1.8
9p21	MTAP	40	70	Deletion	A_14_P117235	1.8
9p21	AK092601	40	70	Deletion	A_16_P18579907	1.8
18q21	ELAC1	40	70	Deletion	A_16_P03366717	1.8
9p21	AF109294	50	80	Deletion	A_14_P121053	1.6
9p21	AF083893	50	80	Deletion	A_16_P38738180	1.6
20q13	NFATC2	40	70	Amplification	A_16_P03531547	1.6
9p22	IFNA2	40	60	Deletion	A_14_P104948	1.5
18q21	BC029860	40	60	Deletion	A_14_P128654	1.5
8p23	CSMD1	50	80	Deletion	A_16_P01853282	1.4
9p21	CDKN2A	50	80	Deletion	A_14_P130650	1.4
22q11	AF336885	20	30	Deletion	A_16_P41491689	1.4
22q11	GSTT1	20	30	Deletion	A_16_P03605972	1.4
9p22	IFNA8	20	30	Deletion	A_14_P109107	1.4
9p21	AK093337	20	30	Deletion	A_14_P104894	1.4
9p21	BC043546	20	30	Deletion	A_16_P18587085	1.4
9p21	AK131322	50	70	Deletion	A_16_P02081957	1.4
18q22	DOK6	40	60	Deletion	A_16_P41086213	1.3
4q22	AB051467	40	60	Deletion	A_14_P131750	1.3
9p22	IFNA14	40	40	Deletion	A_16_P38674029	1.2
9p21	CDKN2B	50	70	Deletion	A_14_P118440	1.2
18q21	RKHD2	40	40	Deletion	A_16_P03367007	1.2
3p21	SCAP	50	60	Deletion	A_16_P16213985	1.1
3q26	BC019327	60	70	Deletion	A_16_P16480002	1.1
4q13	U06641	40	30	Deletion	A_16_P16716224	0.9
6p21	HLA-DRB5	80	70	Deletion	A_16_P17499927	0.8

Table 2 (cont'd)

18q22	CBLN2	50	40	Deletion	A_14_P138114	0.8
6p22	IBRDC2	70	60	Deletion	A_16_P01433929	0.7
9q13	AY098593	70	60	Deletion	A_16_P02099251	0.7
1q21	BC130365	60	40	Deletion	A_14_P100633	0.7
8p23	AK125470	80	60	Deletion	A_16_P01847382	0.7
4q34	GALNT17	60	40	Deletion	A_16_P16956857	0.6
9p21	LRRN6C	40	20	Deletion	A_16_P18593657	0.6
9p21	BC022036	20	10	Deletion	A_16_P18598148	0.6
3p14	FHIT	40	20	Deletion	A_16_P16245334	0.5
18q21	AK094936	60	30	Deletion	A_16_P20860768	0.5
18q23	BC016792	40	20	Deletion	A_16_P20928766	0.5
8p23	ARHGEF10	0.0	40	Deletion	A_16_P01849285	
17p12	MAP2K4	0.0	20	Deletion	A_16_P03215681	

Table 3. Genes with alterations that are selectively enriched in one of the groups. Genes present in more than 50% of cell line in 1 group with 2 fold enrichment in mutation rate between the groups. The percentages in columns 5 and 6 have been rounded off as per the confidence level based on the number of samples. The M/E ratio has been calculated based on the unrounded percentages.

CHR	Gene	Entrez Gene ID	Probe ID	% Epithelial cells showing alteration	% Mesenchymal-like cells showing alteration (M)	M / E	Type of Alteration
8p22	SGCZ	SGCZ(137868)	A_16_P18225623	10	60	9.4	Deletion
8q24	M34428	PVT1(5820)	A_16_P02020073	10	60	4.7	Amplification
8q24	DQ515897	CASC8(727677)	A_16_P18480870	10	60	4.7	Amplification
14q32	AF103097		A_16_P02991441	10	60	4.7	Deletion
9p21	KIAA1797	FOCAD(54914)	A_16_P02074946	20	70	3.8	Deletion
9p21	PTPLAD2	PTPLAD2(401494)	A_16_P38673538	20	70	3.8	Deletion
9p22	MLLT3	MLLT3(4300)	A_16_P18575142	20	60	3.1	Deletion
9p21	IFNB1	IFNB1(3456)	A_14_P124911	20	70	2.8	Deletion
9p22	IFNW1	IFNW1(3467)	A_14_P131521	20	70	2.8	Deletion
9p21	CR627240	LOC101929563 (101929563)	A_16_P18581686	20	60	2.4	Deletion
9p22	V00541	IFNA5(3442)	A_14_P116804	20	60	2.4	Deletion
8p22	TUSC3	TUSC3(7991)	A_16_P18226308	30	70	2.3	Deletion
9p21	DMRTA1	DMRTA1(63951)	A_16_P02077035	30	70	2.3	Deletion
9p21	AK124391	MIR31HG(554202)	A_16_P18577258	30	70	2.3	Deletion
9p22	KLHL9	KLHL9(55958)	A_16_P02075542	30	70	2.3	Deletion

Table 3 (cont'd)

9p23	PTPRD	PTPRD(5789)	A_16_P18547744	20	60	2.3	Deletion
18q21	ME2	ME2(4200)	A_16_P41038127	30	70	2.3	Deletion
18q21	SMAD4	SMAD4(4089)	A_16_P20859969	30	70	2.3	Deletion
18q21	DCC	DCC(1630)	A_16_P20866259	20	60	2.3	Deletion
18q21	MBD2	MBD2(8932)	A_16_P20867858	20	60	2.3	Deletion

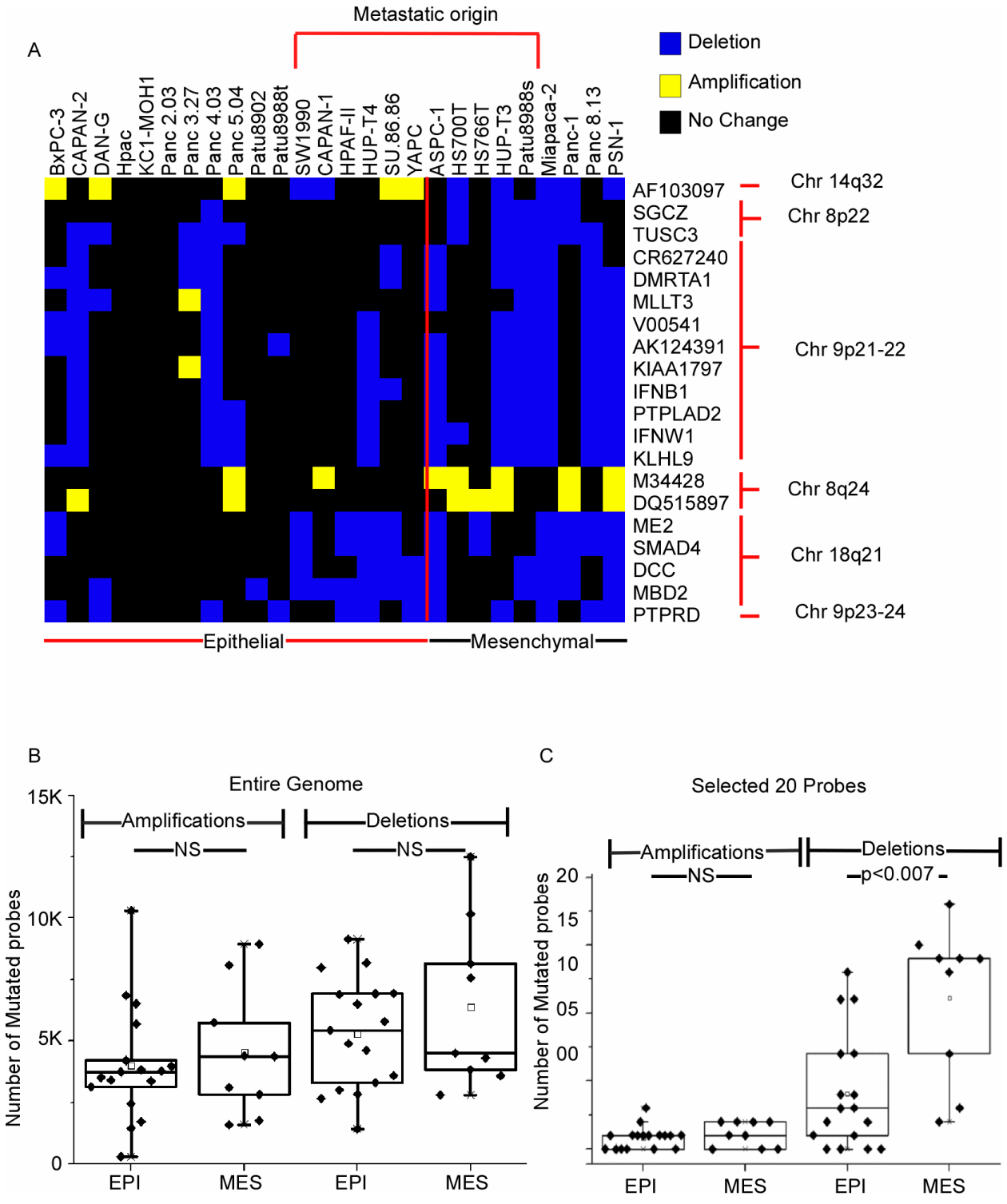

Figure 4. Enriched deletions and amplifications in mesenchymal-like cancer cells. (A) Patterns of amplification and deletion among the most-altered 20 genes. For each gene (given in the row labels) and each cell line (given in the column labels), a blue square indicates deletion, a yellow square indicates amplification, and a black square indicates no change. A clustering algorithm grouped the rows by similarity in pattern.

Figure 4. (cont'd) (B) Total numbers of amplified or deleted probes in each group for the entire genome. (C) Total numbers of amplified or deleted probes in each group for the 17 hits. Each point represents a cell line. EPI, epithelial cell lines; MES, mesenchymal-like cell lines.

The alterations were confined to chromosomes 9 (11 deletions), 18 (4 deletions), 8 (2 amplifications and 2 deletions), and 14 (1 gene showing amplification in the mesenchymal-like group and deletion in the epithelial group). Some cell lines were exceptions to the general trends, like Hs766t, which we classified as mesenchymal-like but had an alteration in only three of the 20 genes (Figure 4A). Such exceptions might result from imperfect classification or diversity in genetic alterations resulting in similar phenotypes. The Hs766t cell line in particular was harder to classify because morphologically it appears somewhat epithelial but has certain molecular characteristics that are mesenchymal-like. Some of the epithelial cells had been derived from a metastatic site and therefore may previously have displayed mesenchymal-like characteristics but returned to the epithelial state via the process of mesenchymal-epithelial transition [79]. Two of the five epithelial cell lines derived from metastatic lesions showed alterations that were akin to the mesenchymal-like cells as opposed to the epithelial cells (Figure 4A). None of the 20 genes, nor their chromosomal regions, was among those previously associated with adaptation to *in vitro* culture conditions [80-83], suggesting that the mutations did not occur after the cells were cultured.

We asked whether the identified mutations were focal or broad when averaged over the cell lines, which may give information about which loci are important functionally. Chromosomes 8, 14, and 9 showed divergent patterns (Figure 5). The deletions of chromosome 8 were clustered in the p arm, whereas the amplifications were clustered in the q arm. In contrast, chromosome 14 showed no clustering but a narrow alteration at the putative gene AF103097, unusual because it was both deleted in the

mesenchymal-like cells and amplified in the epithelial cells. However, not all the probes spanning AF103097 were amplified, so the implication of this change is not evident yet. The deletions of chromosome 9 were clustered on the p arm. The rest of the chromosomes show varying sizes of amplifications and deletions (Figure. 6, 7). The other differences between the mesenchymal-like and epithelial cells (Figure 8) are not as significant as those noted above.

This deletion on chromosome 9p includes the tumor suppressor CDKN2A, suggesting that the alterations neighboring CDKN2A might be passenger mutations. Indeed, in no cases were the identified genes on chromosome 9 deleted when CDKN2A was not (Figure 9). However, neighboring deletions were more frequent in the mesenchymal-like cells, whereas deletions specific to CDKN2A were evenly spread among the epithelial and mesenchymal-like cells (Figure 9). This relationship suggests that the size of the deletion of the CDKN2A locus may affect cell phenotype; loss of CDKN2A promotes tumor formation, but the co-deletion of certain neighboring genes may promote cancer plasticity and invasiveness.

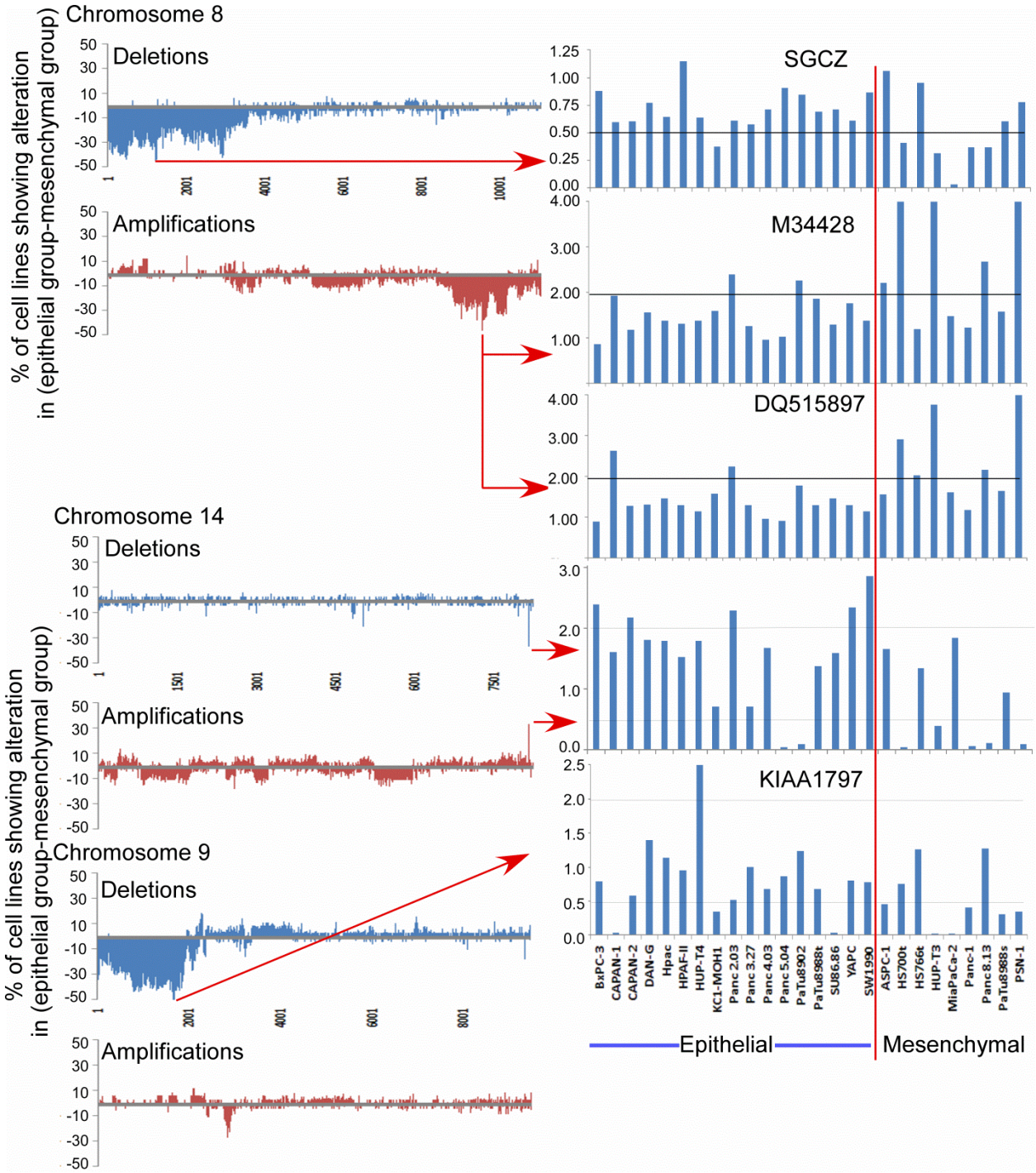

Figure 5. Rates of alterations of selected genes. For each probe, we calculated the difference between the epithelial group and the mesenchymal-like group in the percentage of cell lines showing a deletion or amplification. We smoothed the resulting numbers by a sliding window of 5 probes, using the formula (0.1* probe X-2) + (0.2*probe X-1) + (0.4*probe X) + (0.2* probe X+1) + (0.1* probe X+2), prior to plotting data from all probes for chromosomes 8, 14, and 9. The column graphs at right show the raw CGH values for selected genes across all cell lines.

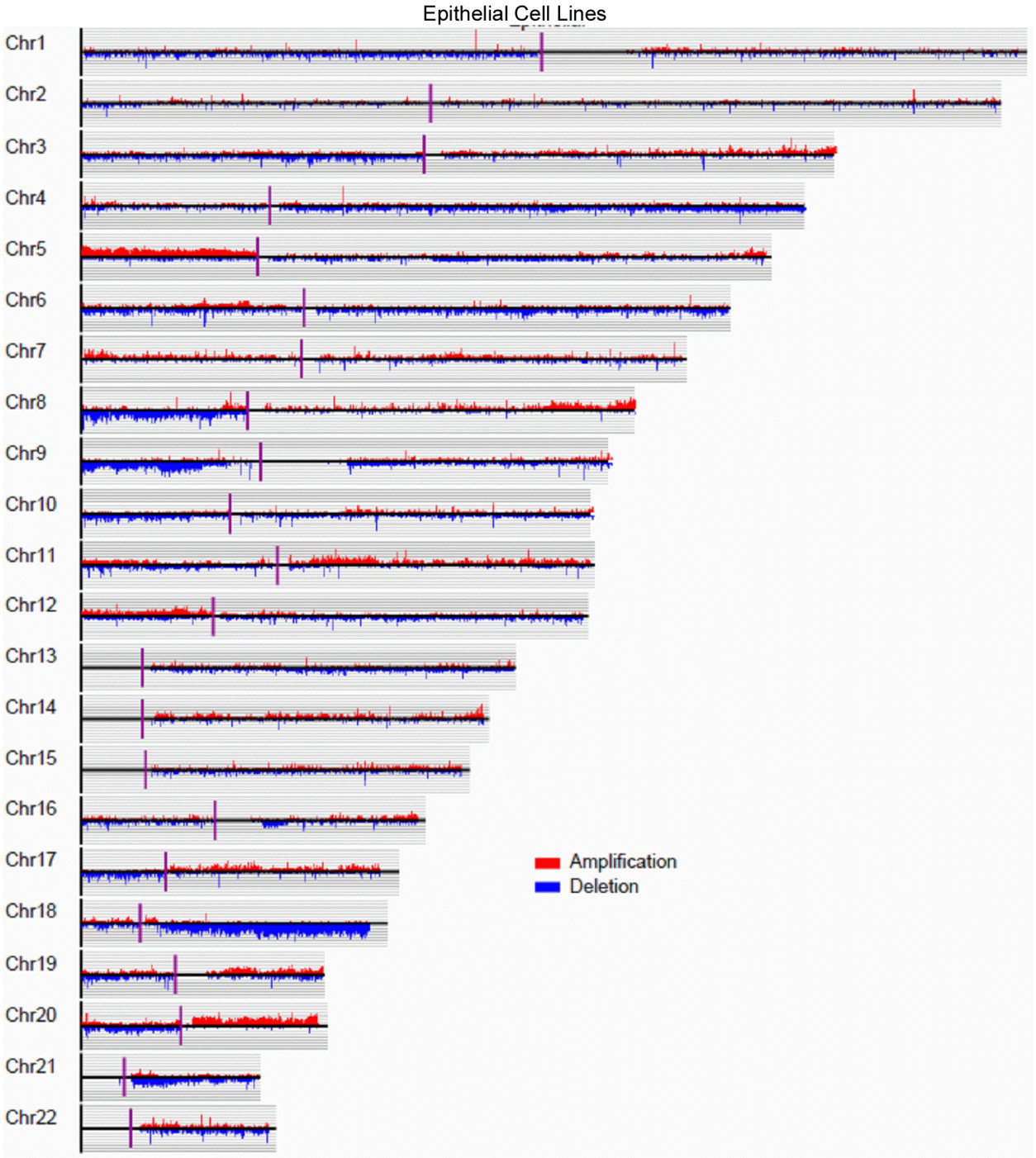

Figure 6. Distribution of altered probes throughout the genome for epithelial cell lines. The raw values (log10) were averaged over all epithelial cell lines for each probe. Probes with an average change of 2-fold or greater relative to the reference DNA were plotted. The y-axis indicates the percentage of number of cell lines showing the alteration.

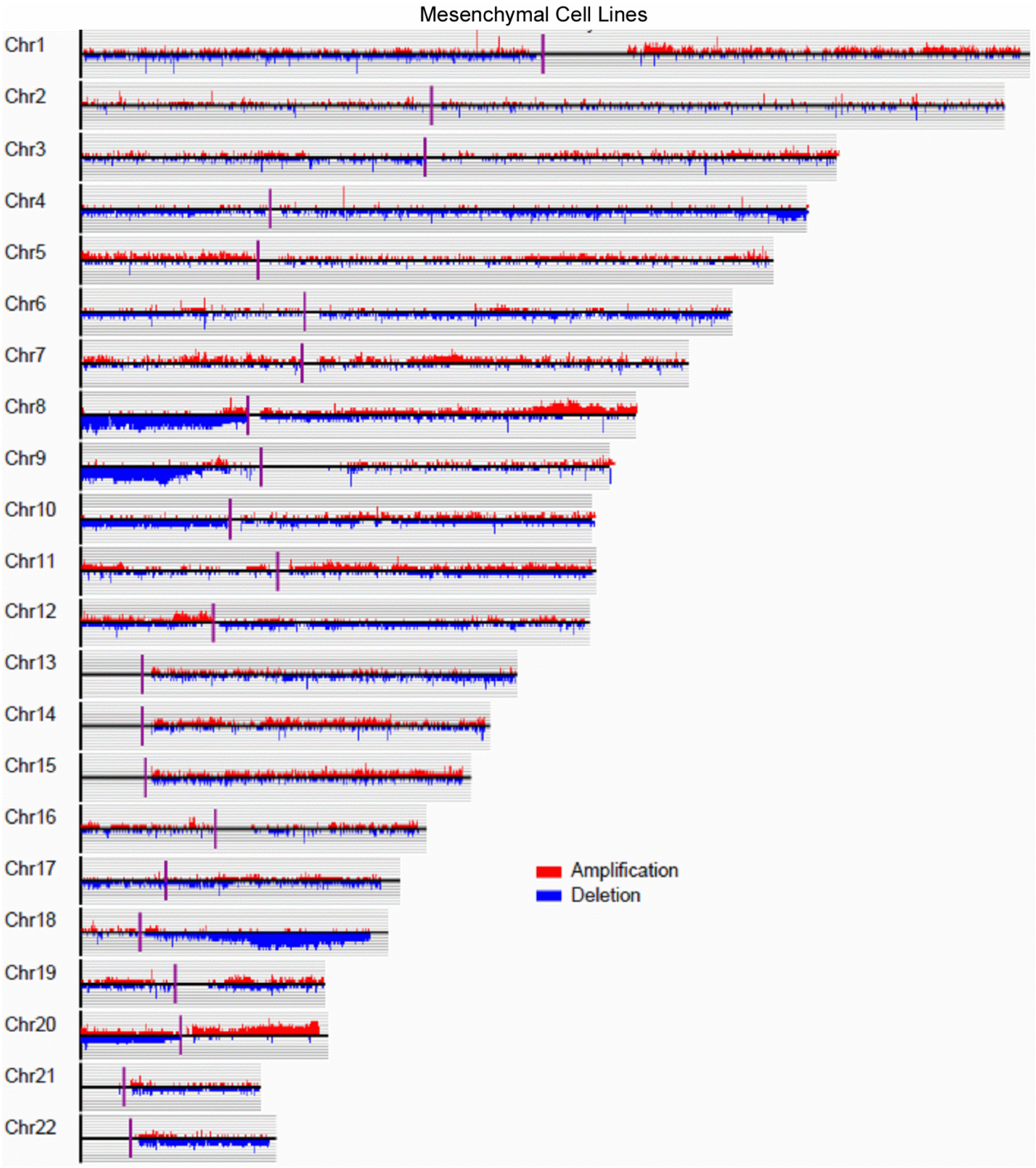

Figure 7. Distribution of altered probes throughout the genome for mesenchymal-like cell lines. The raw values (log10) were averaged over all mesenchymal-like cell lines for each probe. Probes with an average change of 2-fold or greater relative to the reference DNA were plotted. The y-axis indicates the percentage of number of cell lines showing the alteration.

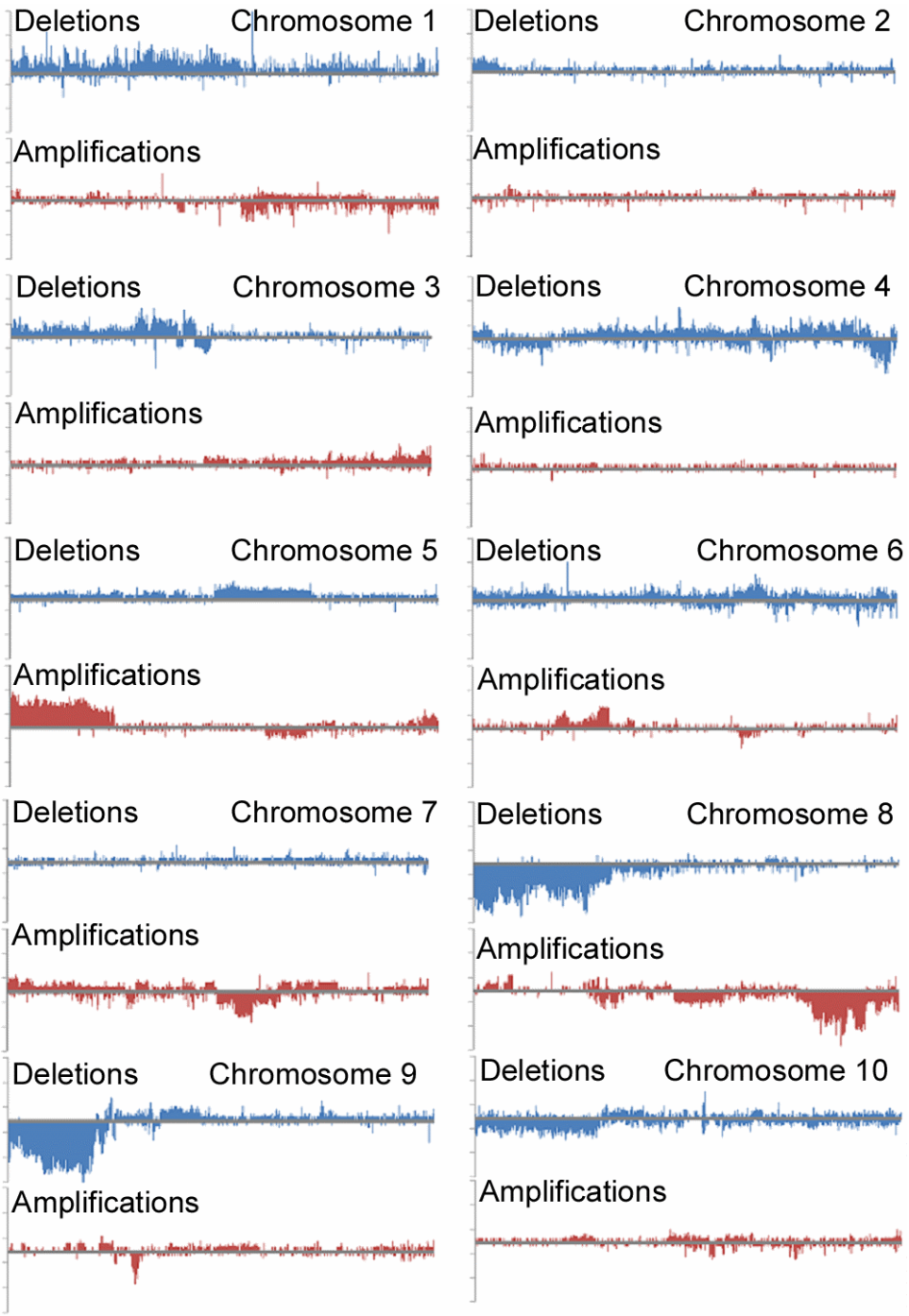

Figure 8. Difference in the incidence of mutations between the epithelial and mesenchymal-like cell lines. The y-axis indicates the difference between the epithelial and mesenchymal-like cells in the percentage of cell lines within each group showing an alteration. A positive value means the mutation at that probe is more prevalent in the epithelial cells whereas a negative value is indicative of probes in the mesenchymal-like cells being more frequently deleted.

Figure 8 (cont'd)

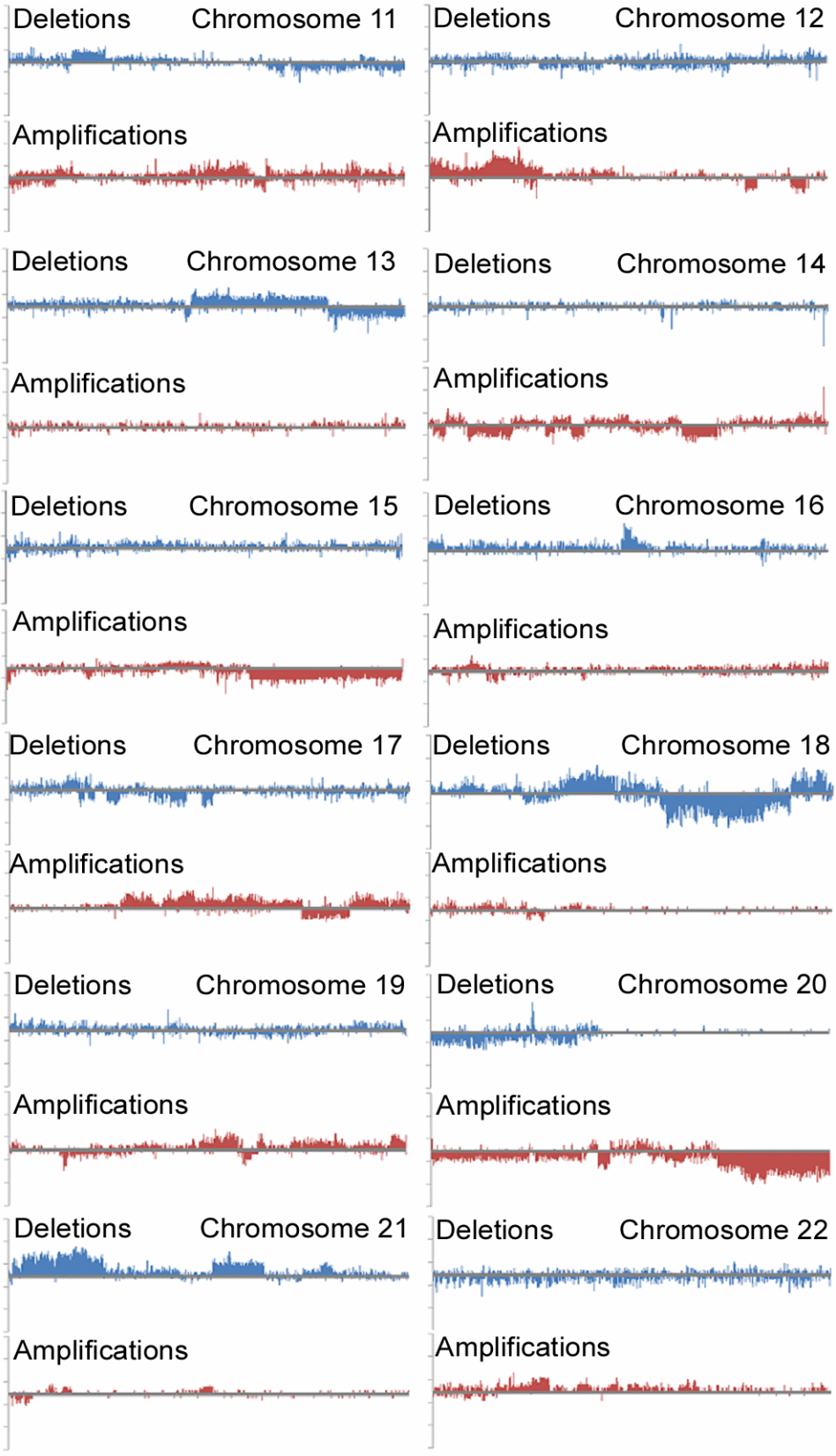

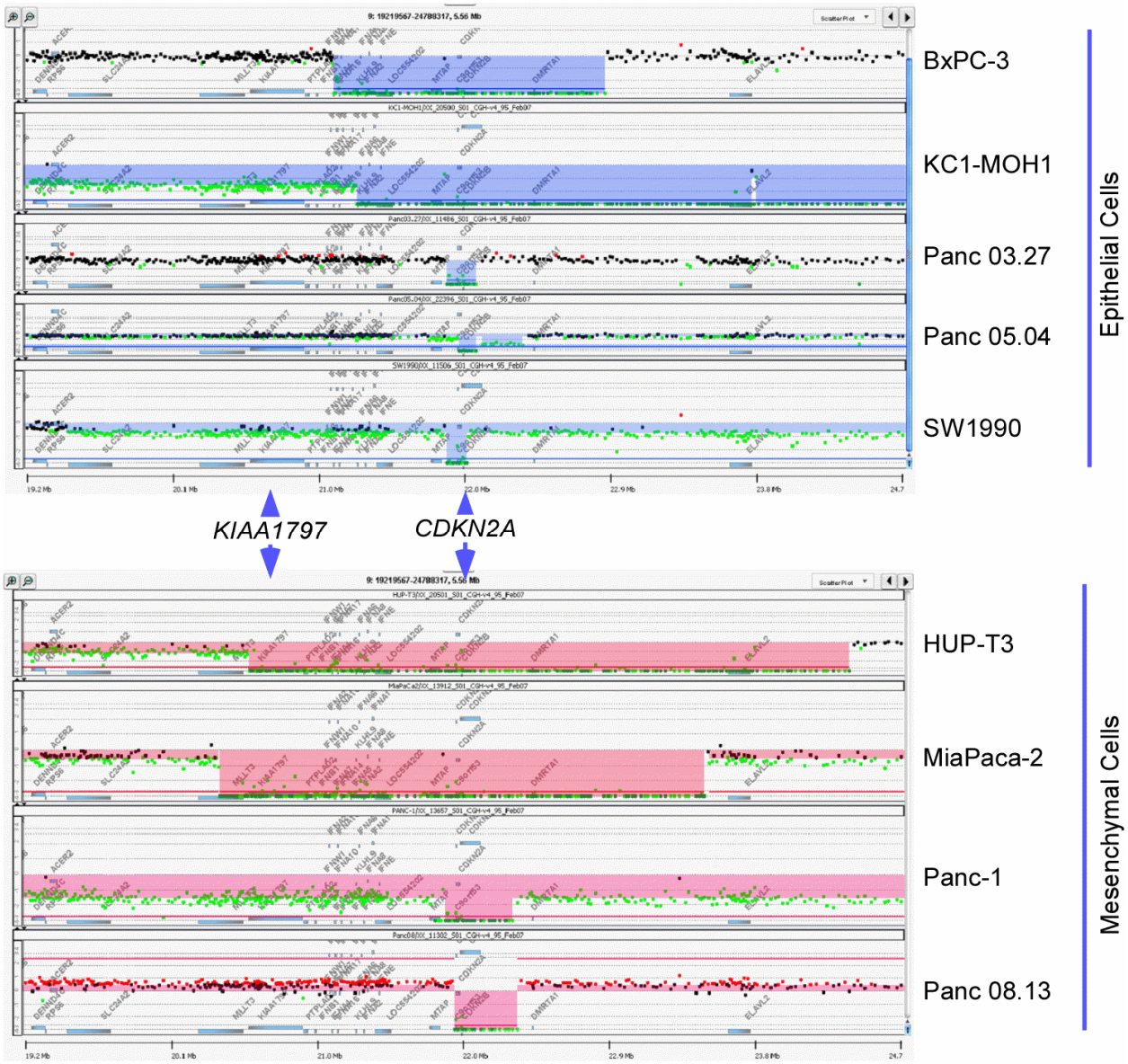

Figure 9. Detailed view of chromosome 9. The highlights indicate regions of deletion in selected epithelial-like cell lines (top) and mesenchymal-like cell lines (bottom). Each point represents data from one probe. The arrows indicate the locations of the KIAA1797 and CDKN2A genes. Note that deletion of CDKN2A is common to all cell lines but that the co-deletion of KIAA1797 is more common in the mesenchymal-like cells.

Genomic alterations common to both groups

To further understand the relationships between all the cell lines in their genomic alterations, we also searched for genes that were altered across both groups with high frequency (at least 50% in each group). Only CDKN2A and CDKN2B were altered in both groups (Table 4), and both were deletions. CDKN2A, also known as P16, is a well-known tumor suppressor and one of the most frequently deleted genes in pancreatic tumors [13, 43, 44, 84]. CDKN2B encodes a cyclin-dependent kinase inhibitor and is a potential effector of TGF-β induced cell cycle arrest [85]. The identification of these two genes is consistent with previous research showing that the most common genetic hits are in tumor suppressors or oncogenes.

Table 4. Alterations common to both mesenchymal-like and epithelial cells. The table presents the genes that were altered in greater than 50% of the cell lines in both the groups. The percentages in columns 5, 6 and 7 have been rounded off as per the confidence level based on the number of samples.

Chromosome	Gene	Entrez Gene ID	Probe Id	% Epithelial cells showing alteration	% Mesenchymal cells showing alteration	Total cells showing alteration	Type of Alteration
9	CDKN2A	CDKN2A(1029)	A_14_P130650	50	80	60	Deletion
9	CDKN2B	CDKN2B(1030)	A_14_P118440	50	70	60	Deletion

Well-known alterations associated with pancreatic cancer, such as MYC amplification, were present in the initial selection of 72 genes (Table 2) but were not included in the final list of 20 genes due to a prevalence of less than 50% in both groups. Other well-

known pancreatic cancer associated genes such as KRAS and TP53 did not show up in the final lists because they typically are affected by point mutations and low copy number aberrations.

Validation of selected copy number changes

We selected at least one gene from each chromosome for validation by qPCR of the alterations found by CGH. We confirmed the integrity of the genomic DNA from the cell lines by gel electrophoresis and normalized the qPCR measurements to NAG, which was within a region of minimum genomic alteration. The qPCR data correlated well with the CGH data for the genes KIAA1797, TUSC3, AF103097, M34428 and SMAD4 (Figure 10). To further test the validity of our findings, we compared the alterations found here to the ones identified in a previous CGH analysis of pancreatic cancer cell lines [47], which shared 14 cell lines in common with our study. Of the 34 genes that were altered in the previous study, all but one was altered in the matched cell lines of this study. We did not find an amplification of STK19 in the SW1990 cell line, for which our analysis only had one probe.

Another test of validity is to randomly permute the grouping and repeat the analysis. We asked, would we achieve similar results with just any grouping of cell lines? We segregated the 26 cell lines into random groups of 17 (group A) and 9 (group B) and performed the exact same analysis as before, searching for genes that were consistently altered in one of the groups, and we then repeated the random grouping and analysis five separate times. For each of the random groupings, we did not see

major differences between the groups. For example, on chromosome 8, only one grouping showed a single difference between any of the groups. We saw similar results with chromosomes 9, 17, and 18 (not shown). This result supports the concept of consistent genetic differences between the mesenchymal-like and epithelial cells.

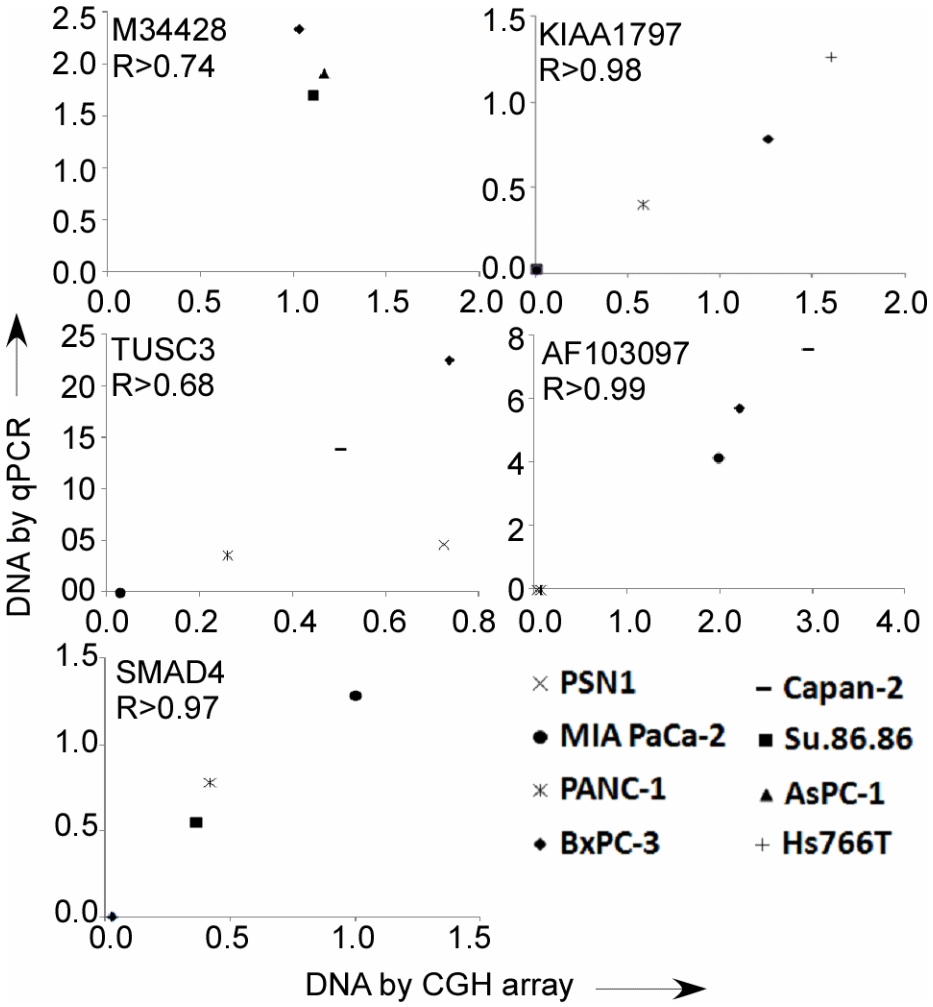

Figure 10. Q-PCR validation of DNA alterations. We used quantitative real time PCR to confirm the genomic alterations at selected loci. We normalized the measurements from each gene to the levels of NAG in the matched cell line. We used NAG because actin was not unaltered in all cell lines.

Relationship of copy number to gene expression

Genomic amplifications and deletions could contribute to cancer progression by affecting the expression levels of certain genes [55, 56, 86, 87]. We obtained gene expression measurements from the CCLE Project [58] for 21 of the 22 genes (including CDKN2A and CDKN2B) identified in our analysis and for 25 of the 26 cell lines. The gene copy numbers correlated significantly with the mRNA expression levels for 9 of 14 genes that had average expression levels above background (Table 5). The strong correlation for SMAD4 was expected, and we also observed strong correlations in genes neighboring CDKN2A, including CDKN2B, KLHL9, and KIAA1797 (Figure 11), supporting the potential cancer-promoting functions of losses near CDKN2A. The amplification of M34428 DNA copy number levels correlated with higher gene expression (Figure 11), supporting a functional component of the DNA alteration. On the other hand, M34428 and DQ515897 are located on either side of the MYC gene, an oncogene that also is amplified in 6 of the cell lines, so they could be co-altered as passengers with MYC. Although we were not able to detect expression of the AF103097 putative gene—interesting due to its gain in epithelial cells and loss in mesenchymal-like cells—genetic alterations to this locus nevertheless could contribute to cancer progression, perhaps through affecting the expression of other genes. Overall, a functional role for gene expression loss caused by DNA deletion is supported mainly for the chromosome 9 loci.

Table 5. DNA-mRNA correlations. Correlation between the DNA copy number and the expression of the gene for 25 cell lines. Significant correlations are highlighted. The percentages in columns 4 and 5 have been rounded off as per the confidence level based on the number of samples.

Chromosome	Probe Id	Gene	% Epithelial cells showing alteration	% Mesenchymal-like cells showing alteration	Average Raw Expression	Correlation	P- Value (1 Tailed)
9	A_16_P02074946	KIAA1797	20	70	715	0.37	p<0.035
9	A_16_P38673538	PTPLAD2	20	70	178	0.24	p<0.124
9	A_16_P18575142	MLLT3	20	60	142	-0.03	p<0.444
8	A_16_P18226308	TUSC3	30	70	447	0.15	p<0.238
9	A_16_P02075542	KLHL9	30	70	861	0.39	p<0.027
18	A_16_P41038127	ME2	30	70	1040	0.66	p<0.0002
18	A_16_P20859969	SMAD4	30	70	231	0.71	p<0.0001
18	A_16_P20867858	MBD2	20	60	3351	0.82	p<0.0001
9	A_14_P130650	CDKN2A	50	80	1831	0.57	p<0.002
9	A_14_P118440	CDKN2B	50	70	291	0.44	p<0.014
9	A_16_P18577258	AK124391	30	70	778	0.39	p<0.027
8	A_16_P02020073	M34428(P1)	10	60	376	0.91	p<0.0001
8	A_16_P02020073	M34428(P2)	10	60	1560	0.08	p<0.352
9	A_16_P18581686	CR627240	20	60	778	0.30	p<0.073
9	A_16_P18547744	PTPRD	20	60	35	0.14	p<0.248
9	A_16_P02077035	DMRTA1	30	70	27	0.28	p<0.088
9	A_14_P116804	VOO541	20	60	36	-0.02	p<0.463

Table 5 (cont'd)

9	A_14_P124911	IFNB1	20	70	5	0.29	p<0.080
9	A_14_P131521	IFNW1	20	70	11	-0.26	p<0.105
8	A_16_P18225623	SGCZ	10	60	12	0.15	p<0.238
18	A_16_P20866259	DCC	20	60	19	0.35	p<0.040

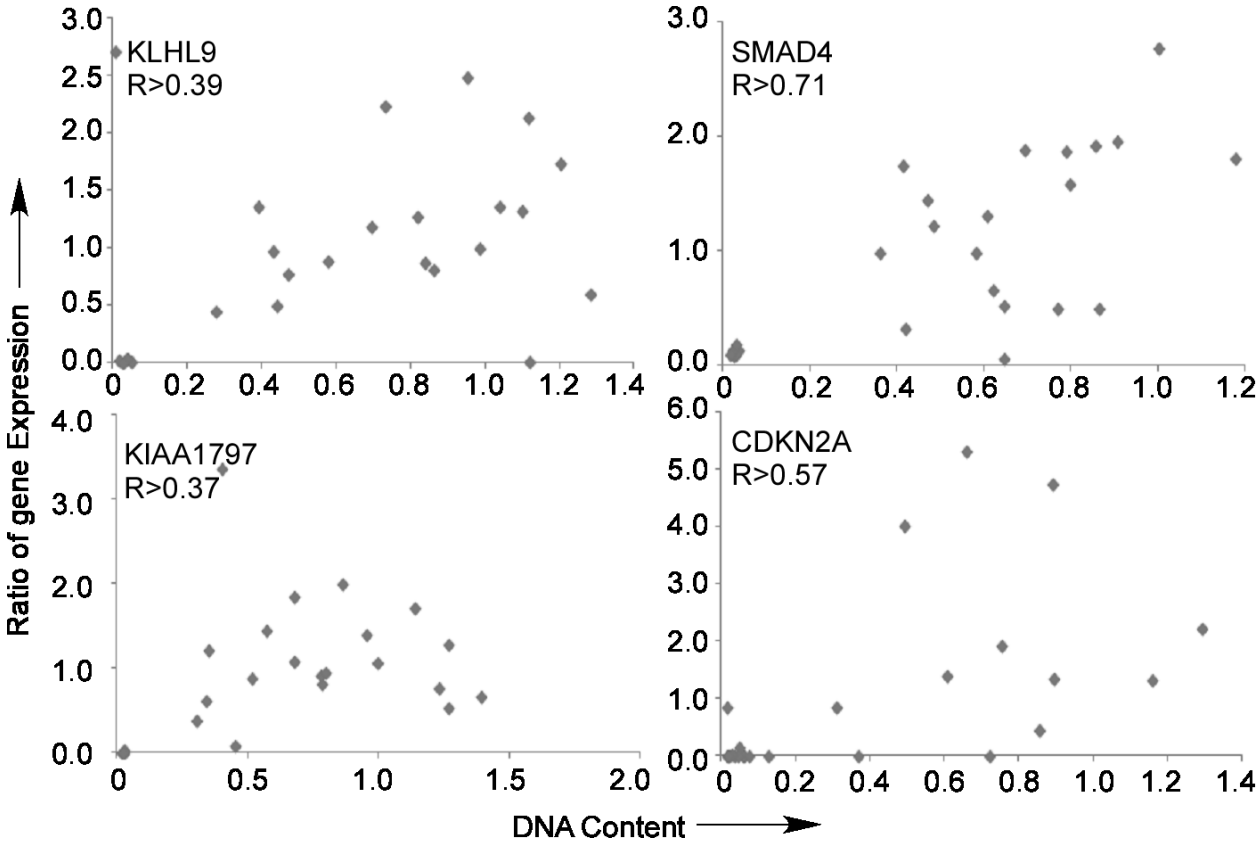

Figure 11. DNA-mRNA correlation. Correlation between the DNA copy numbers (unlogged raw ratios) and the mRNA expression data obtained using U133 Affymetrix mRNA chips

Gains and losses of the selected genes in primary tumors

If any of the identified genes is a driver of a cancer-promoting phenotype, we would expect increased prevalence of the mutation across primary tumors. To test this proposition, we obtained CGH data for 11 primary pancreatic adenocarcinoma samples using the same platform as used for the cell lines. Because a tumor specimen contains a mixture of both normal and neoplastic cells, we flow-sorted the cells based on DNA ploidy and used only the aneuploid cells (the cancer cell population) for the CGH. This system gives a purer look at the DNA of the cancer cells [57] and previously provided information on the clonal origins of metastases [88].

Among all the probes, the rate of alteration was similar between the cell lines and tissue, but the prevalence of deletions in the tissue samples was much higher for the 20 probes (Figure 12, and see Figure 13 for rates of alteration over all chromosomes). For example, 8 (40%) of the 20 genes were deleted in 4 or more tissue samples, compared to less than 2% of all the probes. When we randomly selected 20 different probes 10 separate times and averaged the results, the rate of deletion was similar to that from all probes. Furthermore, the directions of the alterations of the 20 genes were the same between the tissue and cell lines: M34428 and DQ515897 showed amplifications, AF103097 was both amplified and deleted, and the rest showed deletions (Figure 12C). SGCZ, AF103097, KLHL9 and TUSC3 also were aberrant in a high proportion of the samples. CDKN2A, one of the common aberrations, was detected in 7 out of the 11 tumors (not shown), consistent with its major role in pancreatic cancer pathogenesis. The high rate of alteration of the 20 probes, relative to randomly-chosen probes, and the

agreement in direction of change between cell lines and tissue, support the involvement of these alterations in cancer progression.

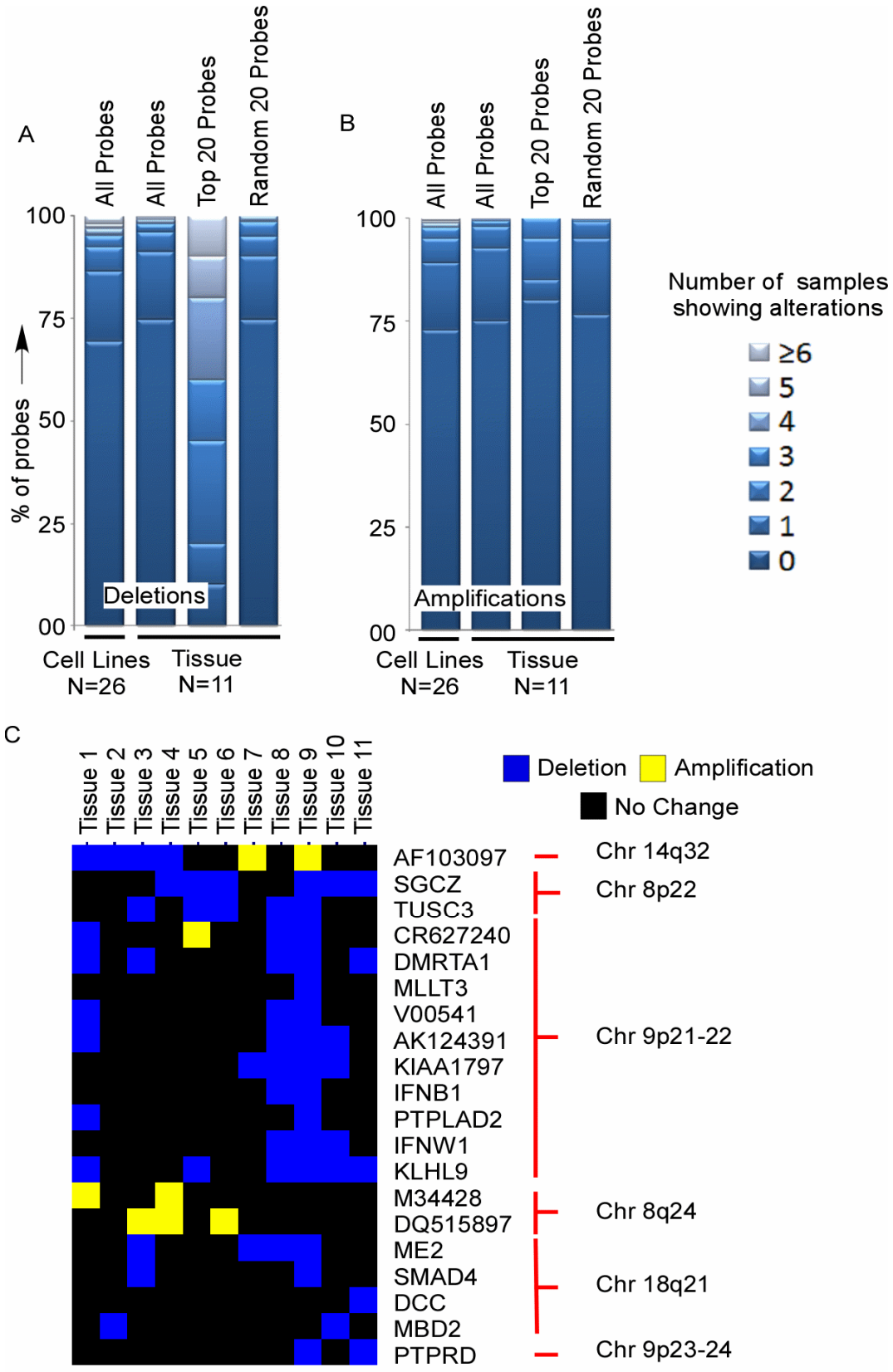

Figure 12. Genomic alterations in primary tumors.

Figure 12. (cont'd) The columns indicate the percentage of probes altered in no sample, one sample, two samples and so on. The percentages were calculated for all the probes in the cell lines and primary tissues, the 20 probes selected from the cell lines in the primary tissue as well as random 20 probes in the primary tissue (averaged over 10 times). (A) Deletions. (B) Amplifications. (C) Amplifications and deletions to the 20 selected probes in individual tissue samples. For each gene (given in the row labels) and each tissue sample (columns), a blue square indicates deletion, a yellow square indicates amplification, and a black square indicates no change.

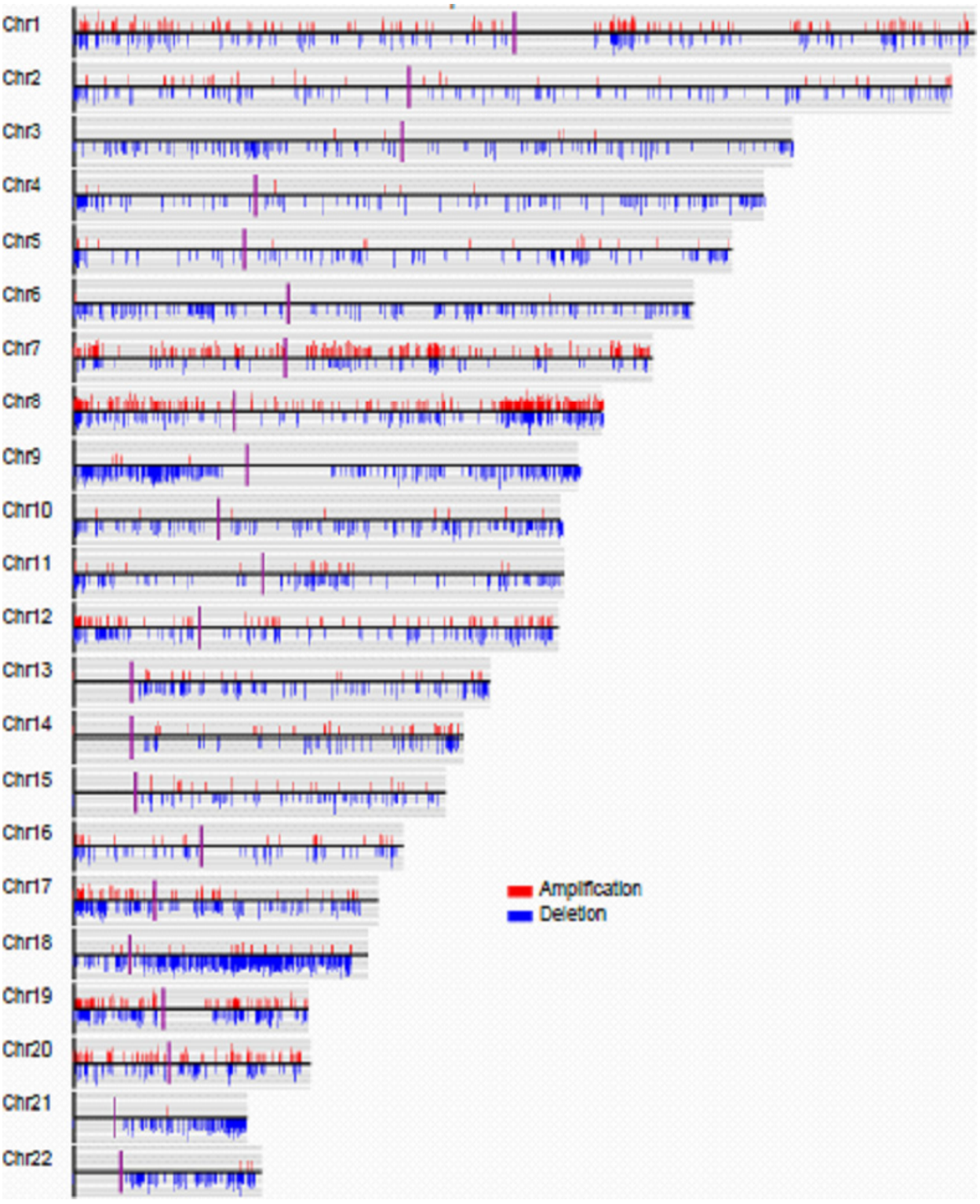

Figure 13. Distribution of Mutated probes throughout the genome for the primary tissues. The raw values (log10) were averaged for each probe. Probes showing an average change of 2-fold or greater relative the reference DNA were plotted. The y-axis indicates the percentage of tissue samples showing the alteration.

Discussion

Cancer cells with a mesenchymal-like phenotype may be responsible for the early dissemination, treatment resistance, and rapid recurrence that are common in pancreatic cancer. Our hypothesis was that certain cancer cells have distinct genetic alterations which could enable a switch to such a phenotype. The switch might be induced by some external factor, like a cytokine from the tumor environment, but the switch acts only in the population containing the right genetic alteration. This model does not preclude conversion back to an epithelial phenotype under the right circumstance, as in the process of mesenchymal-epithelial transition, since the alteration might enable plasticity rather than a permanent change. We found that specific deletions and amplifications are more prevalent in cancer cells with a mesenchymal-like phenotype relative to those with an epithelial phenotype. Several features of the results support the validity of the strategy and findings: the enrichment of specific alterations only in the mesenchymal-like cell lines, despite equivalence between the groups in total alterations; the consistency between the primary tissue and the cell lines in the direction of alterations among the 20 selected genes; and the high prevalence of alterations of the 20 selected genes in primary cancer tissue, relative to all other probes. These findings suggest that some of the identified alterations are cancer promoting rather than initiating, since initiating alterations—such as CDKN2A loss—would appear at equal rates in cells with epithelial and mesenchymal-like phenotypes.

The design of this study was different from previous studies examining DNA copy number alterations in pancreatic cancer, but comparisons of results between the studies could give useful insights. As noted above, our study identified nearly all the alterations previously found in matched cell lines [47]. We did not find some of the alterations that were previously observed in small subsets of cases, such as amplifications in 7q21-q22 [49], most likely because of our more stringent search criteria. Our study is the first to find that some previously identified alterations, including the losses at 8p22 [47, 89], 9p21-p22 [48, 51, 52], and 18q21 [51, 52, 89] and the amplification at 8q24 [48, 50, 89, 90], may be associated with the development of a mesenchymal-like phenotype affecting aggressiveness. The deletion of SMAD4 at 18q21 is one of the most frequent events in pancreatic cancer [91, 92]. SMAD4 is also involved in the EMT pathway but its functional significance is debatable. Intact SMAD4 can lead to EMT through TGF-β signaling which has been shown to increase migration of cells, but SMAD4 inactivation is associated with poor prognosis, presumably through the loss of TGF-β tumor-suppressive capabilities [91, 93, 94], and with widespread metastases [95, 96]. Our data support a dedifferentiation promoted by SMAD4 loss. The loss of SMAD4 might prevent the canonical SMAD-4 dependent TGF-β mediated EMT pathway, but the poor prognosis of SMAD-4

Two features of the present study may be particularly useful in future work. The system of analyzing only the aneuploid population, using flow-sorting by DNA content [97], likely enabled the observation of concordance between the cell lines and the tissue samples. Previous studies using primary cancer samples may have been partially confounded by

the presence of normal stromal cells within the tumors. The analysis of only the aneuploid population may have given us a cleaner, more accurate view of the cancer-associated alterations. Another potentially useful feature of this work is the study design. Instead of searching for abnormalities that are commonly found among cancer cases, we grouped the cancers by phenotype and searched for alterations selectively enriched in one of the groups. A search for genes that were common to both groups, as in a typical study design, turned up only known oncogenes and tumor suppressors, whereas the division of cells by phenotype showed revealed alterations in the mesenchymal-like cell lines that also were present at high prevalence in the primary tissue samples.

Several of the genes identified here are promising subjects for further study. The losses clustered on chromosome 9 were co-deleted with the important tumor suppressor CDKN2A, as none of the genes were lost independently from CDKN2A. However, the higher prevalence of certain co-deletions in the mesenchymal-like cells and the concomitant loss of gene expression argue for the functional importance of the co-deleted genes. One of those genes, KIAA1797, was shown to accelerate colony formation, cell migration, and cell invasion [98]. Another neighboring gene, KLHL9, is a substrate specific adaptor of BCR E3 ligase required for mitotic expression and cytokinesis. This gene is involved in the correct alignment of chromosomes during mitosis, the completion of cytokinesis, and the removal of Aurora B from the complex [85, 99]. The loss of KLHL9 potentially could disrupt regulation of mitosis.

Losses to the p arm of chromosome 8, affecting SGCZ and TUSC3, also were highly prevalent in the mesenchymal-like cells. SGCZ (sarcoglycan zeta) is part of the sarcoglycan complex involved in forming a connection between the cytoskeleton and the extracellular matrix [100]. The loss of sarcoglycans therefore could give ductal epithelial cells increased invasive capability [100]. The downregulation of TUSC3, either through epigenetic silencing or DNA deletion, is prevalent in prostate cancer [101]. It is also associated with poor prognosis in ovarian cancer [102, 103]. TUSC3 shares high sequence homology with OST3P, a subunit of the oligosaccharyltransferase complex involved in protein N-glycosylation. Changes to protein glycosylation influence cancer progression in a variety of ways [104], but the effects of TUSC3 loss on glycosylation are not yet known.

In summary, this study supports the hypothesis that specific genetic alterations are more prevalent in mesenchymal like cancer cells. These genes might enable phenotypic switches or cell plasticity that contributes to cancer progression. Many of these genes are involved in the adhesion between cells or between cells and the ECM either through direct contact, glycoslation alterations as in the cases of SGCZ and TUSC3 while the exact mechanism of KIAA1797 has not been properly deciphered. This might be an important step which affects the induction of EMT. The mesenchymal-like cells tend to show larger losses of the region around CDKN2A on chromosome 9, marked by co-deletion of KLHL9 and KIAA1797 and the associated loss of gene expression. The mesenchymal-like cells also show losses in the p arm of chromosome 8 involving SGCZ and TUSC3, and highly focal amplifications and deletions to the AF103097 putative

gene on chromosome 14. Future studies of human tissue should further explore the relationship of the alterations identified here with the phenotype of the cancer cell. Potentially one could use fluorescence in-situ hybridization (FISH) to examine gains or losses at the single-cell level in tissue and then look at correspondence with histology or specific markers. Alternatively, one could flow-sort the cancer cells by a molecular marker and then examine differences between the groups in genetic gains or losses. A confirmation of the contribution of particular genes to an aggressive phenotype could lead to better strategies to eliminate highly lethal cancer cells and to assess patient prognosis.

CHAPTER THREE: GENE EXPRESSION ALTERATIONS DURING EMT AS CANDIDATE THERAPEUTIC TARGETS & PROGNOSTIC MARKER

The identification of MRC2 as a significant change during TGF-β induced EMT by gene expression microarrays, including Table 6 and Figure 14 were published separately as

Maupin KA, **Sinha A**, Eugster E, Miller J, Ross J, et al. (2010) Glycogene Expression Alterations Associated with Pancreatic Cancer Epithelial-Mesenchymal Transition in Complementary Model Systems. PLoS ONE 5(9): e13002.

Introduction

The process of epithelial-mesenchymal transition (EMT), as already described can generate the subset of cancer cells responsible for many aspects of pancreatic cancer progression [105]. Such cells can acquire stem-cell properties [29, 37, 106] and cultured pancreatic cancer cells with mesenchymal like properties are more invasive and resistant to drugs that those with epithelial properties [39]. Patients with cancer cells showing increased levels of mesenchymal like markers have been shown to have particularly poor outcomes [107-110]. In the previous chapter, we identified that cells that become mesenchymal-like have distinct genetic alterations than their epithelial counterparts ratifying our first specific hypothesis. The genes identified are excellent candidates for further research for their role in metastasis and they can act as excellent biomarkers. However, given that 18 out of the 20 alterations were deletions and the only two amplifications were putative genes, the over-arching aim of targeting the mesenchymal-like cancer cells would be a challenge using those hits. Hence, in a smaller set of cells, we looked at molecular changes that happen during the process of TGF-β induced EMT to identify genes that can be used to target the mesenchymal-like subpopulation.

The only FDA-approved pancreatic cancer biomarker is a carbohydrate molecule, CA19-9, which is associated with poor prognosis. Since, our aim is to molecularly characterize cells causing poor prognosis, we decided to study the cellular glycosylation changes during EMT. The importance of glycosylation in pathologic conditions is well-known with previous evidence showing glycosylation alterations as modulators of tumor-

stromal interactions and invasive potential of tumor cells. The changes in glycosylation are even more paramount in pancreatic cancer because of highly fibrotic nature of the cancer and known glycosylation changes like the elevation of CA19-9 [59, 111]. It is possible that EMT could be driving a lot of these glycosylation changes. However, this association has not been properly investigated. Instead of looking at global transcriptional changes, we decided to take a more focused approach and look into greater detail into the process of glycosylation. Therefore, we hypothesized that EMT is characterized by specific glycosylation alterations that play functional roles in cancer cell differentiation or migration. The aim was to probe these alterations to identify molecules to detect and target mesenchymal-like cancer cells.

To identify the differences between epithelial and mesenchymal-like cells, the expression of glycosylation related genes was examined in cancer cell lines which were either mock-treated or induced to undergo EMT through TGF-β treatment. Monitoring gene expression changes is experimentally more tractable than comprehensively characterizing glycan structures. Hence, looking at the gene expression levels was chosen as the preferred method for the initial investigation. Glycan structures cannot be deduced simply by looking into the gene expression of glycogenes, but it gives indications towards major structural changes and provides candidates for therapeutic interventions. Contrary to previous studies looking at glycogenes using focused microarrays or PCR arrays, we used whole genome expression profiling to capture the information. The advantage of this system is the ability to use standardized platforms as well as use the option of utilizing data from non-glycogenes to gain a holistic image of

the changes happening during EMT. The microarray contained a total of 54675 probes spanning 35,888 genes. A target list of 555 genes was created including glycan-associated genes as well as genes relevant to EMT. We then followed up on the top hits, looking at their known functions to identify candidate genes conferring elevated metastatic capabilities. This was achieved by functional validation assays and determining their association with prognosis.

Materials and Methods

Cell culture and RNA extraction for microarray analysis

Panc-1 and A549 were purchased from the American Type Culture Collection (ATCC, Manassas, VA). For the induced EMT model, Panc-1 and A549 were grown to 70% confluency, cultured for one day in serum-free conditions, and incubated for 48 hours with fresh media containing either 5 nM TGFβ (R&D Systems), or plain media. The cells were rinsed three times in 1× phosphate-buffered saline prior to lysis by the addition of TRIzol reagent (Invitrogen, Carlsbad, CA) followed by repeated passes through an 18-G needle and a 5 min incubation at RT. The lysates were vigorously mixed with chloroform and spun down at 12000×g for 20 minutes at 4°C. The aqueous layers were transferred to an isopropanol solution, mixed vigorously, and centrifuged at 12000×g for 30 minutes at 4°C. The RNA-containing pellet was washed with 75% ethanol, dried, and dissolved in RNase-free water. The RNA quantity and quality was determined using a spectrophotometer (Bio-photometer, Eppendorf, Westbury, NY) and stored at −20°C until all cell lines were ready for cDNA synthesis and polymerase chain reaction (PCR).

Microarray data collection and analysis

All microarray data are compliant with the MIAME standards and are deposited in the GEO database. The induced-EMT model was analyzed on the Affymetrix Human Genome U133 Plus 2.0 chip at the University of Michigan.

A list of 587 genes of interest was assembled using information from the Consortium for Functional Glycomics in addition to project-specific information. These genes include

glycan-transferases (199 genes), glycoproteins (101 genes), lectins (112 genes), glycosidases (62 genes), nucleo-sugar transport (35 genes), nucleo-sugar synthesis (23 genes), golgi transport (8 genes), TGF pathway (19 genes), notch pathway (18 genes), and EMT markers (10 genes).out of which 555 genes were represented on the Affymetrix Human Genome U133 Plus 2.0. A Chi-square test was used to determine whether gene expression changes within this list occurred more frequently than all other changes.

For the analysis of TGF-β–induced EMT of Panc-1, a paired, two-tailed, t-test was performed between the triplicate experiments of each condition, with a p value less then 0.05 considered significant. Probes with mean absolute signal levels below 100 for both conditions were excluded. Analysis of TGFβ treated A549 used the pairwise ratios in transcript levels between the 0 hour and 72 hour time points.

Sulfated glycosaminoglycan assay

The Alcian Blue Assay closely followed a previously established protocol with minor alterations [112]. Cells were lysed in Radio-Immunoprecipitation Assay (RIPA) buffer containing protease inhibitor (Roche). The solution was centrifuged to remove the pellet. The protein-containing supernatant was then quantified using the microBCA assay (Thermo Scientific) and adjusted to equivalent concentrations prior to analysis. All of the following reagents were purchased from Sigma, Samples were initially denatured in 3.3 M urea, 0.1% H_2SO_4, and 0.25% octylphenoxypolyethoxyethanol (Triton X-114) for 30 minutes at room temperature. Alcian Blue stain solution (0.07% Alcian Blue/0.1%

H_2SO_4/0.25% Triton X-114) was then added to give final concentrations of 0.05% Alcian Blue, 0.56 M urea, 0.1% H_2SO_4, and 0.25% Triton X-114. Samples were then left at 4°C overnight to allow precipitation of Alcian Blue bound species. The concentration of H_2SO_4 used should give a pH between 1.5 and 2.0 to allow for the majority of species carrying negative charge to be sulfate residues for specific binding by the cationic dye. The next day the samples were centrifuged at 12,000×g for 15 minutes and the supernatant containing unbound dye was discarded. The pellets containing the dye bound molecules were re-suspended in 1 mL of a solution of 40% dimethylsulfoxide (DMSO) and 0.07M $MgCl_2$ then centrifuged at 12,000×g for 15 minutes and the supernatant was once again discarded. The remaining pellet was re-dissolved in 500 µL of a solution of 5M urea, 33% 1-propanol, and 0.25% Triton X-114 to measure absorbance. Measurements for absorbance at 600 nm were performed in triplicate using a BioPhotometer (Eppendorf). A solution of 5M urea, 33% 1-propanol, and 0.25% Triton X-114 was used as a blank. Heparin (H3393, Sigma) was used as a positive control. The statistical analyses and graphing were performed in Microsoft Excel.

Cell culture and induction of EMT

Cell lines were purchased from American Type Culture Collection (ATCC, Manassas, VA). Panc-1, Hs766T, MIAPaCa-2 and A549 were maintained in Dulbecco's modified Eagle's medium while BxPC-3 was maintained in RPMI1640, both in 10% fetal bovine serum (FBS). To induce EMT, cells were grown to 70% confluency, cultured in serum-free (SF) media for 24 hours, followed by culturing 72 hours in fresh SF media containing 5 nM TGF-β1 (240-B, R&D systems, Minneapolis, MN). Subcellular protein

fractions were obtained using subcellular protein fractionation kit (78840, Thermo Scientific, Rockford, IL).

Immunofluorescence assay

Cells grown on cover slips were fixed using 3.7% paraformaldehyde, permeabilized with 0.3%Triton X-100 in PBS and blocked in blocking buffer (PBS + 0.01% Triton X-100 and 3% BSA). The primary antibody was diluted in blocking buffer to a final concentration of 5 µg/ml and incubated on the cells for one hour at room temperature followed by one hour secondary antibody (4 µg/ml in blocking buffer) incubation at room temperature. The nuclei were counterstained with Hoechst 33258 nuclear dye (83219, AnaSpec Inc., Fremont, CA) at 10 µg/ml concentration in ddH_2O. Cover slips were inverted on glass microscope slides and mounted using Fluoro Gel (17985-10, Electron Microcopy Sciences, Hatfield, PA) and visualized under the Nikon Eclipse TE300 microscope connected to a Photometrics Cool SNAP HQ^2 camera, coupled with a laser from Mager Scientific and NIS-Elements software. The primary antibody used was against MRC2 (ab70132, Abcam, Cambridge, MA) while the secondary antibody was AlexaFluor-conjugated anti-rabbit IgG (A10040, Invitrogen, Grand Island, NY) with excitation and emission at 556 nm and 573 nm, respectively. The nuclear dye was excited at 352 nm and emitted at 461 nm.

Western blot

Cells were lysed in radio-immunoprecipitation assay (RIPA) buffer containing protease inhibitor (Complete Protease Inhibitor, Roche Applied Bioscience, Indianapolis, IN) for

30 minutes. The samples were centrifuged to remove the pellet. Total protein quantification was carried out using the microBCA assay (Thermo Scientific) to ensure equal loading of total protein into 4-12% polyacryamide gels (Criterion Gel, Bio-Rad, Hercules, CA). The proteins were electrophoretically transferred from the gels to polyvinylidene fluoride (PVDF) membranes (BIO-RAD). The membranes were incubated in blocking buffer (1X Tris Buffered Saline + 0.05% Tween-20 + 3% BSA) for 1 hour followed by incubation in primary antibody (diluted in blocking buffer) overnight. The membranes were then washed in Tris-Buffered Saline containing 0.05% Tween-20 (TBST 0.05) three time for 10 minutes each, incubated with horseradish peroxidase (HRP)-conjugated secondary antibody, diluted in blocking buffer for 1 hour, and washed again. The membrane was then incubated with HRP substrate (SuperSignal West Pico, Thermo Scientific) for 3 minutes and visualized using ChemiDOC XRS (Bio-Rad). The resulting spots were quantified using the Quantity One software (Bio-Rad). All quantified protein levels were normalized to the actin levels. The primary antibodies used were against MRC2 (ab70132, Abcam), E-cadherin (MAB1838, R&D Systems), Vimentin (AF2105, R&D Systems), Actin (SC-1616, Santa Cruz Biotechnology, Santa Cruz, CA), HDAC2 (H5109-47E, US Biological, Swampscott, MA).

MRC2 knockdown

MRC2 expression was knocked down in Panc-1 cells using shRNA cassettes from Origene (Rockville, MD). The plasmids were introduced into the cells using Express–In transfection reagent (ETR4621, Thermo Scientific). After 48 hours, cells were positively selected using 1 μg/ml puromycin. After quantification of the level of expression

reduction by western blot, cassettes TR30013 (scrambled), G1345601 (Si 1), G1345604 (Si 2) were selected for subsequent experiments. The cell lines were maintained in 0.5 µg/ml of puromycin.

Scratch assay

Cells were grown to 90% confluency and then serum starved for 24 hours. They were then treated with SF media + 5ng/ml of TGF-β1 for 48 hours. A scratch was introduced into cell monolayer using a pipette tip. The scratched area was washed to remove cell debris and then incubated in media containing 1% FBS. The scratched area was photographed at multiple time points to examine the wound healing rate.

Proliferation assay

3×10^6 cells were seeded in a 60 mm culture dish and incubated with media containing 10% FBS. The cells were harvested after 96 hours and counted using a hemocytometer (Hausser Scientific, Horsham, PA).

Chemotaxis assay

The cells were grown to 70% confluency and then serum starved for 24 hours. The cells were treated with 5 ng/ml TGF-β1 in SF media for 48 hours. The bottom chambers of ChemoTx system (106-8, Neuro Probe, Gaithersburg, MD) were filled with 310 µl of media containing 10% FBS as the chemoattractant. Neuro Probe provided protocol was followed. 20,000 cells were incubated over each well in a 50 µl bubble of SF media. In addition, known numbers of cells were incubated in the bottom wells of a set of

chambers to form a standard curve. After 16 hours in the incubator, the membrane was removed, and the number of cells migrated to each bottom well was calculated using the WST-1 cell proliferation reagent (05015944001, ROCHE). The induction of MRC2 at 48 hours was confirmed by Western blots (data not shown).

Invasion assay

The cells were prepared as for the chemotaxis assay. The Biocoat Matrigel Invasion Chamber (354480, BD Biosciences, Sparks, MD) protocol was followed. The lower well contained 750 µl of media with 10% FBS whereas the upper chamber was incubated with 500 µl SF media containing 25,000 cells. After 22 hours in the incubator, the invaded cells were fixed on the surface of the membrane using the Diff Quik Stain Set (B4132-1A, Siemens) and stained with crystal violet (C3886, Sigma). The membranes were cut out from the invasion chambers and fixed onto microscope slides using Vecta Mount (H-5000, Vector Laboratories, Burlingame, CA). The Aperio Scanscope was used to scan the membranes, and five different sections were manually quantified for the number of invaded cells.

Immunohistochemistry

Tissue microarrays (TMAs) were created using samples gathered from archived paraffin blocks collected from post-retention stores and were coded for TMA construction as human subjects exempt for research purposes. Seven pancreatic cancer TMA blocks were constructed to include 265 tumors of pancreatic origin for evaluation of tumor and tumor associated stroma, and, when available, patient-matched, adjacent non-

cancerous pancreatic tissue (NPT) (N=36) and metastatic lesions (N=22) were included. Most tumor samples had multiple cores taken, for a total of over 800 cores representing 323 samples. The slides were dewaxed, rehydrated and antigen retrieved on the BondMax^{TM} autostainer (Leica Microsystems, Buffalo Grove, IL). Slides stained for MRC2 were subjected to heat-induced epitope retrieval using a proprietary EDTA based retrieval solution for 45 minutes, and SMAD4 slides were subjected to heat-induced epitope retrieval using a proprietary citrate based retrieval solution for 30 minutes. Endogenous peroxidase was blocked. All seven TMAs were incubated for 30 minutes with anti-MRC2 (ab70132, Abcam, 1:150), anti-MRC2 (2h9f12, 1:100), and anti-SMAD4 (sc-7966, Santa Cruz, 1:250). The sections were visualized using the Bond^{TM} Polymer Refine Detection Kit (Leica Microsystems, Buffalo Grove, IL) using diaminobenzidine chromogen as substrate. The TMAs were scanned using the Aperio Scanner. MRC2 staining was semi quantified in a blinded fashion for both the stroma as well as the cancer/epithelial cells and categorized into groups 1, 2 and 3, where 1 indicated minimal and 3 indicated maximum staining. After averaging over the cores, samples with staining intensity of 1-1.5 were considered low, 1.5-2.1 were considered medium, and >2.1 were considered high. Samples with average scores of 1.5 or higher in either compartment were considered as elevated. Anti-MRC2 clone 2h9f12 was kindly provided by Dr. Lars Engelholm (University of Copenhagen, Denmark).

The Positive Pixel Count software identified the total number of pixels in the image along with quantifying the number of weakly positive (Grp A), positive (Grp B) and strongly positive pixels (Grp C) similar to how a histopathologist grades a tumor as 1+,

2+ and 3+. Then we calculate the percentage of pixels in each of the three groups. Then we calculate a score using the following formula, “Score= (Group A % *1 + Group B % *2 + Group C % *3)” similar to the H-scoring system.

The scores of each patient was averaged over the multiple cores present and then divided by the average of the TMA slide to normalize it to account for staining differences (if any) between the multiple TMAs.

Fluroescence Intensity Thresholding and Colocalization (FITC)

50*50 pixels are taken and run through the entire image of 1024 by 1024 pixels. Size was selected so that approximately a single cell is covered in each sliding window. For each window, the mean and standard deviation is calculated. Then the means are plotted and then the median of means is calculated. The standard deviation of the median of means is then used for the calculation of threshold using the following formula-

Threshold= Median of means + X * standard deviation

X was set by using a training set which was graded by a board certified pathologist.

X=1.4 for blue

=1.8 for red

=4.0 for green

The program provides the percentage of positive pixels, threshold, median and standard deviation for each color. The program then calculates the colocalization. Right now, the three channels have to be colocalized in the same pixel and not nearby as smoothing function is challenging to computational abilities of normal desktops.

A lowest threshold is being set for images with low staining and low stdev. Values decided so far include 175 for green 900 for red with the upper limit of staining intensity being 4096. These values were decided upon by looking into the training tissues. Blue staining was pretty robust and the software did not require any minimum value to be set. An upper limit on the threshold can also be set for handling images with high non-specific staining.

Results

Alterations in glycogenes upon TGF-β induced EMT

Panc-1 and A549 were selected for studying changes mediated by TGF-β induced EMT. Panc-1 is a pancreatic cancer cell line while A549 is derived from lung cancer. A549 was included in this study to provide information about the generality of the associations with EMT. Analyzing two different cancer systems also helped in short-listing the list of candidate genes by removing cell line specific alterations. TGF-β treatment resulted in the dissolution of cell-cell junctions and a subset of cells changing their shape to spindle-like, generally seen in fibroblasts. The induction of EMT was confirmed by the E-cadherin and vimentin levels of the cell lines before and after treatment (data not shown). Whole genome expression measurements were obtained for the different cells using Affymetrix gene expression microarrays. The analysis was focused on the previously selected 555 genes related to glycosylation and EMT-associated pathways and the rest of the genes from the microarray were used as control. Among all genes, 1524 unique transcripts were altered. Given that the glycosylation related genes selected in our study represent 1.5% of the total unique transcripts on the Affymetrix chip, random representation of glycogenes approximately 23 genes (1.5% of 1524 transcripts) to be altered amongst the genes that have changed expression. However, 40 of the transcripts with altered expression levels were glycogenes that were found to be significantly different than random distribution by chi-square analysis($X^2=13.05$, $p<0.05$). This suggested an enrichment of transcriptional regulation of glycan-related genes in TGF-β induced EMT (Table 6).

Table 6. Analysis of glycogene enrichment in Panc-1 upon TGF-β treatment. Alterations in total genes probed and specifically the glycogenes during TGF-β induced EMT in Panc-1.

	Induced EMT in Panc-1
Total genes probed	35,888
Glycogenes probed (% of total)	555 (1.5%)
Total genes changing	1524
Glycogenes changing (% of total changing)	40 (2.6%)
Glycogene enrichment (p value, Chi-squared)	$p < 0.05$

An examination of genes that were altered more than 1.5 fold in both cell lines revealed some functional themes. The greatest change was identified in the proteoglycan SPOCK1 which contains glycosaminoglycan side chains of heparin and chondroitin-sulfate. In relation to this protein, genes that modify glycosaminoglycan sulfation including SULF2, CHST3 and CHST11 and HAS2 were up-regulated. An increase in total sulfation levels was identified in the mesenchymal-like cells as assayed by the Alcian blue staining (Figure 14). A lectin-like receptor involved in extracellular matrix remodeling, and known to bind sulfated molecules, MRC2 was upregulated. The alterations of proteoglycans and sulfation enzymes suggest the importance of the control of GAG sulfation in EMT. This finding is consistent with previous research showing alterations to matrix components such as versican and alterations to GAG sulfation in association with cancer particularly in aggressive forms of cancer. Versican is speculated to promote cancer by regulating growth factor activity and by interacting with immune and stromal cells, functions which can be modified by alterations to sulfation. SULF2 is found to be upregulated which acts to remove sulfates from certain GAG chains, has been associated with lung carcinogenesis and the tumorigenicity of pancreatic cancer cells. The association of these functions with cancer EMT suggests that cancer cells undergoing EMT use a reconditioning of the extracellular space to become highly invasive. The evaluation of total sulfation levels using the Alcian blue staining revealed an overall increase in protein sulfation in Panc-1 after treatment with TGF-β.

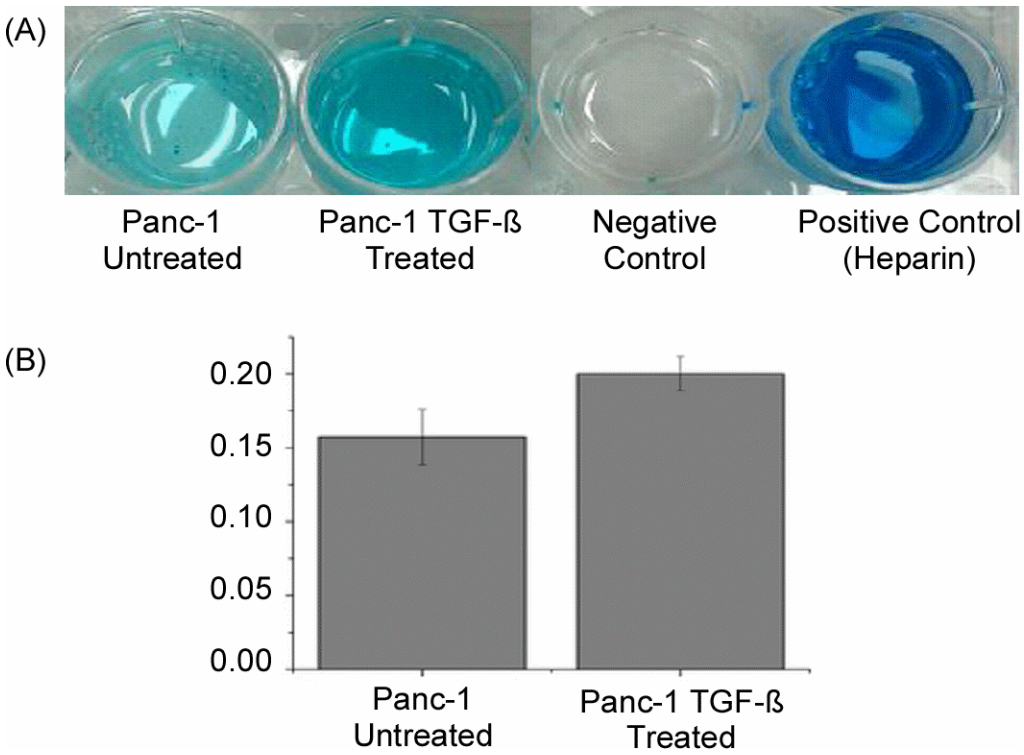

Figure 14. Alcian Blue assay for comparison of overall sulfation levels for treated and untreated Panc-1. An Alcian Blue assay was performed on cells lysates, and the overall sulfation for each cell line was quantified by measuring the absorbance of the dye at 600 nm. A student's t-test (results given by the p value) was performed comparing the absorbances between Panc-1 after 72 hours of TGF-β treatment and untreated Panc-1. Heparin was used as a sulfated GAG control. (A) Photograph of the resulting retention of Alcian Blue dye after the precipitation of sulfated glycans and subsequent re-suspension. Higher staining intensity indicates the presence of higher levels of sulfated glycans in the cell lysate of TGF-β treated Panc-1. (B) Bar graphs showing the differences in absorbance at 600 nm for Panc-1 after 72 hours exposure to 5 ng/mL TGF-β or untreated under serum starvation. Panc-1 after TGF-β treatment had significantly higher levels of absorbance than the untreated Panc-1 ($p = 0.027$).

The alterations in mannose receptor could have implications for cellular interactions with a reconditioned local environment. Mannose receptor family members have specificity for various matrix components such as collagen and sulfation [47]. Collagen was up-regulated in the media of both A549 and Panc-1 as determined by mass-spectrometry profiling (data not shown), and multiple other matrix components are altered by cancer cells, as discussed above. Considering these factors, altered regulation of mannose receptors such as MRC2 could be a means to conditioning the cellular response to the new matrix environment or acting to mediate autocrine loops. Considering the ECM remodeling is an integral part of metastasis, we hypothesized that during TGF-β mediated EMT, the increase in migration and invasion rates happen through the upregulation of MRC2.

The other hits that were identified were unsuitable for use as drug targets because of them being transcriptional factors or glycosyltransferases which affect multiple genes and hence are unsuitable for therapeutic interference. However, given that many of those proteins are secreted, they might have potential as biomarkers. Hence the other hits especially alterations in sulfation are being investigated by other members of the Haab laboratory for their merit as a biomarker. However, they have not been discussed further in this thesis.

Functional assessment of top alterations

Some of the top hits were transcription factors and enzymes affecting multiple proteins/pathways downstream; making them not ideal to be targeted. This left us with

some proteins like SPOCK1, ITGB3, LAMC2, MRC2, ITGA5 and ITGA3. The involvement of MRC2 in ECM remodeling, which is considered to be an integral part of cellular metastasis was one of the major reasons why we decided to follow-up on MRC2 despite it not being the top hit. Also, given the role of MRC2 as a constitutive endocytic receptor, if established as a marker of mesenchymal-like cancer cells, the endocytic receptor function can be utilized to specifically deliver drugs to the MRC2 expressing mesenchymal-like cancer cells by conjugation to an anti-MRC2 antibody ensuring high specificity with minimal side effects. MRC2 might have a role in cellular response to the ECM remodeling associated with EMT, especially the increase in collagen and protein sulfation. Keeping these points in mind, we decided to investigate the role of MRC2 in the progression of pancreatic cancer.

Mannose Receptor C-Type 2 (MRC2)

MRC2 is a type 1 transmembrane protein which is part of the mannose receptor family which includes 3 other proteins-mannose receptor (MR), PLA(2)R and DEC-205. All the mannose receptor family proteins including MRC2 have 3 extracellular domains. It has a cysteine rich domain which has been shown to bind to negatively charged oligosaccharides in the members of mannose receptor family. However, no known biological ligand is known for MRC2. The most well characterized function of MRC2 is collagen uptake and turnover [112-115], which can be attributed to the fibronectin type II domain. It has been experimentally shown to BIND at least collagen 1, 4 and 5. Its ability to uptake MMP-degraded collagen is higher than its ability to uptake native collagen. This collagen turnover has been demonstrated to be extremely important in biological processes like fibrosis and wound healing with possible role in even cancer metastasis. In addition to these 2 domains, mannose receptor family proteins have multiple C-type lectin like domains which number eight in the case of MRC2 [117]. They have been shown to bind various sugar moieties in vitro but biological ligands are still unknown [118].

In normal human tissue, MRC2 (also known as endo180 or UPARAP) has been shown to be mainly restricted to activated stromal fibroblasts and immune cells, with most organs showing no to low staining for MRC2 [119, 120]. In addition to expression on stromal fibroblasts, MRC2 expression also has been observed in breast cancer cell lines with invasive properties and in a subset of breast cancer cells from invasive tumors [121]. The expression of MRC2 on certain breast cancer [121] and glioma cell

lines [122] can be induced by TGF-β1, and expression in cell lines promotes chemotactic migration and invasion [123], likely through signaling from the endosomal compartment [124]. It has been shown to promote breast tumor growth and prostate cancer progression, but other than with high throughput gene expression studies, the importance of MRC2 in pancreatic cancer has not been studied yet [121, 125].

Pancreatic cancer typically shows severe desmoplasia, often with the major part of a tumor mass filled with fibrotic material and stromal cells. The remodeling and partial clearance of this matrix could be important in pancreatic cancer cell migration. These previous findings provide support for a potential role of MRC2 in pancreatic cancer aggressiveness.

We first investigated the conditions in which MRC2 is expressed and upregulated in cultured pancreatic cancer cells. Consistent with the gene expression profiling, MRC2 protein was upregulated during TGF-β1-induced EMT in Panc-1 and A549 cells as confirmed by western blotting and immunofluorescence (Figure 15A, 15B). Panc-1 and A549 cells have an intact SMAD4 pathway, but the cell lines BXPC3, Hs766T and Miapaca-2, which lack wild-type SMAD4 [126, 127] neither undergo TGF-β induced EMT nor show upregulation of MRC2 levels upon TGF-β1 treatment (Figure 15C). These results concord with a previous study showing that TGF-β1-induced MRC2 expression occurs through the SMAD4 pathway [128]. However, Miapaca-2, which has a mesenchymal-like phenotype under normal culture conditions, produces low levels of MRC2, whereas no cell lines with an epithelial phenotype express MRC2 under normal

culture conditions [59]. These observations indicate that MRC2 can be expressed by mesenchymal-like cancer cells through non-SMAD4 pathways under certain conditions and that it is strongly upregulated in TGF-β1-induced EMT. To investigate this observation in primary tumor tissues, we determined the correlation between SMAD4 and MRC2 staining in the primary tissues (Figure 16). Among the 21 PDAC cases scored for SMAD4 in the cancer cells, 12 (57%) were negative, in accordance to known rates of SMAD4 deletions/mutations in pancreatic cancers [129]. 50% of the SMAD4-negative cases showed some elevation in MRC2 in the cancer cells, indicating that MRC2 can be induced by alternate routes besides SMAD4. This result suggests MRC2 elevation in cancer cells may relate more closely to the differentiation state or EMT rather than a specific pathway, which is in agreement with the *in vitro* observations (Figure 15C).

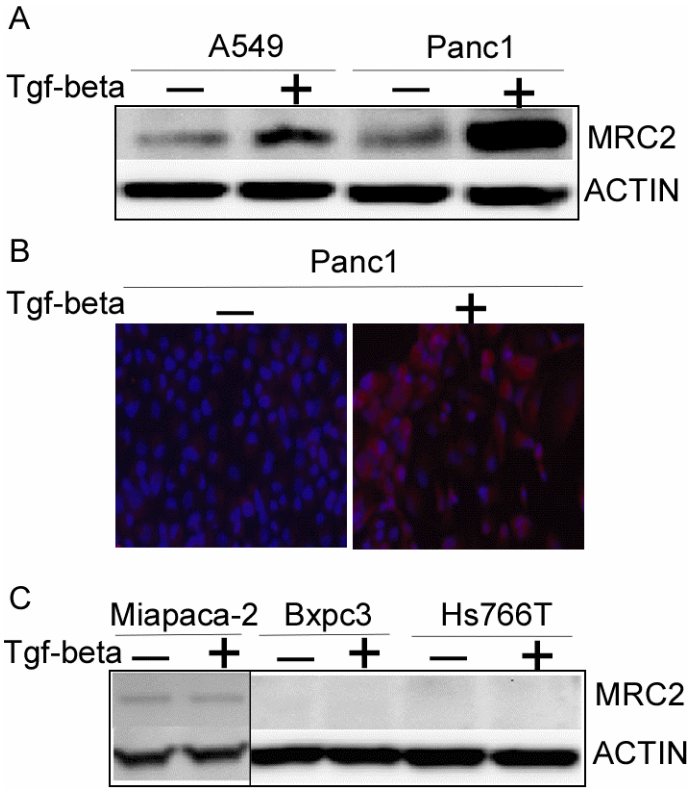

Figure 15. TGF-β1-induced changes in MRC2 protein levels. Cell lines with an active TGF-β signaling pathway (Panc-1, A549) showed upregulation of MRC2 as confirmed by (A) Western blots and (B) immunofluorescence, whereas cells lacking a SMAD4 dependent TGF-β pathway (Bxpc3, Miapaca-2 and Hs766T) did not show any change (C). The cells were treated with TGF-β1 or buffer for 72 hours prior to analysis.

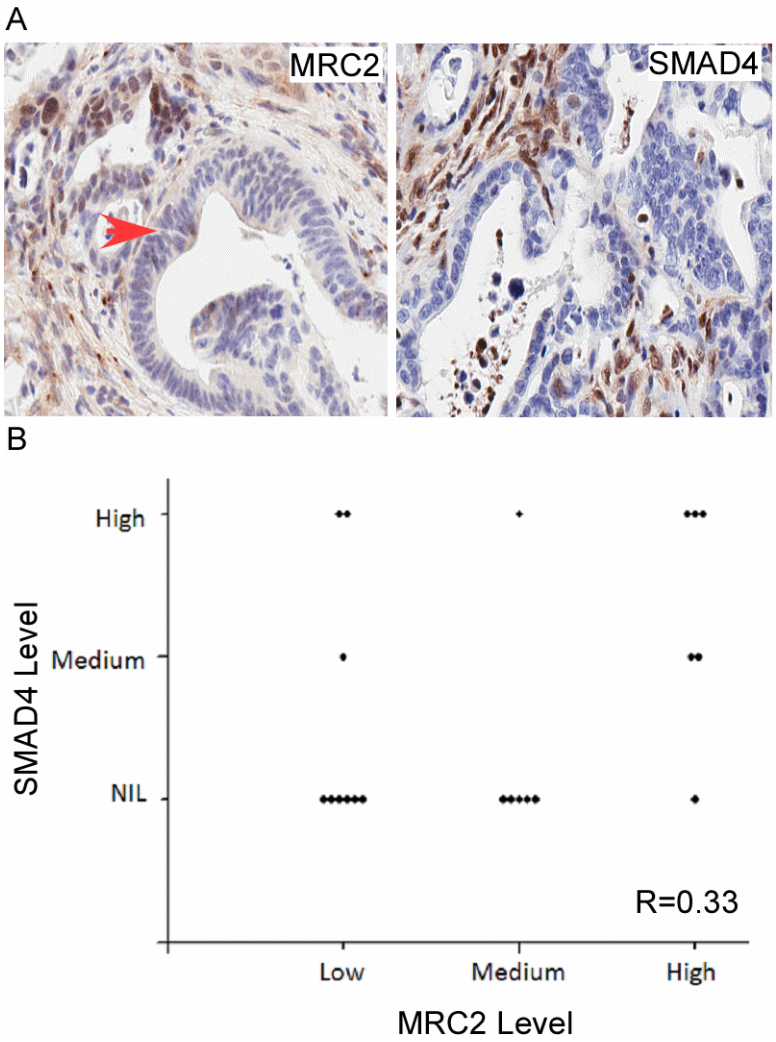

Figure 16. Correlation between SMAD4 and MRC2 staining intensity. (A) Representative image showing a tissue with cancer cells negative for SMAD4 but still expressing MRC2. (B) Each point represents a tumor section on the tissue microarray. For each tumor section, the staining intensity for SMAD4 in the cancer cells (y axis) was plotted with respect to the intensity of MRC2 in the cancer cells (x axis).

MRC2 in primary tissues

After confirming the validity of the microarray data, we evaluated the expression of MRC2 in pancreatic cancer patient samples. Immunohistochemistry on tissue microarrays was used to quantify MRC2 in pancreatic carcinoma samples and adjacent non-cancerous tissue. The specificity of the antibody was confirmed by the use of another anti-MRC2 antibody kindly provided by Dr. Lars Engelholm (Figure 17).

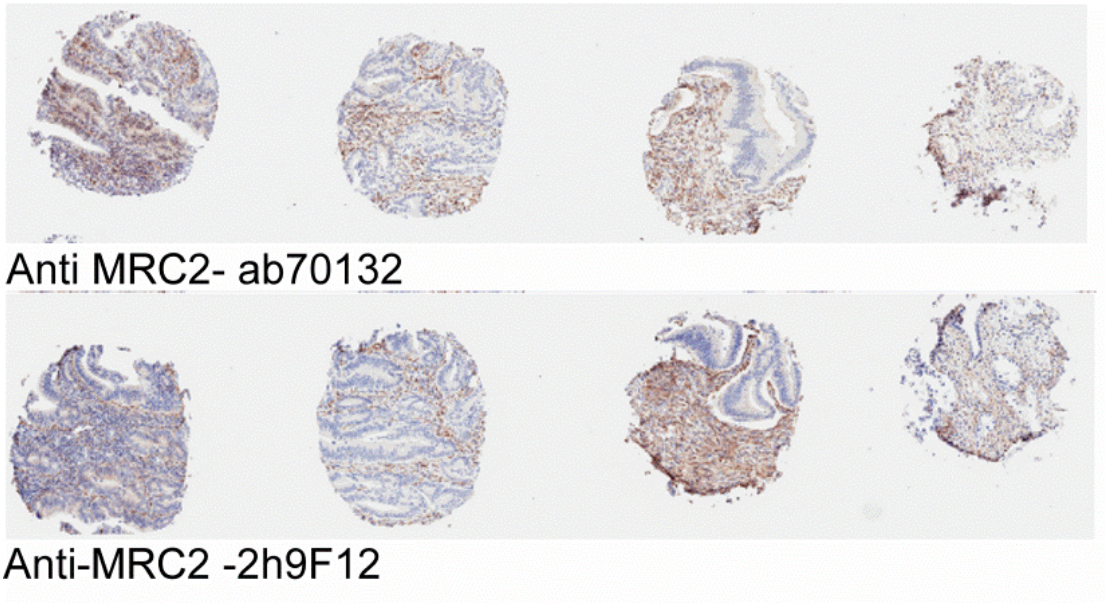

Figure 17. Correlation between different MRC2 antibodies. TMAs showing similar staining patterns for MRC2 using 2 different antibodies; ab70132 (abcam) and 2h9f12 (Lars H. Engelholm).

In total, we performed staining on 179 tissues with most tissues having multiple cores to avoid regional bias. The 179 tissues included 121 cancer tissues, 36 adjacent non-cancerous tissues and 22 metastatic lesions. The staining was quantified using the Aperio Imagescope software utilizing the Positive Pixel Count V9 software. MRC2 was found to be significantly upregulated in the cancer tissues in comparison to the normal tissue (Figure 18). The metastatic lesions had the highest average intensity but the difference was not significant. The high variability in the metastatic lesions might be because of mesenchymal to epithelial transition in a subset of tissues as metastatic lesions are being formed. Also, the adjacent non-cancerous tissues still expressed a significant amount of MRC2 possibly because of these tissues possibly being under the effect of cytokines secreted by the tumor cells in the vicinity. Unfortunately completely normal pancreatic tissue from patients expired from ailments other than that related to the pancreas were not found in significant numbers. In addition, because the MRC2 staining appeared to localize to the nucleus in many cases, we investigated whether MRC2 can shuttle to the nucleus upon TGF-β1 stimulation *in vitro* in Panc-1. MRC2 was found only in the cytoplasmic and membrane fractions, suggesting that the *in vivo* observations are due to perinuclear, rather than nuclear localization (data not shown). A potential mechanism of MRC2 modulation in cancer cells is genomic amplification or deletion [121], but no genomic alteration was observed at the MRC2 locus in any of these cell lines as assessed by comparative genomic hybridization (data not shown).

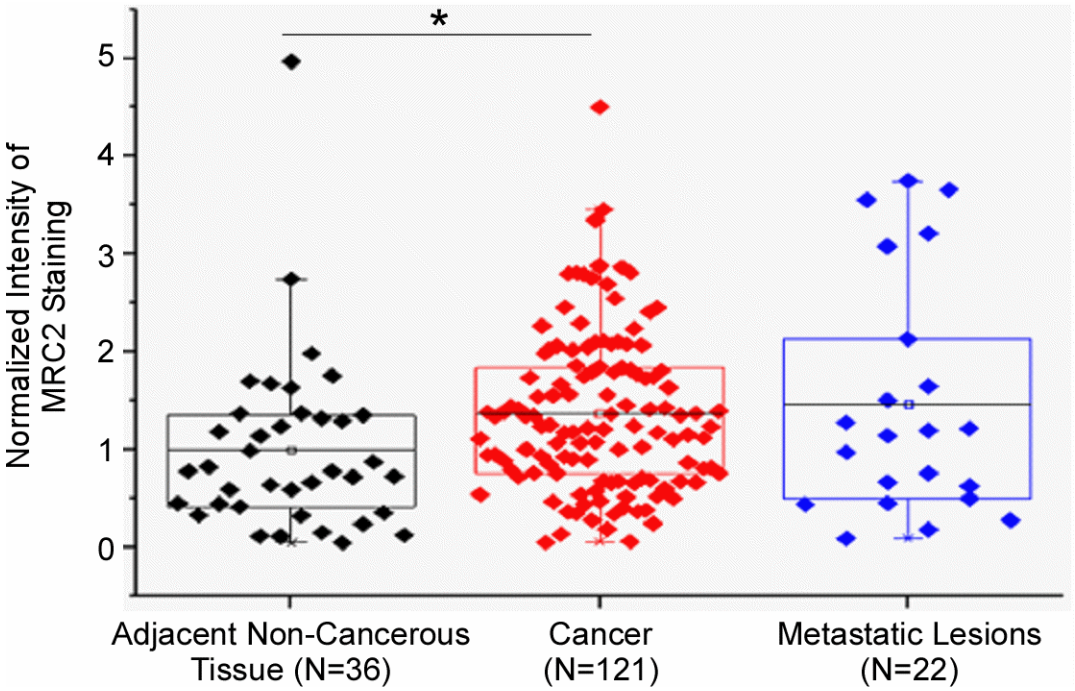

Figure 18. MRC2 staining *in vivo*. Quantification of MRC2 staining using immunohistochemistry in Cancer tissues, metastatic lesions and adjacent non-cancerous tissues.

Functional role of MRC2

After confirming the overexpression of MRC2 in pancreatic cancer, we wanted to identify the role of MRC2 in the elevated migratory phenotype conferred by TGF-β induced EMT. To test for MRC2 function, a couple of shRNA constructs were used to downregulate MRC2 along with a scrambled RNA construct as a control in Panc-1. Panc-1, a pancreatic cancer cell line was used for the study because of its ability to undergo TGF-β mediated EMT and shows MRC2 overexpression along with EMT induction. Even though Panc-1 is inclined more towards the mesenchymal side based on its expression of EMT markers. At the same time, the morphology of Panc-1 is not completely mesenchymal-like and hence provides an opportunity to turn it more-mesenchymal with TGF-β treatment. Knockdowns were confirmed by western blots (Figure 19A, 19B). Also, the cell morphologies were not significantly different, with the cells attaining a scattered look with spindle formation upon TGF-β treatment (Figure 19C), confirming that full MRC2 upregulation is not required for EMT induction.

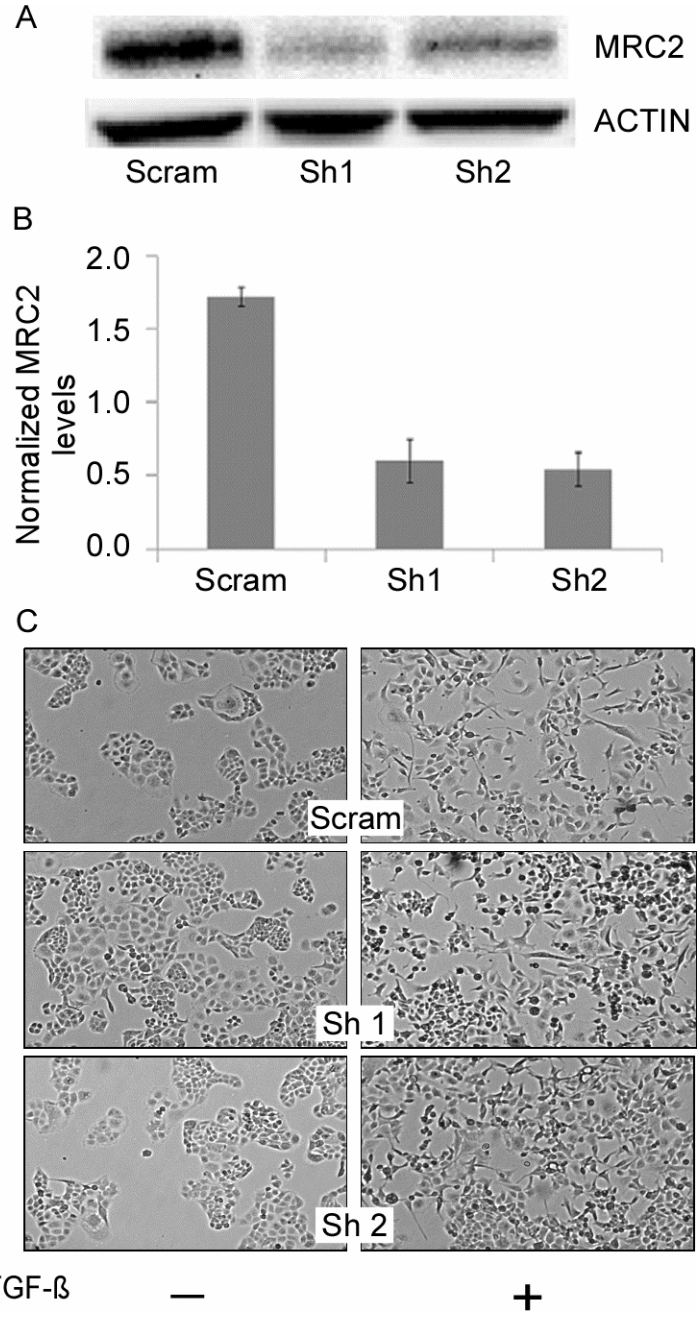

Figure 19. MRC2 Knockdown. Confirmation of MRC2 knockdown (A) Western Blot (B) Quantification of MRC2 levels relative to actin in the scrambled and shRNA constructs. (C) Morphology of Panc-1 after MRC2 knockdown.

MRC2 downregulation did not affect cell migration in the absence of a chemical gradient, as assessed by a scratch assay (Figure 20A). Cell proliferation was also found to be equivalent between the 3 cell lines created (Figure 20B), confirming a lack of effect of MRC2 on non-directional migration of cells. However, using matrigel-coated invasion chambers, we observed a significant reduction in cellular invasion through the matrigel layer upon downregulation of MRC2 (Figure 20D). This is in accordance to the role of MRC2 as observed in other systems. At the same time, using Boyden chambers, we observed an identical reduction of chemotaxis of cells towards the chemo attractant, which was serum in this case (Figure 20C). However, the number of cells that invaded in the invasion assay and the number of cells that migrated in the chemotaxis assay were similar. The chemotaxis assay, suggests that MRC2 has a role in directional migration. Given that invasion assay is a combination of directional migration and degradation of matrigel and MRC2 is known to have a role in matrix remodeling especially collagen degradation, an additive effect was expected from the chemotaxis results. However, the number of cells that invaded were similar to the number of cells that migrated in the chemotaxis assay showing no additive effect of the MRC2 degrading the ECM. Similar results were also observed in Takahashi et al. [130]. There are two possibilities in this regard, the residual MRC2 might be sufficient for degrading the matrigel layer, or MRC2 might be primarily involved in chemotactic rather than invasive mechanisms. Therefore, MRC2 might be involved in the directional migration of cells in a chemical gradient and can help cancer cells make their way through the extracellular matrix. However, more research is needed to identify the contribution of the chemotactic ability and the ability to degrade ECM to this phenotype.

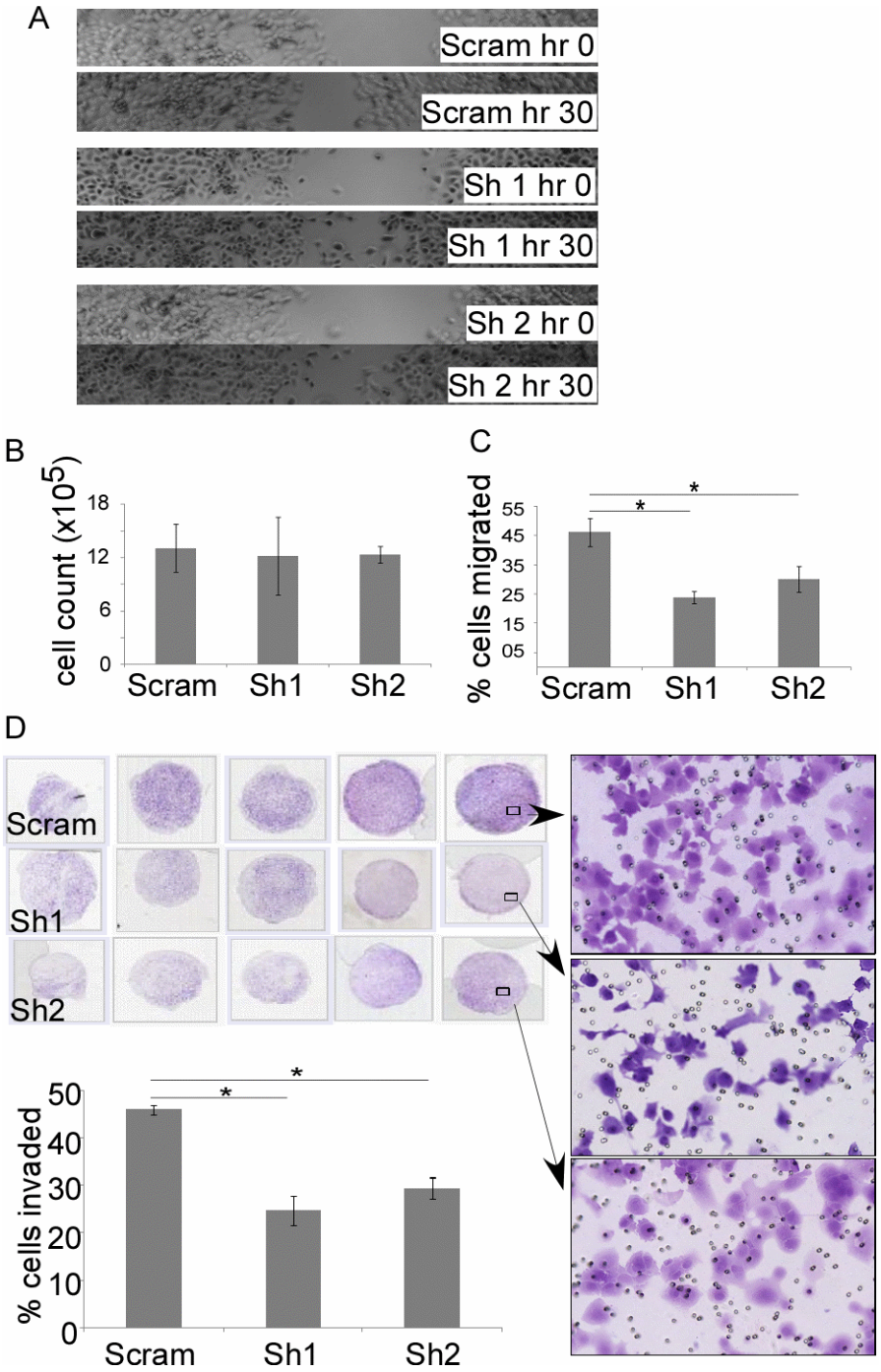

Figure 20. MRC2 contribution to migration, chemotaxis, and invasion. (A) Scratch assay. The cells were treated with TGF-β1 for 72 hours before the initiation of the scratch to induce MRC2 expression. (B) Cell proliferation rates. Cell counts after 96 hours of growth were quantified and averaged over three repeats. (C) Chemotaxis assay. A Boyden chamber was used to quantify the migration of cells through 8 μm pores toward the chemoattractant (10% fetal bovine serum) in the bottom chamber.

Figure 20. (cont'd) The percentage of migrated cells was averaged over four experiments, with each experiment having at least three technical repeats. (D) Invasion assay. The representative images show the invasion of cells through Matrigel. The cells were fixed on the membrane, stained using crystal violet, and manually counted. Five different frames from each chamber were counted and averaged, and the values from five different chambers were averaged. In each column graph, the error bars represent standard deviations over the repeat experiments, and the asterisks indicate significant differences ($p < 0.05$, Student's t test).

Prognostic value of MRC2

A consequence of the above observations could be reduced survival in association with MRC2 upregulation. To test that relationship, MRC2 staining was scored in a blinded fashion, using the approach used in the previous section, on three TMAs containing 144 different pancreatic cancer tissues in triplicate (three cores per block) for which survival information was available. These tissues were different from the ones used in the previous section.

Short survivors (63 subjects) were classified as those who succumbed to the disease within 12 months, whereas long survivors (81 subjects) were those with a life span of over 30 months from the time of surgery. No relationship between MRC2 staining and survival was found when examining the entire tissue (Figure 21A). The traditional way of immunohistochemistry analysis, where the analyst grades the tissue as either 1+, 2+ or 3+ based on the level of intensity was also used wherein the images were scored for both the stromal compartment and the epithelial cancer cells. In the stromal cells, high MRC2 staining (3+) was significantly associated with short survival ($p < 0.05$, Fisher's Exact Test) (Figure 21B). This relationship suggests that MRC2 upregulation in the cancer-associated stroma contributes to the progression of pancreatic cancer. No relationship was found between MRC2 expression in the cancer cells and prognosis even though *in vitro* studies hint towards a role of MRC2 in the invasion and Chemotaxis of cells. The potentially transient nature of the upregulation and the occurrence in a small subset of cells may preclude associations with prognosis.

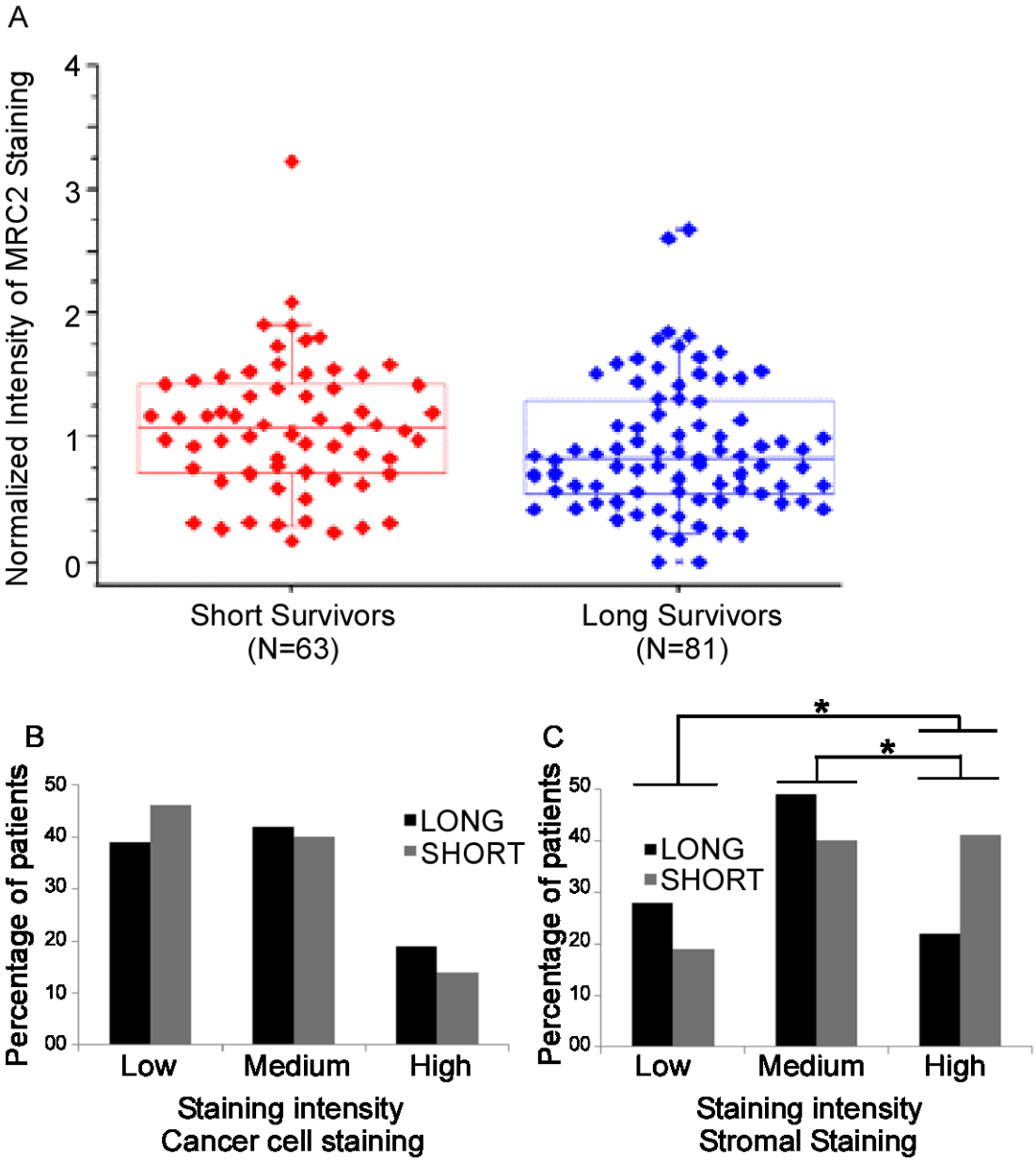

Figure 21. Association of MRC2 staining with prognosis. (A) Quantifiation of staining intensity in blinded cancer samples for prognosis. (B, C) The percentage of long survivors (>30 months) or short survivors (<12 months) was determined for each staining intensity in both the cancer cells (B) and the stromal cells (C). The asterisks indicate a significant difference ($p<0.05$, Fisher's Exact Test) for comparing the ratios of long to short survivors between the staining intensities.

MRC2/Epcam dual positive cells as prognostic biomarker

In a tumor, it is only a subset of cells that undergo EMT and those cells are responsible for spreading metastatic lesions and cause poor prognosis. However while grading, a pathologist looks for the overall staining of the cancer cells, an overwhelming majority of which is in an epithelial state and hence negative for MRC2. Hence, instead of looking qualitatively at an image from a pathologist's point of view, if we can quantify the number of cancer cells that overexpress MRC2, it might be more informative. So, the aim was to identify individual MRC2 positive cancer cells. Dual staining of MRC2 and Epcam was decided to use to identify such cells. Epcam is an epithelial cell marker that is absent in mesenchymal cells. However, when cells undergo EMT, their epcam levels is reduced but not lost, making it the marker of choice for isolating circulating tumor cells. At the same time, MRC2 is not normally expressed in epithelial cells unless they have undergone EMT. Hence cells that express both MRC2 and Epcam will most likely be cancer cells that have undergone EMT. The size and shape of the nuclei can be used to verify its cancerous origin. To identify these two molecules, we tried various different methods starting with dual immunohistochemistry. DAB and alkaline phosphatase were used to provide brown and red color for Epcam and MRC2 respectively. The Nuance system was used to differentiate between the spectral properties of these dyes and the colors were permanent with no bleaching. However, it is not an automated system and requires manual focusing on every tissue core. Another major hurdle we ran into was the inability of the software to optimally differentiate between the red and brown stains in regions which overlapped thereby defeating the purpose of the program. The failure of the program can be attributed to the overlapping

spectral properties of the two dyes. Another major issue that we ran into was the difference in the quantified numbers between consecutive tissue sections making it unreliable.

We also tried fluorescence using a microarray scanning machine as the sizes of TMAs and microarrays are identical. Alexa dye conjugated secondary antibodies were used for the fluorescence purposes. The green channel was used to visualize MRC2 while the red channel was used to measure Epcam. No spectral overlaps were identified in this method and the entire image capture method was really fast and an entire TMA could be scanned under 10 minutes. Some of the drawbacks of this method include low resolution, auto fluorescence issues especially in the channel for MRC2 as well as the system's limitation to only two colors. A big advantage of this system was that after scanning the slides for IF purposes, the same slide could be used for Hematoxylin and Eosin (H&E) staining and then the two images could be accurately overlaid with the features matching perfectly. Using this method, we were able to identify cells that were dual positive for Epcam and MRC2. Upon overlaying the images with the H&E, the cells with dual staining looked like cells that were in the process of migrating as they were breaking away from the ductal structures and their cellular structures also looked mesenchymal-like. This supported our hypothesis that migrating cancer cells overexpress MRC2 (Figure 22).

Unfortunately, red blood cells auto-fluoresce in both the channels giving false positive signals. To counter this problem, the absence of nuclei in red blood cells was utilized to

discriminate signals from red blood cells from the nucleated cells. To include a third channel for the nucleus, we moved our system to confocal microscopy. The advantages included much better resolution and the availability of 4 different channels which gave us the ability to stain for nucleus along with MRC2 and Epcam (Figure 23, 24).

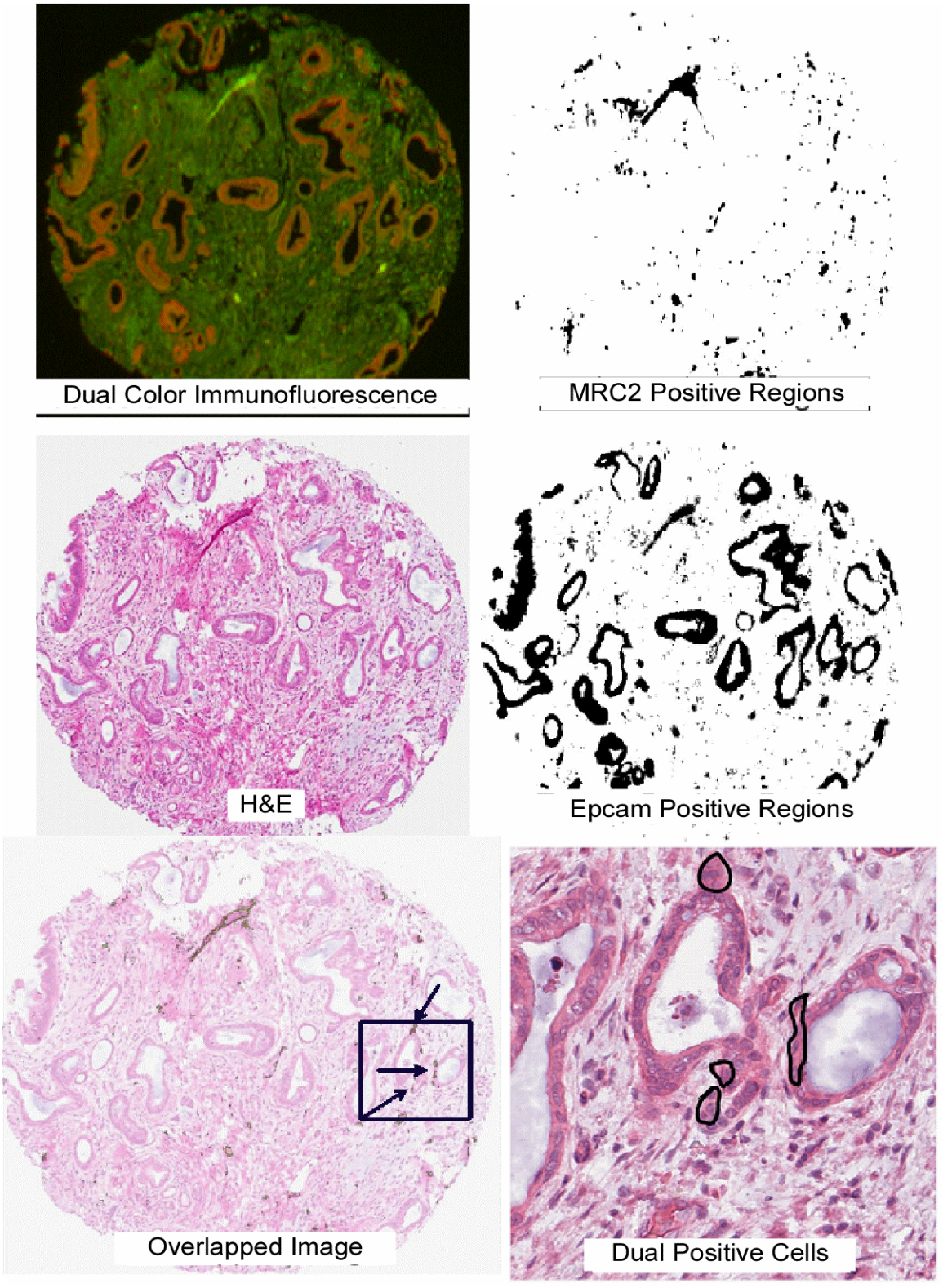

Figure 22. Dual fluorescence images along with H&E.

Figure 22. (cont'd) The fluorescent image along with the positive pixels identified by ImageJ in each channel along with the H&E as well as the overlapped image.

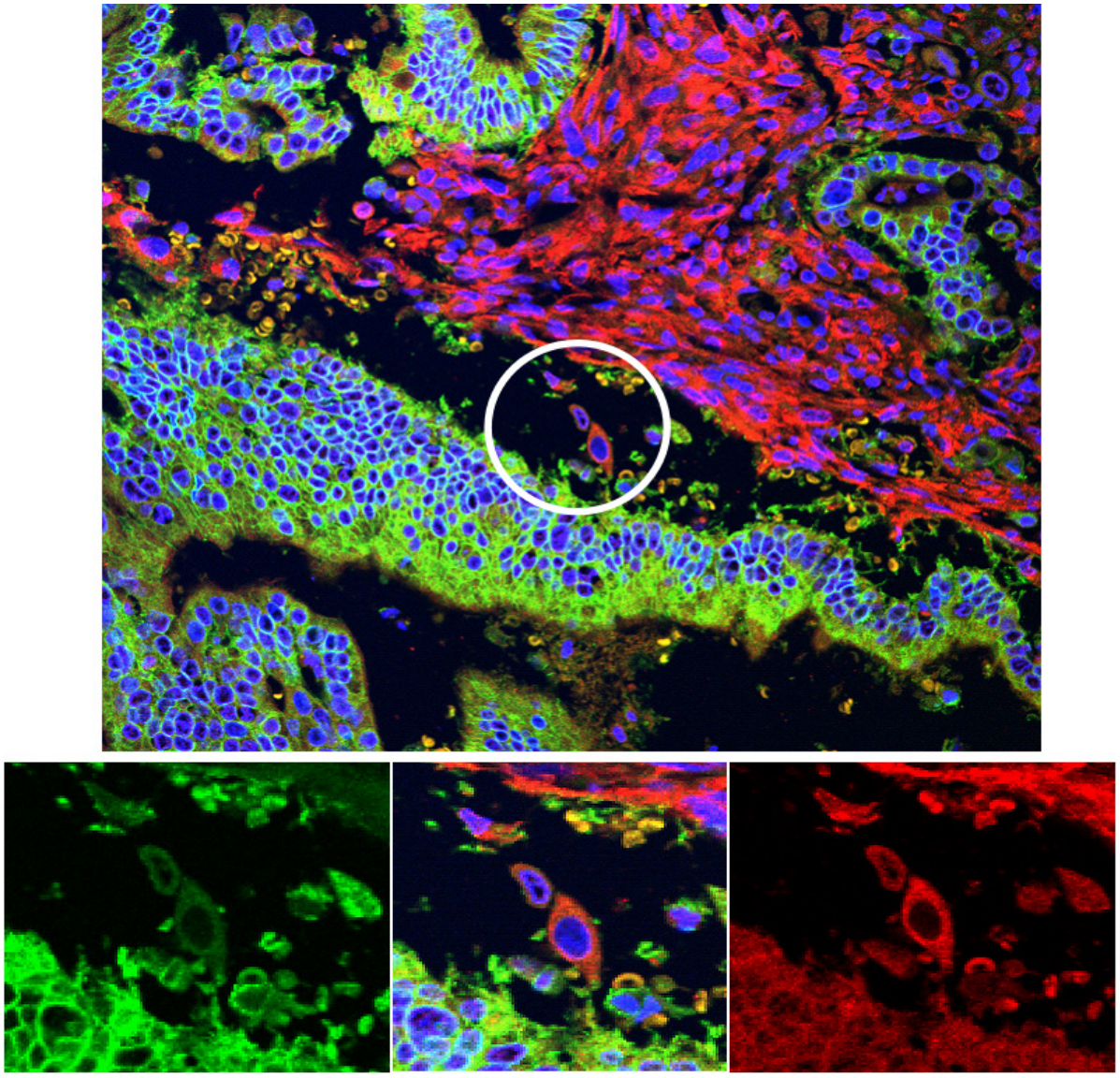

Figure 23. Confocal Images showing presence of probable dual positive cancer cells. Red- MRC2, Green-Epcam and blue-Nucleus.

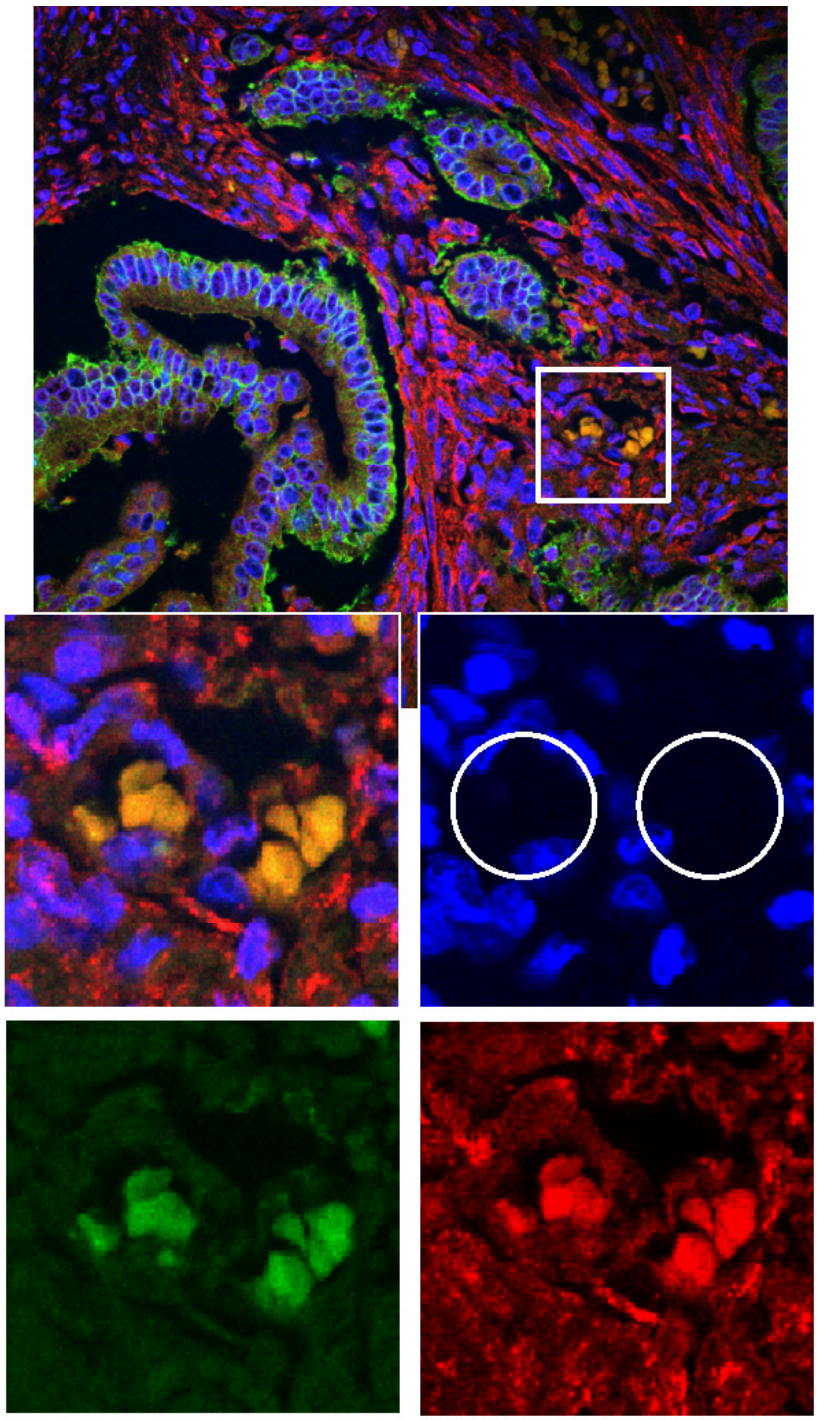

Figure 24. Confocal Images able to distinguish red blood cells from true positives. The yellow region observed in upper left corner are RBCs. RBCs auto-fluoresce but do not have a nuclei, which can be used to tag them as false positive.

Following the staining of tissues, a major and time consuming exercise is the thresholding of images to identify positive and negative staining regions. Generally, this is achieved by staining a consecutive tissue section with the same secondary antibodies minus the primary antibody. Not only is this process a hindrance in cases of limited tissue, it is also a really time consuming process. The FFPE (Formalin fixed and paraffin embedded) tissues in a TMA are generally collected over a period of time and the amount of fixation on each tissue is also different depending on the measure of the tissue. Hence, given the variables of time and fixation, it was not surprising that a single threshold did not work for all tissues. So, careful examination of the adjacent tissue section to identify thresholds for each tissue and then apply them to the actual stained tissues was a really labor intensive and error prone method depending exclusively on the decision of the personnel. So, we realized the need for a thresholding program which, while staying within the confines of a formula will set individual thresholds for each tissue. Also, existing image analysis programs for determining co-localization worked very well for cell lines which are regularly shaped and have distinct boundaries and uniform nuclei. However, in primary tissues, with multiple different cell types, irregular nuclei shape, presence of fibrotic mass, the performance comes down markedly. Hence, we developed a MATLAB based program FITC to address the following requirements,

- Automation of individual thresholding.
- Calculation of staining percentage in each fluorescent channel

  and
- Calculate the colocalization between the three channels.

The thresholding part of the program used the formula ‘threshold=Median of means + X*standard deviation’. The variable X can be set by the operator for each color channel thereby helping the program to be optimized for any system. We utilized a TMA to optimize the system; dividing a subset of those images into a training set and a validation set. The images were evaluated by a board-certified pathologist, Dr. Galen Hostetter who identified positive and negative regions on the tissues. Utilizing the program, we then varied the variable ‘X’ from the formula to identify the optimal ‘X’ value which identifies the true positives as identified by Dr. Hostetter while minimizing the negative regions. Once, the optimal X value was identified, we applied the same variable to the validation set to verify whether the X value can be applied to the actual samples. Using this process, the values of X were set for all the three channels for DNA, epcam and MRC2.

Then the values were applied to analyze 102 pancreatic cancer samples in triplicates, spread over two different TMAs provided by Dr. Peter Allen from Memorial Sloan Kettering. The samples on these TMAs were collected from patients who survived over 30 months or succumbed to the disease within 12 months. By excluding samples from patients with survival between 12-30 months, it minimizes bias due to differences in treatment regimens and also other factors like age. The TMAs were blindly evaluated and the co-localization percentage of each core was calculated, followed by averaging over the three repeats.

Representative images from the program show its ability to identify genuine dual positive cells as well as remove signals from red blood cells which lack nuclei. Also the ability to perform H&E staining on the same tissues gives us more information about the morphology of the cells (Figure 25). This will help us in identifying whether the subset of aggressive cells is preferentially enriched at a particular location like the invasive front of a tumor. This process improves current methods of immunohistochemistry/immunofluorescence by allowing us to looking at multiple markers and test their relationship with a phenotype. The results from these samples are being analyzed currently for testing the second hypothesis that the presence of mesenchymal-like cancer cells is an indicator of poor prognosis and shows that individual cancer cells expressing MRC2 are a better prognostic marker than total MRC2 staining.

The advantages of the system include the ability to quantify the results allowing more accurate statistical comparisons and various types of mathematical transformations to the data. Along with the advantage of being high throughput, it is able to pick up small subpopulations of cell showing staining which is an extremely difficult and cumbersome process for a pathologist. It also takes away the variability that is associated with the subjective view of a pathologist.

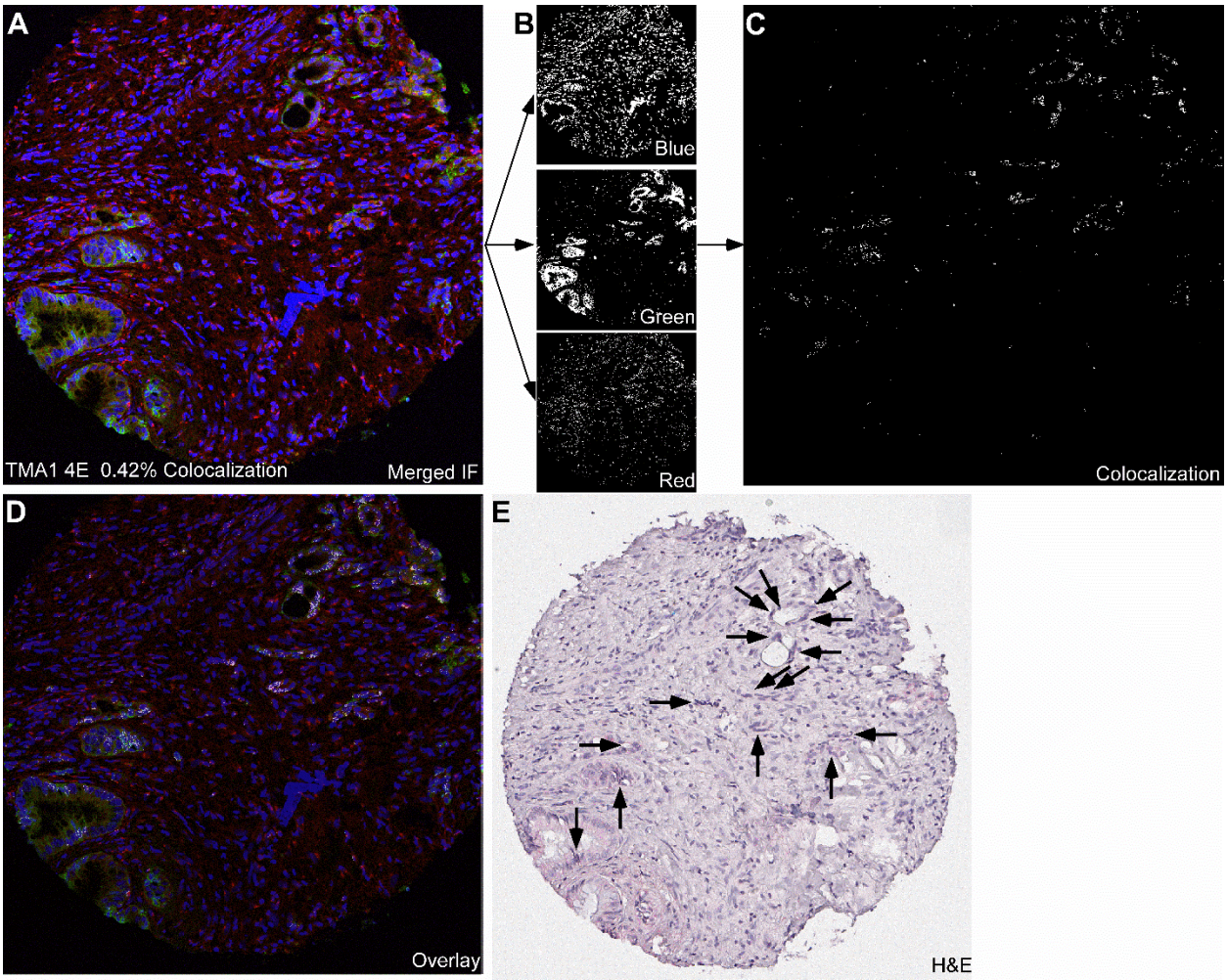

Figure 25. FITC results. (A) Confocal Image showing staining MRC2 staining in red, Epcam staining in green and nuclear stain in blue. (B) Output images of FITC program showing the pixels over the threshold in each of the three channels individually. (C) Image showing the colocalization of all three channels. (D) Overlay of the colocalized pixels over the fluorescent image. The colocalization pixels are in white. (E) H&E image of the same section showing the cells which have both Epcam and MRC2 staining.

Discussion

Pancreatic cancer cells with mesenchymal features tend to be more invasive and resistant to treatment than those with epithelial features. The identification of the molecular characteristics of mesenchymal-like cancer cells is an important step in developing therapies that might have more durable responses. Similar to our approach in the previous chapter, we identified the molecular differences between epithelial and mesenchymal-like cells but at a transcriptional level. We determined that during TGF-β induced EMT; there is a significant change in the glycosylation pattern of mesenchymal-like cells, especially with the genes involved in the process of sulfation. Another major change was observed in MRC2, a gene that binds sulfated molecules and is an integral part of ECM remodeling. Our current study showed that MRC2 upregulation is a common feature among primary pancreatic cancer cells, as well as tumor-associated stromal cells, which uniformly are mesenchymal. Upregulation of MRC2 in cancer cells seems to play a role in chemotactic migration and invasion *in vitro*. Furthermore, peritumoral expression of MRC2 was observed suggesting a local activation of the microenvironment by the cancer cells in preparation for invasion. The high prevalence in pancreatic tumors and the potential mechanistic involvement in cancer invasion warrant the further study of MRC2 in pancreatic cancer progression.

To test our second hypothesis, we looked at the correlation of MRC2 staining with prognosis. Using immunohistochemistry, stromal MRC2 staining was found to be correlative of poor prognosis. MRC2-mediated matrix turnover and remodeling by the stromal cells could promote cancer cell migration [113-115, 131], and collagen

breakdown by MRC2 also could affect cancer cells through the release of trapped signaling factors or bioactive fragments. Macrophages were found to be one of the subset of cells that express MRC2 in the stromal cells. Further studies regarding the role of macrophages especially the macrophages expressing MRC2 might lead to better understanding of the stromal MRC2's role in the invasion and metastatic cascade.

The alteration of protein sulfation during the process of EMT and the simultaneous upregulation of MRC2, known to bind sulfated molecules also suggest a role of MRC2 in cellular communication and signal transduction. The expression of MRC2 on cancer cells also could contribute to cancer progression through the promotion of chemotactic migration and invasion, as observed *in vitro*. However, no association was found between MRC2 expression in the cancer cells and prognosis. The lack of association between cancer cell MRC2 expression and prognosis could be due to only a small subset of cells undergoing the process whereas the pathologist looks at the bulk of the tissue. We have developed a program, FITC to calculate individual cancer cells that overexpress MRC2 from tissue microarrays. This would remove the variability associated with manual grading and also pick up signals oblivious to the human eye. We used confocal microscopy using a combination of Epcam, an epithelial marker and MRC2, a traditionally mesenchymal marker to identify mesenchymal-like cancer cells in primary tissues. Experiments are underway to test the relationship of cancer cells expressing MRC2 with pancreatic cancer prognosis.

Recent work showed that EMT derived dissemination of pancreatic cancer cells may happen even before the development of a defined tumor mass [29], highlighting the need for treatment options that are effective against invasive cancer cells which may develop through EMT. MRC2 provides a suitable target for targeting these subset of cells as it has been shown to be overexpressed in cancer cells that undergo TGF-β mediated EMT. With results showing the association of MRC2 with invasiveness *in vitro* as well as the association of stromal MRC2 with poor prognosis, the endocytic pathway of MRC2 could provide a route to selectively deliver drugs to the mesenchymal like subpopulation of cancer cells and associated stroma with minimal side effects.

CHAPTER FOUR: SYNTHESIS AND FUTURE WORK

Summary

Pancreatic cancer cells with mesenchymal features tend to be more invasive and resistant to treatment than those with epithelial features. The identification of the molecular characteristics of mesenchymal cancer cells is an important step in developing therapies that might have more durable responses. The goal of this research was to test the hypotheses that mesenchymal cancer cells have distinct gene expression features and genetic alterations relative to their epithelial counterparts and that the presence of mesenchymal cancer cells in tumors indicates poor prognosis. We tested the first hypothesis using gene expression profiling and genome-wide CGH. Both approaches supported the hypothesis. We tested the second hypothesis through studies of the molecule MRC2. We developed a novel approach of detecting co-expression of MRC2 and an epithelial marker to show that MRC2 is expressed in a subpopulation of cancer cells in primary tissue, and we currently are testing the hypothesis that the dual-expression feature is an indicator of poor prognosis. The confirmation of this hypothesis would establish a new way to detect an aggressive subpopulation of cancer cells and would point to a viable target for eliminating those cells.

Copy number differences between epithelial and mesenchymal cancer cells

Using whole-genome CGH measurements on 26 pancreatic cancer cell lines with either an epithelial (17 cell lines) or mesenchymal (9 cell lines) phenotype *in vitro*, we identified 20 genes with differential copy numbers between the two groups. Previous studies have employed similar means to identify genes associated with an aggressive

phenotype. However, most of their findings are present in a very small subset of cells and hence have been unsuccessful in developments towards a cure for pancreatic cancer. We designed our algorithm to identify alterations that are present in at least 50% of cell lines in either the epithelial or mesenchymal group, and they have a minimum of two-fold enrichment in the prevalence between the two groups. All 20 alterations (18 deletions and 2 amplifications) were more prevalent in the mesenchymal group, confirming the advanced nature of this cellular subtype. CDKN2A was altered in more than 50% of both groups, but co-deletions in neighboring genes, and concomitant loss of gene expression, were more prevalent in the mesenchymal group, suggesting that the size of the loss around CDKN2A affects cell phenotype. Whole-genome CGH on 11 primary cancer tissues revealed that the 20 genes were altered at a higher prevalence (up to 55% of the cases for certain genes) than randomly-selected sets of 20 genes, with the same direction of alteration as in the cell lines. The identified genes have functions ranging from glycosylation to cellular adhesion; functions known to play important roles in cellular aggressiveness. Another gene identified by our study, KIAA1797 has since been identified by Brockschmidt et al. to have a role in cell migration and invasion. These findings support the idea that specific genetic alterations enable phenotype plasticity and provide promising candidate genes for further research.

Gene expression changes during EMT

The aim of this study was to identify the molecular differences between epithelial and mesenchymal cells and identify a gene that can not only be used to identify mesenchymal cancer cells but also be used to target it with minimal side effects. Using

gene expression microarrays in a TGF-β-induced EMT model, we determined that glycosylation related genes especially those related to sulfation are upregulated during a transition to a mesenchymal phenotype. At the same time, MRC2, a transmembrane protein with affinity for sulfated molecules and a role in ECM remodeling was also upregulated. We validated the upregulation of MRC2 in primary tissues and also determined that it increases the invasive ability of cancer cells *in vitro*. The involvement of MRC2 in the invasive capability of cells reveals that it might be one of the multiple ways by which the process of EMT increases the metastatic ability of cancer cells.

MRC2 association with prognosis

Using immunohistochemistry, stromal MRC2 staining was found to be associated with poor prognosis of pancreatic cancer. MRC2-mediated matrix turnover and remodeling by the stromal cells could promote cancer cell migration, through the release of trapped signaling factors or bioactive fragments. Even though *in vitro* experiments showed that higher MRC2 levels can lead to increased invasion and metastasis, no association was found between MRC2 levels and prognosis in primary tissues. One of the reasons for this may be only a small subset of cancer cells undergo the process whereas the pathologist looks at the bulk of the tissue. Using a dual staining model of epcam and MRC2, we were able to identify individual mesenchymal cancer cells in primary tissues. These cells looked morphologically different that their peers. The same model was used to test the association between the presence of mesenchymal cancer cells and prognosis. This led to the development of a new program FITC to analyze such fluorescent images.

Fluorescence intensity thresholding and colocalization

With the aim of identifying a minority population in a tumor tissue; a need arose for swift image analysis, functional capabilities like colocalization along with minimal operator variation. Keeping all these requirements in mind, the FITC program was developed to determine individual thresholds for each image core to account for differences between FFPE tissues. At the same time, it calculates the number of epcam and MRC2 positive pixels as well as colocalized pixels. The program also helps remove false positives in the form of red blood cells which autofluoresce. Using this program, we are testing whether MRC2/Epcam colocalization is a better marker to predict pancreatic cancer prognosis than MRC2 alone. This will also evaluate the value of looking at multiple markers to test as biomarkers.

Future studies

If MRC2 overexpression in cancer cells is found to be associated with poor prognosis, it will set a proper background for testing the hypothesis that targeting the mesenchymal-like cancer cells will improve the prognosis of pancreatic cancer. Utilizing the endocytic pathway of MRC2, drugs can be specifically delivered to a particular subset of tumor cells. Because of the endocytosis, drugs which cannot pass through the cell membrane can be used. Also, being a targeted therapy, this will facilitate the administration of highly toxic drugs which cannot be administered in standard chemotherapy.

This could be achieved by conjugating a drug to a compound that is endocytosed by MRC2. This will provide entry for the drug into the cell. Alternatively, the drug can also

be conjugated to an antibody against MRC2 as antibodies against MRC2 have been shown to be endocytosed. If drugs are acid labile, endosomal escape of drugs can be acquired by the use of cationic molecules like poly (DL-lactide-co-glycolide) (PLGA) which can carry small drug molecules and has been previously ratified to escape the endosomal compartment.

Since the stromal MRC2 staining was also found to be associated with poor prognosis and macrophages have been found to be one of the MRC2 carriers in the stromal compartment, Dr. Hostetter is checking the role of MRC2 expressing macrophages in cancer invasion and metastasis. Additionally, the mechanism by which MRC2 affects invasion and chemotaxis is a question that warrants further research.

If the MRC2 molecule is not successful in conferring better prognosis because of its transient nature, we have also identified genomic changes like KIAA1797 that occur in selective cells that undergo EMT. These molecules can be tested for their association with poor prognosis using FISH assay and the best candidates can be used for targeting cancer cells. These being permanent changes can counter the problems associated with a transient change like MRC2. Since most of them are deletions, their downstream signaling molecules might be an appropriate choice for targeting. Also, the role of the 20 genes identified in the CGH study can be tested for their role in the induction of EMT.

The FITC can be used to combine various candidate molecules to look for complementary or co expression of molecules in search for better biomarkers. For example, cancer cells that do not express CA19-9 can be analyzed for expression of other complementary biomarkers using the program to identify false negatives. Also, Epcam might not be the most reliable marker to identify mesenchymal like cells and in that case, other molecules smooth muscle actin and others can be tried in its place.

These studies will help in the identification of better drug targets as well as diagnostic tools to eventually improve not only the prognosis but also the quality of life of pancreatic cancer patients.

BIBILIOGRAPHY

BIBILIOGRAPHY

1. FREDERIC H. MARTINI MJT: **HUMAN ANATOMY**: PRENTICE HALL; 1997.
2. SLACK JM: **DEVELOPMENTAL BIOLOGY OF THE PANCREAS**. *DEVELOPMENT* 1995, **121**(6):1569-1580.
3. FREDERIC H. MARTINI EFB: **ESSENTIALS OF ANATOMY AND PHYSIOLOGY**: PRENTICE-HALL INCORPORATED; 1997.
4. MURTAUGH LC: **PANCREAS AND BETA-CELL DEVELOPMENT: FROM THE ACTUAL TO THE POSSIBLE**. *DEVELOPMENT* 2007, **134**(3):427-438.
5. PIELER T, CHEN Y: **FORGOTTEN AND NOVEL ASPECTS IN PANCREAS DEVELOPMENT**. *BIOL CELL* 2006, **98**(2):79-88.
6. PREVENTION CFDCA: **NATIONAL DIABETICS STATISTICAL REPORT, 2014**. IN.; 2014.
7. HYUN JJ, LEE HS: **EXPERIMENTAL MODELS OF PANCREATITIS**. *CLIN ENDOSC*, **47**(3):212-216.
8. **NATIONAL CANCER INSTITUTE** [HTTP://WWW.CANCER.GOV/CANCERTOPICS/TYPES/PANCREATIC]
9. SCHMID RM: **ACINAR-TO-DUCTAL METAPLASIA IN PANCREATIC CANCER DEVELOPMENT**. *J CLIN INVEST* 2002, **109**(11):1403-1404.
10. RYAN DP, HONG TS, BARDEESY N: **PANCREATIC ADENOCARCINOMA**. *N ENGL J MED*, **371**(11):1039-1049.
11. HIDALGO M: **PANCREATIC CANCER**. *N ENGL J MED*, **362**(17):1605-1617.
12. TUMMALA P, JUNAIDI O, AGARWAL B: **IMAGING OF PANCREATIC CANCER: AN OVERVIEW**. *J GASTROINTEST ONCOL*, **2**(3):168-174.
13. BARDEESY N, DEPINHO RA: **PANCREATIC CANCER BIOLOGY AND GENETICS**. *NAT REV CANCER* 2002, **2**(12):897-909.
14. REICHERT M, RUSTGI AK: **PANCREATIC DUCTAL CELLS IN DEVELOPMENT, REGENERATION, AND NEOPLASIA**. *J CLIN INVEST*, **121**(12):4572-4578.
15. WAUTERS E, SANCHEZ-AREVALO LOBO VJ, PINHO AV, MAWSON A, HERRANZ D, WU J, COWLEY MJ, COLVIN EK, NJICOP EN, SUTHERLAND RL *ET AL*: **SIRTUIN-1 REGULATES ACINAR-TO-DUCTAL METAPLASIA AND SUPPORTS CANCER CELL VIABILITY IN PANCREATIC CANCER**. *CANCER RES*, **73**(7):2357-2367.
16. DEY P, RACHAGANI S, VAZ AP, PONNUSAMY MP, BATRA SK: **PD2/PAF1 DEPLETION IN PANCREATIC ACINAR CELLS PROMOTES ACINAR-TO-DUCTAL METAPLASIA**. *ONCOTARGET*, **5**(12):4480-4491.

17. HRUBAN RH, WILENTZ RE, KERN SE: **GENETIC PROGRESSION IN THE PANCREATIC DUCTS**. *AM J PATHOL* 2000, **156**(6):1821-1825.

18. WILENTZ RE, IACOBUZIO-DONAHUE CA, ARGANI P, MCCARTHY DM, PARSONS JL, YEO CJ, KERN SE, HRUBAN RH: **LOSS OF EXPRESSION OF DPC4 IN PANCREATIC INTRAEPITHELIAL NEOPLASIA: EVIDENCE THAT DPC4 INACTIVATION OCCURS LATE IN NEOPLASTIC PROGRESSION**. *CANCER RES* 2000, **60**(7):2002-2006.

19. HANAHAN D, WEINBERG RA: **THE HALLMARKS OF CANCER**. *CELL* 2000, **100**(1):57-70.

20. HANAHAN D, WEINBERG RA: **HALLMARKS OF CANCER: THE NEXT GENERATION**. *CELL*, **144**(5):646-674.

21. HIYAMA E, KODAMA T, SHINBARA K, IWAO T, ITOH M, HIYAMA K, SHAY JW, MATSUURA Y, YOKOYAMA T: **TELOMERASE ACTIVITY IS DETECTED IN PANCREATIC CANCER BUT NOT IN BENIGN TUMORS**. *CANCER RES* 1997, **57**(2):326-331.

22. ITAKURA J, ISHIWATA T, FRIESS H, FUJII H, MATSUMOTO Y, BUCHLER MW, KORC M: **ENHANCED EXPRESSION OF VASCULAR ENDOTHELIAL GROWTH FACTOR IN HUMAN PANCREATIC CANCER CORRELATES WITH LOCAL DISEASE PROGRESSION**. *CLIN CANCER RES* 1997, **3**(8):1309-1316.

23. MAITRA A, HRUBAN RH: **PANCREATIC CANCER**. *ANNU REV PATHOL* 2008, **3**:157-188.

24. HAY ED: **AN OVERVIEW OF EPITHELIO-MESENCHYMAL TRANSFORMATION**. *ACTA ANAT (BASEL)* 1995, **154**(1):8-20.

25. LAMOUILLE S, XU J, DERYNCK R: **MOLECULAR MECHANISMS OF EPITHELIAL-MESENCHYMAL TRANSITION**. *NAT REV MOL CELL BIOL*, **15**(3):178-196.

26. KALLURI R, WEINBERG RA: **THE BASICS OF EPITHELIAL-MESENCHYMAL TRANSITION**. *J CLIN INVEST* 2009, **119**(6):1420-1428.

27. KALLURI R: **EMT: WHEN EPITHELIAL CELLS DECIDE TO BECOME MESENCHYMAL-LIKE CELLS**. *J CLIN INVEST* 2009, **119**(6):1417-1419.

28. KATSUNO Y, LAMOUILLE S, DERYNCK R: **TGF-BETA SIGNALING AND EPITHELIAL-MESENCHYMAL TRANSITION IN CANCER PROGRESSION**. *CURR OPIN ONCOL*, **25**(1):76-84.

29. RHIM AD, MIREK ET, AIELLO NM, MAITRA A, BAILEY JM, MCALLISTER F, REICHERT M, BEATTY GL, RUSTGI AK, VONDERHEIDE RH *ET AL*: **EMT AND DISSEMINATION PRECEDE PANCREATIC TUMOR FORMATION**. *CELL* 2012, **148**(1-2):349-361.

30. PHILIP PA: **TARGETED THERAPIES FOR PANCREATIC CANCER**. *GASTROINTEST CANCER RES* 2008, **2**(4 SUPPL):S16-19.

31. KINDLER HL, FRIBERG G, SINGH DA, LOCKER G, NATTAM S, KOZLOFF M, TABER DA, KARRISON T, DACHMAN A, STADLER WM *ET AL*: **PHASE II TRIAL OF BEVACIZUMAB PLUS GEMCITABINE IN PATIENTS WITH ADVANCED PANCREATIC CANCER**. *J CLIN ONCOL* 2005, **23**(31):8033-8040.

32. MOORE MJ, GOLDSTEIN D, HAMM J, FIGER A, HECHT JR, GALLINGER S, AU HJ, MURAWA P, WALDE D, WOLFF RA *ET AL*: **ERLOTINIB PLUS GEMCITABINE COMPARED WITH GEMCITABINE ALONE IN PATIENTS WITH ADVANCED PANCREATIC CANCER: A PHASE III TRIAL OF THE NATIONAL CANCER INSTITUTE OF CANADA CLINICAL TRIALS GROUP**. *J CLIN ONCOL* 2007, **25**(15):1960-1966.

33. HERMANN PC, HUBER SL, HERRLER T, AICHER A, ELLWART JW, GUBA M, BRUNS CJ, HEESCHEN C: **DISTINCT POPULATIONS OF CANCER STEM CELLS DETERMINE TUMOR GROWTH AND METASTATIC ACTIVITY IN HUMAN PANCREATIC CANCER**. *CELL STEM CELL* 2007, **1**(3):313-323.

34. RASHEED ZA, YANG J, WANG Q, KOWALSKI J, FREED I, MURTER C, HONG SM, KOORSTRA JB, RAJESHKUMAR NV, HE X *ET AL*: **PROGNOSTIC SIGNIFICANCE OF TUMORIGENIC CELLS WITH MESENCHYMAL FEATURES IN PANCREATIC ADENOCARCINOMA**. *J NATL CANCER INST* 2010, **102**(5):340-351.

35. LI C, HEIDT DG, DALERBA P, BURANT CF, ZHANG L, ADSAY V, WICHA M, CLARKE MF, SIMEONE DM: **IDENTIFICATION OF PANCREATIC CANCER STEM CELLS**. *CANCER RESEARCH* 2007, **67**(3):1030-1037.

36. LI C, WU JJ, HYNES M, DOSCH J, SARKAR B, WELLING TH, PASCA DI MAGLIANO M, SIMEONE DM: **C-MET IS A MARKER OF PANCREATIC CANCER STEM CELLS AND THERAPEUTIC TARGET**. *GASTROENTEROLOGY*, **141**(6):2218-2227 E2215.

37. MANI SA, GUO W, LIAO MJ, EATON EN, AYYANAN A, ZHOU AY, BROOKS M, REINHARD F, ZHANG CC, SHIPITSIN M *ET AL*: **THE EPITHELIAL-MESENCHYMAL TRANSITION GENERATES CELLS WITH PROPERTIES OF STEM CELLS**. *CELL* 2008, **133**(4):704-715.

38. MASUGI Y, YAMAZAKI K, HIBI T, AIURA K, KITAGAWA Y, SAKAMOTO M: **SOLITARY CELL INFILTRATION IS A NOVEL INDICATOR OF POOR PROGNOSIS AND EPITHELIAL-MESENCHYMAL TRANSITION IN PANCREATIC CANCER**. *HUMAN PATHOLOGY* 2010, **41**(8):1061-1068.

39. ARUMUGAM T, RAMACHANDRAN V, FOURNIER KF, WANG H, MARQUIS L, ABBRUZZESE JL, GALLICK GE, LOGSDON CD, MCCONKEY DJ, CHOI W: **EPITHELIAL TO MESENCHYMAL TRANSITION CONTRIBUTES TO DRUG RESISTANCE IN PANCREATIC CANCER**. *CANCER RESEARCH* 2009, **69**(14):5820-5828.

40. ZEISBERG M, HANAI J, SUGIMOTO H, MAMMOTO T, CHARYTAN D, STRUTZ F, KALLURI R: **BMP-7 COUNTERACTS TGF-BETA1-INDUCED EPITHELIAL-TO-MESENCHYMAL TRANSITION AND REVERSES CHRONIC RENAL INJURY**. *NAT MED* 2003, **9**(7):964-968.

41. GREGORY PA, BERT AG, PATERSON EL, BARRY SC, TSYKIN A, FARSHID G, VADAS MA, KHEW-GOODALL Y, GOODALL GJ: **THE MIR-200 FAMILY AND MIR-205 REGULATE EPITHELIAL TO MESENCHYMAL TRANSITION BY TARGETING ZEB1 AND SIP1**. *NAT CELL BIOL* 2008, **10**(5):593-601.

42. SU GH, HILGERS W, SHEKHER MC, TANG DJ, YEO CJ, HRUBAN RH, KERN SE: **ALTERATIONS IN PANCREATIC, BILIARY, AND BREAST CARCINOMAS SUPPORT MKK4**

AS A GENETICALLY TARGETED TUMOR SUPPRESSOR GENE. *CANCER RES* 1998, **58**(11):2339-2342.

43. MOSKALUK CA, HRUBAN RH, KERN SE: **P16 AND K-RAS GENE MUTATIONS IN THE INTRADUCTAL PRECURSORS OF HUMAN PANCREATIC ADENOCARCINOMA**. *CANCER RES* 1997, **57**(11):2140-2143.

44. CALDAS C, HAHN SA, DA COSTA LT, REDSTON MS, SCHUTTE M, SEYMOUR AB, WEINSTEIN CL, HRUBAN RH, YEO CJ, KERN SE: **FREQUENT SOMATIC MUTATIONS AND HOMOZYGOUS DELETIONS OF THE P16 (MTS1) GENE IN PANCREATIC ADENOCARCINOMA**. *NAT GENET* 1994, **8**(1):27-32.

45. JONES S, ZHANG X, PARSONS DW, LIN JC, LEARY RJ, ANGENENDT P, MANKOO P, CARTER H, KAMIYAMA H, JIMENO A *ET AL*: **CORE SIGNALING PATHWAYS IN HUMAN PANCREATIC CANCERS REVEALED BY GLOBAL GENOMIC ANALYSES**. *SCIENCE* 2008, **321**(5897):1801-1806.

46. GOGGINS M, SCHUTTE M, LU J, MOSKALUK CA, WEINSTEIN CL, PETERSEN GM, YEO CJ, JACKSON CE, LYNCH HT, HRUBAN RH *ET AL*: **GERMLINE BRCA2 GENE MUTATIONS IN PATIENTS WITH APPARENTLY SPORADIC PANCREATIC CARCINOMAS**. *CANCER RES* 1996, **56**(23):5360-5364.

47. BASHYAM MD, BAIR R, KIM YH, WANG P, HERNANDEZ-BOUSSARD T, KARIKARI CA, TIBSHIRANI R, MAITRA A, POLLACK JR: **ARRAY-BASED COMPARATIVE GENOMIC HYBRIDIZATION IDENTIFIES LOCALIZED DNA AMPLIFICATIONS AND HOMOZYGOUS DELETIONS IN PANCREATIC CANCER**. *NEOPLASIA (NEW YORK, NY* 2005, **7**(6):556-562.

48. HEIDENBLAD M, SCHOENMAKERS EF, JONSON T, GORUNOVA L, VELTMAN JA, VAN KESSEL AG, HOGLUND M: **GENOME-WIDE ARRAY-BASED COMPARATIVE GENOMIC HYBRIDIZATION REVEALS MULTIPLE AMPLIFICATION TARGETS AND NOVEL HOMOZYGOUS DELETIONS IN PANCREATIC CARCINOMA CELL LINES**. *CANCER RES* 2004, **64**(9):3052-3059.

49. MAHLAMAKI EH, KAURANIEMI P, MONNI O, WOLF M, HAUTANIEMI S, KALLIONIEMI A: **HIGH-RESOLUTION GENOMIC AND EXPRESSION PROFILING REVEALS 105 PUTATIVE AMPLIFICATION TARGET GENES IN PANCREATIC CANCER**. *NEOPLASIA (NEW YORK, NY* 2004, **6**(5):432-439.

50. HOLZMANN K, KOHLHAMMER H, SCHWAENEN C, WESSENDORF S, KESTLER HA, SCHWOERER A, RAU B, RADLWIMMER B, DOHNER H, LICHTER P *ET AL*: **GENOMIC DNA-CHIP HYBRIDIZATION REVEALS A HIGHER INCIDENCE OF GENOMIC AMPLIFICATIONS IN PANCREATIC CANCER THAN CONVENTIONAL COMPARATIVE GENOMIC HYBRIDIZATION AND LEADS TO THE IDENTIFICATION OF NOVEL CANDIDATE GENES**. *CANCER RESEARCH* 2004, **64**(13):4428-4433.

51. AGUIRRE AJ, BRENNAN C, BAILEY G, SINHA R, FENG B, LEO C, ZHANG Y, ZHANG J, GANS JD, BARDEESY N *ET AL*: **HIGH-RESOLUTION CHARACTERIZATION OF THE PANCREATIC ADENOCARCINOMA GENOME**. *PROCEEDINGS OF THE NATIONAL ACADEMY OF SCIENCES OF THE UNITED STATES OF AMERICA* 2004, **101**(24):9067-9072.

52. GYSIN S, RICKERT P, KASTURY K, MCMAHON M: **ANALYSIS OF GENOMIC DNA ALTERATIONS AND MRNA EXPRESSION PATTERNS IN A PANEL OF HUMAN PANCREATIC CANCER CELL LINES**. *GENES CHROMOSOMES CANCER* 2005, **44**(1):37-51.

53. HARADA T, CHELALA C, CRNOGORAC-JURCEVIC T, LEMOINE NR: **GENOME-WIDE ANALYSIS OF PANCREATIC CANCER USING MICROARRAY-BASED TECHNIQUES**. *PANCREATOLOGY* 2009, **9**(1-2):13-24.

54. LOUKOPOULOS P, SHIBATA T, KATOH H, KOKUBU A, SAKAMOTO M, YAMAZAKI K, KOSUGE T, KANAI Y, HOSODA F, IMOTO I *ET AL*: **GENOME-WIDE ARRAY-BASED COMPARATIVE GENOMIC HYBRIDIZATION ANALYSIS OF PANCREATIC ADENOCARCINOMA: IDENTIFICATION OF GENETIC INDICATORS THAT PREDICT PATIENT OUTCOME**. *CANCER SCI* 2007, **98**(3):392-400.

55. KWEI KA, SHAIN AH, BAIR R, MONTGOMERY K, KARIKARI CA, VAN DE RIJN M, HIDALGO M, MAITRA A, BASHYAM MD, POLLACK JR: **SMURF1 AMPLIFICATION PROMOTES INVASIVENESS IN PANCREATIC CANCER**. *PLOS ONE* 2011, **6**(8):E23924.

56. LAURILA E, SAVINAINEN K, KUUSELO R, KARHU R, KALLIONIEMI A: **CHARACTERIZATION OF THE 7Q21-Q22 AMPLICON IDENTIFIES ARPC1A, A SUBUNIT OF THE ARP2/3 COMPLEX, AS A REGULATOR OF CELL MIGRATION AND INVASION IN PANCREATIC CANCER**. *GENES CHROMOSOMES CANCER* 2009, **48**(4):330-339.

57. RUIZ C, LENKIEWICZ E, EVERS L, HOLLEY T, ROBESON A, KIEFER J, DEMEURE MJ, HOLLINGSWORTH MA, SHEN M, PRUNKARD D *ET AL*: **ADVANCING A CLINICALLY RELEVANT PERSPECTIVE OF THE CLONAL NATURE OF CANCER**. *PROC NATL ACAD SCI U S A* 2011, **108**(29):12054-12059.

58. BARRETINA J, CAPONIGRO G, STRANSKY N, VENKATESAN K, MARGOLIN AA, KIM S, WILSON CJ, LEHAR J, KRYUKOV GV, SONKIN D *ET AL*: **THE CANCER CELL LINE ENCYCLOPEDIA ENABLES PREDICTIVE MODELLING OF ANTICANCER DRUG SENSITIVITY**. *NATURE* 2012, **483**(7391):603-607.

59. MAUPIN KA, SINHA A, EUGSTER E, MILLER J, ROSS J, PAULINO V, KESHAMOUNI VG, TRAN N, BERENS M, WEBB C *ET AL*: **GLYCOGENE EXPRESSION ALTERATIONS ASSOCIATED WITH PANCREATIC CANCER EPITHELIAL-MESENCHYMAL TRANSITION IN COMPLEMENTARY MODEL SYSTEMS**. *PLOS ONE* 2010, **5**(9):E13002.

60. SCHOCK F, PERRIMON N: **MOLECULAR MECHANISMS OF EPITHELIAL MORPHOGENESIS**. *ANNU REV CELL DEV BIOL* 2002, **18**:463-493.

61. NEUREITER D, ZOPF S, DIMMLER A, STINTZING S, HAHN EG, KIRCHNER T, HEROLD C, OCKER M: **DIFFERENT CAPABILITIES OF MORPHOLOGICAL PATTERN FORMATION AND ITS ASSOCIATION WITH THE EXPRESSION OF DIFFERENTIATION MARKERS IN A XENOGRAFT MODEL OF HUMAN PANCREATIC CANCER CELL LINES**. *PANCREATOLOGY* 2005, **5**(4-5):387-397.

62. ZEISBERG M, NEILSON EG: **BIOMARKERS FOR EPITHELIAL-MESENCHYMAL TRANSITIONS**. *J CLIN INVEST* 2009, **119**(6):1429-1437.

63. BUCK E, EYZAGUIRRE A, BARR S, THOMPSON S, SENNELLO R, YOUNG D, IWATA KK, GIBSON NW, CAGNONI P, HALEY JD: **LOSS OF HOMOTYPIC CELL ADHESION BY EPITHELIAL-MESENCHYMAL TRANSITION OR MUTATION LIMITS SENSITIVITY TO EPIDERMAL GROWTH FACTOR RECEPTOR INHIBITION**. *MOLECULAR CANCER THERAPEUTICS* 2007, **6**(2):532-541.

64. ATCC: **AMERICAN TYPE CULTURE COLLECTION (ATCC)**. IN.

65. FRIXEN UH, BEHRENS J, SACHS M, EBERLE G, VOSS B, WARDA A, LOCHNER D, BIRCHMEIER W: **E-CADHERIN-MEDIATED CELL-CELL ADHESION PREVENTS INVASIVENESS OF HUMAN CARCINOMA CELLS**. *J CELL BIOL* 1991, **113**(1):173-185.

66. CLS: **CELL LINE SERVICE**. IN.

67. NISHIMURA N, SAITO S, KUBOTA Y, MOTO-O N, TAGUCHI K, YAMAZAKI K, WATANABE A, SASAKI H: **NEWLY ESTABLISHED HUMAN PANCREATIC CARCINOMA CELL LINES AND THEIR LECTIN BINDING PROPERTIES**. *INT J PANCREATOL* 1993, **13**(1):31-41.

68. MOHAMMAD RM, DUGAN MC, MOHAMED AN, ALMATCHY VP, FLAKE TM, DERGHAM ST, SHIELDS AF, AL-KATIB AA, VAITKEVICIUS VK, SARKAR FH: **ESTABLISHMENT OF A HUMAN PANCREATIC TUMOR XENOGRAFT MODEL: POTENTIAL APPLICATION FOR PRECLINICAL EVALUATION OF NOVEL THERAPEUTIC AGENTS**. *PANCREAS* 1998, **16**(1):19-25.

69. MOHAMMAD RM, LI Y, MOHAMED AN, PETTIT GR, ADSAY V, VAITKEVICIUS VK, AL-KATIB AM, SARKAR FH: **CLONAL PRESERVATION OF HUMAN PANCREATIC CELL LINE DERIVED FROM PRIMARY PANCREATIC ADENOCARCINOMA**. *PANCREAS* 1999, **19**(4):353-361.

70. BIOINFORMATIONWEB: **BIOINFORMATIONWEB**. IN.

71. ONCOMINE: **ONCOMINE**. IN.

72. ELSASSER HP, LEHR U, AGRICOLA B, KERN HF: **STRUCTURAL ANALYSIS OF A NEW HIGHLY METASTATIC CELL LINE PATU 8902 FROM A PRIMARY HUMAN PANCREATIC ADENOCARCINOMA**. *VIRCHOWS ARCH B CELL PATHOL INCL MOL PATHOL* 1993, **64**(4):201-207.

73. JESSE S, KOENIG A, ELLENRIEDER V, MENKE A: **LEF-1 ISOFORMS REGULATE DIFFERENT TARGET GENES AND REDUCE CELLULAR ADHESION**. *INT J CANCER*, **126**(5):1109-1120.

74. JESSE S, KOENIG A, ELLENRIEDER V, MENKE A: **LEF-1 ISOFORMS REGULATE DIFFERENT TARGET GENES AND REDUCE CELLULAR ADHESION**. *INT J CANCER* 2010, **126**(5):1109-1120.

75. ELSASSER HP, LEHR U, AGRICOLA B, KERN HF: **ESTABLISHMENT AND CHARACTERISATION OF TWO CELL LINES WITH DIFFERENT GRADE OF DIFFERENTIATION DERIVED FROM ONE PRIMARY HUMAN PANCREATIC ADENOCARCINOMA**. *VIRCHOWS ARCH B CELL PATHOL INCL MOL PATHOL* 1992, **61**(5):295-306.

76. KYRIAZIS AP, MCCOMBS WB, 3RD, SANDBERG AA, KYRIAZIS AA, SLOANE NH, LEPERA R: **ESTABLISHMENT AND CHARACTERIZATION OF HUMAN PANCREATIC ADENOCARCINOMA CELL LINE SW-1990 IN TISSUE CULTURE AND THE NUDE MOUSE**. *CANCER RES* 1983, **43**(9):4393-4401.

77. YAMADA T, OKAJIMA F, ADACHI M, OHWADA S, KONDO Y: **GROWTH DEPENDENCY OF A NEW HUMAN PANCREATIC CANCER CELL LINE, YAPC, ON AUTOCRINE INTERLEUKIN-1ALPHA STIMULATION**. *INT J CANCER* 1998, **76**(1):141-147.

78. OWENS RB: **SELECTIVE CULTIVATION OF MAMMALIAN EPITHELIAL CELLS**, VOL. 14: ACADEMIC PRESS INCORPORATED; 1976.

79. THIERY JP: **EPITHELIAL-MESENCHYMAL TRANSITIONS IN TUMOUR PROGRESSION**. *NAT REV CANCER* 2002, **2**(6):442-454.

80. BAKER DE, HARRISON NJ, MALTBY E, SMITH K, MOORE HD, SHAW PJ, HEATH PR, HOLDEN H, ANDREWS PW: **ADAPTATION TO CULTURE OF HUMAN EMBRYONIC STEM CELLS AND ONCOGENESIS IN VIVO**. *NAT BIOTECHNOL* 2007, **25**(2):207-215.

81. IMREH MP, GERTOW K, CEDERVALL J, UNGER C, HOLMBERG K, SZOKE K, CSOREGH L, FRIED G, DILBER S, BLENNOW E *ET AL*: **IN VITRO CULTURE CONDITIONS FAVORING SELECTION OF CHROMOSOMAL ABNORMALITIES IN HUMAN ES CELLS**. *J CELL BIOCHEM* 2006, **99**(2):508-516.

82. ENVER T, SONEJI S, JOSHI C, BROWN J, IBORRA F, ORNTOFT T, THYKJAER T, MALTBY E, SMITH K, ABU DAWUD R *ET AL*: **CELLULAR DIFFERENTIATION HIERARCHIES IN NORMAL AND CULTURE-ADAPTED HUMAN EMBRYONIC STEM CELLS**. *HUM MOL GENET* 2005, **14**(21):3129-3140.

83. BAHARVAND H, AGHDAMI N, HARRISON N, BAKER D, ANDREWS P: **THE SIGNIFICANCE OF CULTURE ADAPTATION OF EMBRYONIC STEM CELLS FOR REGENERATIVE MEDICINE**. IN: *ADVANCES IN STEM CELL RESEARCH.* HUMANA PRESS; 2012: 17-27.

84. OSHIMA M, OKANO K, MURAKI S, HABA R, MAEBA T, SUZUKI Y, YACHIDA S: **IMMUNOHISTOCHEMICALLY DETECTED EXPRESSION OF 3 MAJOR GENES (CDKN2A/P16, TP53, AND SMAD4/DPC4) STRONGLY PREDICTS SURVIVAL IN PATIENTS WITH RESECTABLE PANCREATIC CANCER**. *ANN SURG* 2013, **258**(2):336-346.

85. UNIPROT: **UNIPROT**. IN.

86. LEGOFFIC A, CALVO EL, BARTHET M, DELPERO JR, DAGORN JC, IOVANNA JL: **IDENTIFICATION OF GENOMIC ALTERATIONS ASSOCIATED WITH THE AGGRESSIVENESS OF PANCREATIC CANCER USING AN ULTRA-HIGH-RESOLUTION CGH ARRAY**. *PANCREATOLOGY* 2009, **9**(3):267-272.

87. KWEI KA, SHAIN AH, BAIR R, MONTGOMERY K, KARIKARI CA, VAN DE RIJN M, HIDALGO M, MAITRA A, BASHYAM MD, POLLACK JR: **SMURF1 AMPLIFICATION PROMOTES INVASIVENESS IN PANCREATIC CANCER**. *PLOS ONE*, **6**(8):E23924.

88. YACHIDA S, JONES S, BOZIC I, ANTAL T, LEARY R, FU B, KAMIYAMA M, HRUBAN RH, ESHLEMAN JR, NOWAK MA *ET AL*: **DISTANT METASTASIS OCCURS LATE DURING THE GENETIC EVOLUTION OF PANCREATIC CANCER**. *NATURE* 2010, **467**(7319):1114-1117.

89. GRIFFIN CA, MORSBERGER L, HAWKINS AL, HADDADIN M, PATEL A, RIED T, SCHROCK E, PERLMAN EJ, JAFFEE E: **MOLECULAR CYTOGENETIC CHARACTERIZATION OF PANCREAS CANCER CELL LINES REVEALS HIGH COMPLEXITY CHROMOSOMAL ALTERATIONS**. *CYTOGENET GENOME RES* 2007, **118**(2-4):148-156.

90. HEIDENBLAD M, LINDGREN D, VELTMAN JA, JONSON T, MAHLAMAKI EH, GORUNOVA L, VAN KESSEL AG, SCHOENMAKERS EF, HOGLUND M: **MICROARRAY ANALYSES REVEAL STRONG INFLUENCE OF DNA COPY NUMBER ALTERATIONS ON THE TRANSCRIPTIONAL PATTERNS IN PANCREATIC CANCER: IMPLICATIONS FOR THE INTERPRETATION OF GENOMIC AMPLIFICATIONS**. *ONCOGENE* 2005, **24**(10):1794-1801.

91. HERREROS-VILLANUEVA M, GIRONELLA M, CASTELLS A, BUJANDA L: **MOLECULAR MARKERS IN PANCREATIC CANCER DIAGNOSIS**. *CLIN CHIM ACTA* 2013, **418**:22-29.

92. KOWALSKI J, MORSBERGER LA, BLACKFORD A, HAWKINS A, YEO CJ, HRUBAN RH, GRIFFIN CA: **CHROMOSOMAL ABNORMALITIES OF ADENOCARCINOMA OF THE PANCREAS: IDENTIFYING EARLY AND LATE CHANGES**. *CANCER GENET CYTOGENET* 2007, **178**(1):26-35.

93. DERYNCK R, AKHURST RJ, BALMAIN A: **TGF-BETA SIGNALING IN TUMOR SUPPRESSION AND CANCER PROGRESSION**. *NAT GENET* 2001, **29**(2):117-129.

94. BLACKFORD A, SERRANO OK, WOLFGANG CL, PARMIGIANI G, JONES S, ZHANG X, PARSONS DW, LIN JC, LEARY RJ, ESHLEMAN JR *ET AL*: **SMAD4 GENE MUTATIONS ARE ASSOCIATED WITH POOR PROGNOSIS IN PANCREATIC CANCER**. *CLIN CANCER RES* 2009, **15**(14):4674-4679.

95. IACOBUZIO-DONAHUE CA, FU B, YACHIDA S, LUO M, ABE H, HENDERSON CM, VILARDELL F, WANG Z, KELLER JW, BANERJEE P *ET AL*: **DPC4 GENE STATUS OF THE PRIMARY CARCINOMA CORRELATES WITH PATTERNS OF FAILURE IN PATIENTS WITH PANCREATIC CANCER**. *J CLIN ONCOL* 2009, **27**(11):1806-1813.

96. MAITRA A, MOLBERG K, ALBORES-SAAVEDRA J, LINDBERG G: **LOSS OF DPC4 EXPRESSION IN COLONIC ADENOCARCINOMAS CORRELATES WITH THE PRESENCE OF METASTATIC DISEASE**. *AM J PATHOL* 2000, **157**(4):1105-1111.

97. MAHLAMAKI EH, HOGLUND M, GORUNOVA L, KARHU R, DAWISKIBA S, ANDREN-SANDBERG A, KALLIONIEMI OP, JOHANSSON B: **COMPARATIVE GENOMIC HYBRIDIZATION REVEALS FREQUENT GAINS OF 20Q, 8Q, 11Q, 12P, AND 17Q, AND LOSSES OF 18Q, 9P, AND 15Q IN PANCREATIC CANCER**. *GENES CHROMOSOMES CANCER* 1997, **20**(4):383-391.

98. BROCKSCHMIDT A, TROST D, PETERZIEL H, ZIMMERMANN K, EHRLER M, GRASSMANN H, PFENNING PN, WAHA A, WOHLLEBER D, BROCKSCHMIDT FF *ET AL*: **KIAA1797/FOCAD ENCODES A NOVEL FOCAL ADHESION PROTEIN WITH TUMOUR SUPPRESSOR FUNCTION IN GLIOMAS**. *BRAIN* 2012, **135**(PT 4):1027-1041.

99. SUMARA I, QUADRONI M, FREI C, OLMA MH, SUMARA G, RICCI R, PETER M: **A CUL3-BASED E3 LIGASE REMOVES AURORA B FROM MITOTIC CHROMOSOMES, REGULATING MITOTIC PROGRESSION AND COMPLETION OF CYTOKINESIS IN HUMAN CELLS**. *DEVELOPMENTAL CELL* 2007, **12**(6):887-900.

100. ARCO A, FAVALORO A, GIOFFRE M, SANTORO G, SPECIALE F, VERMIGLIO G, CUTRONEO G: **SARCOGLYCANS IN THE NORMAL AND PATHOLOGICAL BREAST TISSUE OF HUMANS: AN IMMUNOHISTOCHEMICAL AND MOLECULAR STUDY**. *CELLS TISSUES ORGANS* 2012, **195**(6):550-562.

101. BOVA GS, CARTER BS, BUSSEMAKERS MJ, EMI M, FUJIWARA Y, KYPRIANOU N, JACOBS SC, ROBINSON JC, EPSTEIN JI, WALSH PC *ET AL*: **HOMOZYGOUS DELETION AND FREQUENT ALLELIC LOSS OF CHROMOSOME 8P22 LOCI IN HUMAN PROSTATE CANCER**. *CANCER RESEARCH* 1993, **53**(17):3869-3873.

102. PILS D, HORAK P, VANHARA P, ANEES M, PETZ M, ALFANZ A, GUGERELL A, WITTINGER M, GLEISS A, AUNER V *ET AL*: **METHYLATION STATUS OF TUSC3 IS A PROGNOSTIC FACTOR IN OVARIAN CANCER**. *CANCER* 2013, **119**(5):946-954.

103. PILS D, HORAK P, GLEISS A, SAX C, FABJANI G, MOEBUS VJ, ZIELINSKI C, REINTHALLER A, ZEILLINGER R, KRAINER M: **FIVE GENES FROM CHROMOSOMAL BAND 8P22 ARE SIGNIFICANTLY DOWN-REGULATED IN OVARIAN CARCINOMA: N33 AND EFA6R HAVE A POTENTIAL IMPACT ON OVERALL SURVIVAL**. *CANCER* 2005, **104**(11):2417-2429.

104. DENNIS JW, GRANOVSKY M, WARREN CE: **GLYCOPROTEIN GLYCOSYLATION AND CANCER PROGRESSION**. *BIOCHIMICA ET BIOPHYSICA ACTA* 1999, **1473**(1):21-34.

105. YANG J, WEINBERG RA: **EPITHELIAL-MESENCHYMAL TRANSITION: AT THE CROSSROADS OF DEVELOPMENT AND TUMOR METASTASIS**. *DEVELOPMENTAL CELL* 2008, **14**(6):818-829.

106. MOREL AP, LIEVRE M, THOMAS C, HINKAL G, ANSIEAU S, PUISIEUX A: **GENERATION OF BREAST CANCER STEM CELLS THROUGH EPITHELIAL-MESENCHYMAL TRANSITION**. *PLOS ONE* 2008, **3**(8):E2888.

107. JAVLE MM, GIBBS JF, IWATA KK, PAK Y, RUTLEDGE P, YU J, BLACK JD, TAN D, KHOURY T: **EPITHELIAL-MESENCHYMAL TRANSITION (EMT) AND ACTIVATED EXTRACELLULAR SIGNAL-REGULATED KINASE (P-ERK) IN SURGICALLY RESECTED PANCREATIC CANCER**. *ANN SURG ONCOL* 2007, **14**(12):3527-3533.

108. OIDA Y, YAMAZAKI H, TOBITA K, MUKAI M, OHTANI Y, MIYAZAKI N, ABE Y, IMAIZUMI T, MAKUUCHI H, UEYAMA Y *ET AL*: **INCREASED S100A4 EXPRESSION COMBINED WITH DECREASED E-CADHERIN EXPRESSION PREDICTS A POOR OUTCOME OF PATIENTS WITH PANCREATIC CANCER**. *ONCOLOGY REPORTS* 2006, **16**(3):457-463.

109. NAKAJIMA S, DOI R, TOYODA E, TSUJI S, WADA M, KOIZUMI M, TULACHAN SS, ITO D, KAMI K, MORI T *ET AL*: **N-CADHERIN EXPRESSION AND EPITHELIAL-MESENCHYMAL TRANSITION IN PANCREATIC CARCINOMA**. *CLIN CANCER RES* 2004, **10**(12 PT 1):4125-4133.

110. YIN T, WANG C, LIU T, ZHAO G, ZHA Y, YANG M: **EXPRESSION OF SNAIL IN PANCREATIC CANCER PROMOTES METASTASIS AND CHEMORESISTANCE**. *THE JOURNAL OF SURGICAL RESEARCH* 2007, **141**(2):196-203.

111. FREIRE-DE-LIMA L: **SWEET AND SOUR: THE IMPACT OF DIFFERENTIAL GLYCOSYLATION IN CANCER CELLS UNDERGOING EPITHELIAL-MESENCHYMAL TRANSITION**. *FRONT ONCOL*, **4**:59.

112. IOZZO RV (ED.): **METHODS IN MOLECULAR BIOLOGY** 2001.

113. EAST L, MCCARTHY A, WIENKE D, STURGE J, ASHWORTH A, ISACKE CM: **A TARGETED DELETION IN THE ENDOCYTIC RECEPTOR GENE ENDO180 RESULTS IN A DEFECT IN COLLAGEN UPTAKE**. *EMBO REPORTS* 2003, **4**(7):710-716.

114. ENGELHOLM LH, LIST K, NETZEL-ARNETT S, CUKIERMAN E, MITOLA DJ, AARONSON H, KJOLLER L, LARSEN JK, YAMADA KM, STRICKLAND DK *ET AL*: **UPARAP/ENDO180 IS ESSENTIAL FOR CELLULAR UPTAKE OF COLLAGEN AND PROMOTES FIBROBLAST COLLAGEN ADHESION**. *THE JOURNAL OF CELL BIOLOGY* 2003, **160**(7):1009-1015.

115. WIENKE D, MACFADYEN JR, ISACKE CM: **IDENTIFICATION AND CHARACTERIZATION OF THE ENDOCYTIC TRANSMEMBRANE GLYCOPROTEIN ENDO180 AS A NOVEL COLLAGEN RECEPTOR**. *MOL BIOL CELL* 2003, **14**(9):3592-3604.

116. KJOLLER L, ENGELHOLM LH, HOYER-HANSEN M, DANO K, BUGGE TH, BEHRENDT N: **UPARAP/ENDO180 DIRECTS LYSOSOMAL DELIVERY AND DEGRADATION OF COLLAGEN IV**. *EXPERIMENTAL CELL RESEARCH* 2004, **293**(1):106-116.

117. EAST L, ISACKE CM: **THE MANNOSE RECEPTOR FAMILY**. *BIOCHIM BIOPHYS ACTA* 2002, **1572**(2-3):364-386.

118. EAST L, RUSHTON S, TAYLOR ME, ISACKE CM: **CHARACTERIZATION OF SUGAR BINDING BY THE MANNOSE RECEPTOR FAMILY MEMBER, ENDO180**. *J BIOL CHEM* 2002, **277**(52):50469-50475.

119. ISACKE CM, VAN DER GEER P, HUNTER T, TROWBRIDGE IS: **P180, A NOVEL RECYCLING TRANSMEMBRANE GLYCOPROTEIN WITH RESTRICTED CELL TYPE EXPRESSION**. *MOLECULAR AND CELLULAR BIOLOGY* 1990, **10**(6):2606-2618.

120. ZAHEDI K: **CHARACTERIZATION OF THE BINDING OF SERUM AMYLOID P TO TYPE IV COLLAGEN**. *THE JOURNAL OF BIOLOGICAL CHEMISTRY* 1996, **271**(25):14897-14902.

121. WIENKE D, DAVIES GC, JOHNSON DA, STURGE J, LAMBROS MB, SAVAGE K, ELSHEIKH SE, GREEN AR, ELLIS IO, ROBERTSON D *ET AL*: **THE COLLAGEN RECEPTOR ENDO180 (CD280) IS EXPRESSED ON BASAL-LIKE BREAST TUMOR CELLS AND PROMOTES TUMOR GROWTH IN VIVO**. *CANCER RES* 2007, **67**(21):10230-10240.

122. HUIJBERS IJ, IRAVANI M, POPOV S, ROBERTSON D, AL-SARRAJ S, JONES C, ISACKE CM: **A ROLE FOR FIBRILLAR COLLAGEN DEPOSITION AND THE COLLAGEN INTERNALIZATION RECEPTOR ENDO180 IN GLIOMA INVASION**. *PLOS ONE* 2010, **5**(3):E9808.

123. STURGE J, WIENKE D, EAST L, JONES GE, ISACKE CM: **GPI-ANCHORED UPAR REQUIRES ENDO180 FOR RAPID DIRECTIONAL SENSING DURING CHEMOTAXIS**. *THE JOURNAL OF CELL BIOLOGY* 2003, **162**(5):789-794.

124. STURGE J, WIENKE D, ISACKE CM: **ENDOSOMES GENERATE LOCALIZED RHO-ROCK-MLC2-BASED CONTRACTILE SIGNALS VIA ENDO180 TO PROMOTE ADHESION DISASSEMBLY**. *THE JOURNAL OF CELL BIOLOGY* 2006, **175**(2):337-347.

125. KOGIANNI G, WALKER MM, WAXMAN J, STURGE J: **ENDO180 EXPRESSION WITH COFUNCTIONAL PARTNERS MT1-MMP AND UPAR-UPA IS CORRELATED WITH PROSTATE CANCER PROGRESSION**. *EUR J CANCER* 2009, **45**(4):685-693.

126. FINK SP, MIKKOLA D, WILLSON JK, MARKOWITZ S: **TGF-BETA-INDUCED NUCLEAR LOCALIZATION OF SMAD2 AND SMAD3 IN SMAD4 NULL CANCER CELL LINES**. *ONCOGENE* 2003, **22**(9):1317-1323.

127. GRAU AM, ZHANG L, WANG W, RUAN S, EVANS DB, ABBRUZZESE JL, ZHANG W, CHIAO PJ: **INDUCTION OF P21WAF1 EXPRESSION AND GROWTH INHIBITION BY TRANSFORMING GROWTH FACTOR BETA INVOLVE THE TUMOR SUPPRESSOR GENE DPC4 IN HUMAN PANCREATIC ADENOCARCINOMA CELLS**. *CANCER RES* 1997, **57**(18):3929-3934.

128. HUIJBERS IJ, IRAVANI M, POPOV S, ROBERTSON D, AL-SARRAJ S, JONES C, ISACKE CM: **A ROLE FOR FIBRILLAR COLLAGEN DEPOSITION AND THE COLLAGEN INTERNALIZATION RECEPTOR ENDO180 IN GLIOMA INVASION**. *PLOS ONE*, **5**(3):E9808.

129. HAHN SA, SCHUTTE M, HOQUE AT, MOSKALUK CA, DA COSTA LT, ROZENBLUM E, WEINSTEIN CL, FISCHER A, YEO CJ, HRUBAN RH *ET AL*: **DPC4, A CANDIDATE TUMOR SUPPRESSOR GENE AT HUMAN CHROMOSOME 18Q21.1**. *SCIENCE* 1996, **271**(5247):350-353.

130. TAKAHASHI S, YAMADA-OKABE H, HAMADA K, OHTA S, KAWASE T, YOSHIDA K, TODA M: **DOWNREGULATION OF UPARAP MEDIATES CYTOSKELETAL REARRANGEMENTS AND DECREASES INVASION AND MIGRATION PROPERTIES IN GLIOMA CELLS**. *J NEUROONCOL*, **103**(2):267-276.

131. CURINO AC, ENGELHOLM LH, YAMADA SS, HOLMBECK K, LUND LR, MOLINOLO AA, BEHRENDT N, NIELSEN BS, BUGGE TH: **INTRACELLULAR COLLAGEN DEGRADATION MEDIATED BY UPARAP/ENDO180 IS A MAJOR PATHWAY OF EXTRACELLULAR MATRIX TURNOVER DURING MALIGNANCY**. *THE JOURNAL OF CELL BIOLOGY* 2005, **169**(6):977-985.